N71-33214

NASA CONTRACTOR REPORT

NASA CR-1778

NASA CR-1778

CASE FILE COPY

ADAPTIVE OPTIMIZATION OF SIGNAL TO NOISE RATIO IN RECEIVING ARRAYS

by Robert L. Riegler

Prepared by
ELECTROSCIENCE LABORATORY
THE OHIO STATE UNIVERSITY
Columbus, Ohio 43212
for Electronics Research Center

NATIONAL AERONAUTICS AND SPACE ADMINISTRATION • WASHINGTON, D. C. • AUGUST 1971

1. Report No.	2. Government Accession No.	3. Recipient's Catalog No.
NASA CR-1778		

4. Title and Subtitle	5. Report Date
ADAPTIVE OPTIMIZATION OF SIGNAL TO NOISE RATIO IN RECEIVING ARRAYS	August 1971
	6. Performing Organization Code
7. Author(s)	8. Performing Organization Report No.
Robert L. Riegler	Technical Report 2902-1
	10. Work Unit No.
9. Performing Organization Name and Address	11. Contract or Grant No.
The Ohio State University ElectroScience Laboratory Department of Electrical Engineering Columbus, Ohio 20546	NGL 36-008-138
	13. Type of Report and Period Covered
12. Sponsoring Agency Name and Address	Contractor Report
National Aeronautics and Space Administration Washington, DC 20546	14. Sponsoring Agency Code

15. Supplementary Notes

16. Abstract

This report discusses adaptive optimization of signal-to-noise ratio in receiving arrays. Both background sky noise and coherent noise interference are considered.

First, the array weighting coefficients which maximize SNR are derived for an array subjected to uniform background antenna noise. An array model of half-wavelength dipoles over a ground plane is analyzed to show the effects of mutual coupling.

Second, an adaptive array that rejects undesired or interfering signals is presented. The array pattern is controlled by an adaptive feedback system based on a steepest-descent minimization of mean square error. Here error is defined as the difference between the array output and a locally generated reference signal. Minimization of mean square error is closely related to maximization of signal-to-noise ratio.

An experimental version, a 2-element S-band adaptive array, is discussed. Typical antenna patterns for various desired and interfering signals are shown, as well as measured transient response. Finally, some experiments showing the array behavior with modulated signals are described.

The results show that such an antenna system is capable of automatically rejecting interfering signals, subject only to certain basic constraints. No a priori information concerning the angles of arrival of the signals is required. Detailed knowledge of the waveforms of the desired and interfering signals is also not needed, although the spectral density of the desired signal must be known.

17. Key Words (Suggested by Author(s))	18. Distribution Statement
Antennas, arrays, adaptive antenna arrays, antenna arrays having optimized signal to noise ratio	Unclassified-Unlimited

19. Security Classif. (of this report)	20. Security Classif. (of this page)	21. No. of Pages	22. Price*
Unclassified	Unclassified	120	$3.00

*For sale by the National Technical Information Service, Springfield, Virginia 22151

ACKNOWLEDGMENT

It is a pleasure to acknowledge several people for their assistance in the preparation of this report.

First, special thanks are due to Dr. C.H. Walter and Dr. W.H. Peake for their technical assistance, counseling, and encouragement, not only during the work covered in this report but all through my graduate program.

Dr. R.T. Compton contributed many valuable ideas and comments throughout the writing of this report and during the preceding experimental and theoretical research work.

Finally, Dr. J.H. Richmond deserves recognition for his assistance in computer solution techniques for determining mutual coupling parameters.

The material contained in this report was also used as a dissertation submitted to the Department of Electrical Engineering, The Ohio State University, as partial fulfillment for the degree Doctor of Philosophy.

CONTENTS

Chapter		Page
I	INTRODUCTION	1
II	OPTIMIZATION OF SNR FOR BACKGROUND SKY NOISE	5
	A. Output Signal Power	5
	B. Output Noise Power	8
	C. Optimization of SNR	10
	D. Dipole Array Model	14
III	OPTIMIZATION FOR COHERENT INTERFERENCE	27
	A. The LMS Feedback Algorithm	30
	B. Relationship between SNR and LMS Error	37
	C. The Steepest Descent Optimization	43
IV	EXPERIMENTAL RESULTS	47
	A. Description of Equipment	47
	B. Description of Measured Results	50
	i. Phase Tracking	52
	ii. Amplitude Tracking	52
	C. Interference Rejection	52
	D. Speed of Response	66
V	CONCLUSIONS	85
Appendix		
I	BACKGROUND SKY NOISE	87
II	ARRAY IMPEDANCE	98
III	CIRCUIT DIAGRAM FOR PROCESSING UNIT	105
IV	COMPUTER PROGRAM	108
REFERENCES		115

CHAPTER I
INTRODUCTION

The optimization of antenna arrays has been studied for many years. Many types of criteria and parameters have been used as the variable to be optimized but most of the work has been concerned only with properties of the antenna pattern. For example in 1946 Dolph[1] developed a synthesis technique which minimized the beamwidth subject to a specified sidelobe level. About the same time Uzkov[2] showed how to maximize the gain of a uniformly spaced array. In particular, he showed that the optimum gain of an endfire array of isotropic sources was equal to the square of the number of elements (and occured when the interelement spacing approached zero). In addition he showed that for half-wavelength spacing the optimum gain was equal to the number of elements. Tai[3] determined the optimum broadside gain of uniformly spaced arrays of directive elements (dipoles). Jennetti[4] maximized gain with the constraint of a pattern null in a specified direction.

For receiving arrays, such as those used in communication and radar systems, the most important parameter is not simply gain but output signal to noise ratio (SNR). For a specified modulation scheme this parameter can also be related to probability of error.

It is highly desirable that this optimization be automatic. That is for each change in the array's environment (e.g., change in angle of arrival of the signal) or operating condition (e.g., changes in the properties of the electronic components) the system should adapt itself to this new condition by suitable internal feedback modifications until the SNR is again optimum. This class of antenna systems is called adaptive arrays.

The first adaptive array of this type was the phase lock loop[5,6] or self-phasing array. This type of array operates by aligning the phase of the signal from each element with that of a reference before they are combined, thus assuring that coherent addition occurs. This type of processing forces the main beam to point in the direction of the incident signal and automatically track it as its angle of arrival changes. It will be shown in Chapter II that this type of processing does maximize the output SNR if the array consists of widely spaced (no mutual coupling) identical elements and the noise is generated internally by identical components in each channel. Unfortunately the phase locked array does not have the ability to reject undesired signals which are incident upon it. Even worse, if the interfering signal is stronger than the desired signal the array has a tendency to "lock-on" to the interference and track it rather than the desired signal (the so-called capture effect)[6].

Shor[7] was one of the first to suggest an adaptive process which maximized the SNR of an array of hydraphones, with both desired and undesired signals present. Widrow[8] et al suggested a technique which minimized the mean square error between an array output and a reference signal, also for the case of both desired and undesired signals present. It will be shown in Chapter III that for certain conditions this is equivalent to maximizing SNR.

The techniques suggested by Shor and Widrow are both iterative processes using a steepest descent optimization approach and both tend to point the main beam in the direction of the desired signal, while simultaneously generating antenna pattern nulls in the direction of undesired or interfering signals.

The basic problem to be studied here is how to organize or process the elements of an array in order to achieve optimum SNR, for two distinct situations. Chapter II considers the case of spatially uncorrelated sky noise in the array's environment plus noise generated internally by electronic components. Specific examples are presented which quantitatively show the performance of an array when mutual coupling effects are considered.

Chapter III considers the case of coherent interference or jamming signals. The scheme suggested by Widrow is discussed; in particular the behavior of the LMS algorithm for communication type (i.e., modulated) signals is analyzed. An actual array based on this technique was constructed and experimental results (antenna

patterns, power spectra, etc.) are presented in Chapter IV to demonstrate that the principles upon which this theory is based are correct and within state of the art technology.

CHAPTER II
OPTIMIZATION OF SNR FOR BACKGROUND SKY NOISE

In this chapter the array weighting coefficients which yield maximum output SNR are derived for the case of uncorrelated background sky noise with internally generated noise. That is, the array is assumed to be operating in an environment where no coherent interference or jamming signals are present; the only noise from the environment is "antenna or sky noise". Intuitively it is expected that the improvement in SNR due to signal processing will be less than when "plane wave" interference from a particular spatial angle is incident upon the array.

The basic array system is shown in Fig. 1. The output of each antenna element is weighted by a complex weighting coefficient w_i before being added together to form the array output. The actual weighting coefficient component may be an amplifier with complex (i.e., magnitude and phase) voltage gain or an attenuator and phase shifter and may be continuously changing due to internal feedback control circuitry.

A. Output Signal Power

The signal power at the output may be expressed as

$$(1) \qquad S_o = \left| \left(\sum_{i=1}^{N} w_i \, x_i \right) \right|^2$$

where: w_i is the complex voltage weighting coefficient which may be seperated into its amplitude and phase components, i.e., $w_i = A_i e^{j\phi_i}$

x_i is the complex signal voltage appearing at the terminals of the ith antenna element, $x_i = V_i e^{j\psi_i}$

N= number of elements in the array.

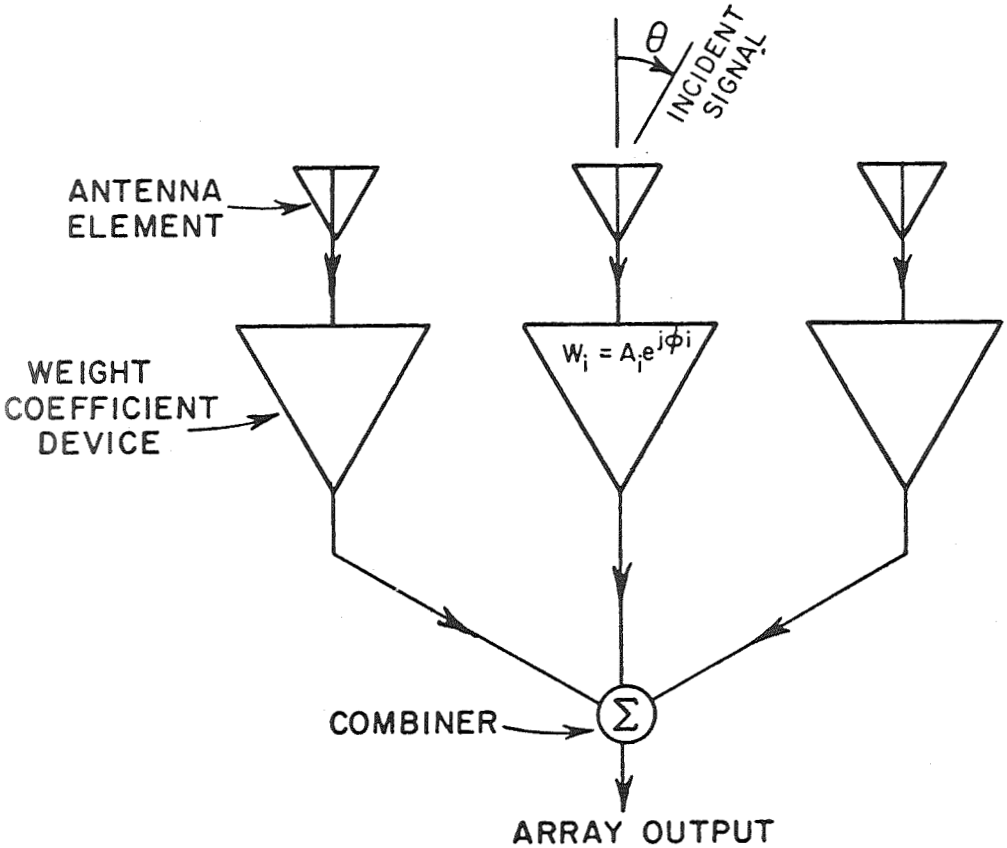

Fig. 1--Basic array system.

Unity output impedance has been assumed in the above equation; since the ratio of signal to noise is the parameter of interest the impedance will cancel, so this represents no loss of generality. Note that the terminal voltage is a function of spatial angle θ, the direction from which a plane wave is incident upon the array. That is $X_i(\theta) = V_i(\theta)e^{j\psi_i(\theta)}$.

Based on simple array theory (neglecting any mutual coupling) the expression for X_i due to a constant amplitude plane wave with identical antenna elements and identical load terminations would have the form:

$$X_i(\theta) = V\, e^{-jk(i-1)d \sin \theta} \tag{2}$$

where V = a constant

$k = 2\pi/\lambda$ = propagation factor

d = separation distance between elements (assumed equal)

λ = wavelength of incident source.

That is, the voltage at each element would have the same magnitude (determined by the strength of the incident wave and physical properties of the antennas) and differ from one another only in phase. However, for many arrays the effects of mutual coupling from element to element cause this simple theory to yield poor results. When mutual coupling is significant the simplified expression for X_i cannot be used, instead the more general form must be retained. The manner in which the actual X_i's are

obtained for this case is discussed in more detail in Appendices II and IV.

B. Output Noise Power

The noise power at the array output consists of two distinct types, a contribution generated by the array system, and a component which originates from outside the system and enters the system via the antennas. The component generated by the system includes shot noise from electronic components (mixers, amplifiers, etc.) as well as thermal noise produced by lossy materials (coax lines, etc.). For convenience all of these internally generated contributions can be referred to the input of the device which performs the weighting operation, so that the output noise power due to this type is given by

$$N_g = \sum_{i=1}^{N} |w_i|^2 N_i \tag{3}$$

where N_g = total output noise power generated by the system

$|w_i|^2 = w_i \cdot w_i^* = A_i^2$ the power gain of the weighting coefficient device

N_i = total mean square noise voltage generated in the ith channel and referred to the input of the weighting coefficient device.

A common source of noise N_i is the amplifier in each channel. If the noise figure F_i of channel i is known then

(4) $N_i = k(F_i-1)T_o\Delta f$

where k = Boltzmann's constant = 1.38×10^{-23} joule/^oK

F_i = noise figure of ith channel

$T_o = 290^oK$

Δf = bandwidth of the channel.

If the internally generated noise is due to lossy materials, say a length of transmission line with power transfer ratio α then the available noise is given by

(5) $N_{th} = k(1-\alpha)T_\ell \Delta f$

where N_{th} = available thermal noise

α = the power transmission factor = $\frac{\text{output power from transmission line}}{\text{input power into transmission line}}$

T_ℓ = physical temperature of transmission line in ^oK

If both of these sources of internal noise are present the total noise in the channel will be the sum of each contribution. The addition is done on a power basis rather than voltage due to the uncorrelated nature of these two types of noise.

In addition to this internally generated noise there exists a component due to noise sources in the environment of the antenna, i.e., antenna or sky noise. This component is extremely difficult to describe in practice because it may vary considerably with time, location, direction, and frequency. In principal the output noise

power due to external sky noise sources can be expressed as:

$$(6) \qquad N_e = \iint B(\theta',\phi')\, A_e(\theta',\phi')\, d\Omega$$

(for a more complete description of sky noise see Appendix I)

where $B(\theta',\phi')$ is the brightness of the sky in the direction θ',ϕ' with dimensions $\frac{\text{watts}}{m^2 - \text{sterad}}$

$A_e(\theta',\phi')$ is the effective collecting aperture of array (m^2) which may also be expressed in terms of its normalized power pattern $f(\theta',\phi')$ as $A_{e_m} f(\theta',\phi')$ with A_{e_m} the maximum value of $A_e(\theta\ ,\phi\ )$

$d\Omega$ = element of solid angle = $\sin\theta'\, d\theta'\, d\phi'$

If $v_i^u(\theta',\phi')$ is the voltage induced on element i due to a principal polarized plane wave which has unit power density (i.e., 1 watt/m^2) from direction θ',ϕ' then the effective aperture is given by

$$(7) \qquad A_e(\theta',\phi') = \left| \left(\sum w_i v_i^u(\theta',\phi') \right) \right|^2$$

C. Optimization of SNR

It is now possible to write the expression for output SNR as:

$$(8) \qquad \frac{S_o}{N_o} = \frac{\left(\sum_{i=1}^{N} w_i\, x_i(\theta_o,\phi_o) \right)^2}{\sum_{i=1}^{N} |w_i|^2 N_i + \iint B(\theta',\phi') A_e(\theta',\phi') d\Omega}$$

substituting the expression for A_e yields

$$(9)\quad \frac{S_o}{N_o} = \frac{\left(\sum w_i X_i(\theta_o,\phi_o)\right)^2}{\sum |w_i|^2 N_i + \iint B(\theta',\phi')\left(\sum_{i=1}^{N} w_i v_i^u(\theta',\phi')\right)^2 d\Omega}$$

or writing the complex quantities in terms of their amplitude and phase functions, i.e., $w_i = A_i e^{j\phi_i}$ $x_i(\theta',\phi') = V_i(\theta',\phi')e^{j\psi_i(\theta',\phi')}$

$$(10)\quad \frac{S_o}{N_o} = \frac{\left|\left(\sum_{i=1}^{N} A_i V_i(\theta',\phi')e^{j(\phi_i+\psi_i(\theta_o,\phi_o)}\right)\right|^2}{\sum_{i=1}^{N} A_i^2 N_i + \iint B(\theta',\phi')\left|\left(\sum A_i V_i^u(\theta',\phi')e^{j\phi_i+\psi_i(\theta',\phi')}\right)\right|^2 d\Omega}$$

In principal those values of A_i and ϕ_i ($i = 1,\cdots N$) which maximize the output SNR can be found by setting the partial derivatives of Eq. (10) with respect to A_i and ϕ_i equal to zero. This would yield a system of 2N equations containing integral expressions which must be solved. Unfortunately a completely general solution valid for arbitrary brightness, array geometry, etc., cannot be found. Rather some specific cases must be considered.

One of the most important cases (because it frequently occurs in practice) is that of uniform noise background. For this case $B(\theta',\phi')$ becomes a constant and can be taken outside the integral sign. In addition maximum SNR will occur for this case when all the signal components are added coherently at the output, i.e., when

$$(11)\qquad \psi_1(\theta_o,\phi_o) + \phi_1 = \psi_2(\theta_o,\phi_o) + \phi_2 = \psi_3(\theta_o,\phi_o) + \phi_3 = \cdots$$

or

$$\psi_i(\theta_o,\phi_o) + \phi_i = \text{constant.}$$

Equation (10) can then be written in a much simpler form as

$$(12) \qquad \frac{S_o}{N_o} = \frac{\left(\sum_{i=1}^{N} A_i V_i(\theta_o,\phi_o)\right)^2}{\sum_{i=1}^{N} A_i^2 N_i + B \sum \sum A_m A_n C_{mn}}$$

where $C_{mn} = \iint V^u(\theta',\phi') V^u(\theta',\phi')$ Real $\left[e^{j(\phi_m-\phi_n+\psi_m(\theta',\phi')-\psi_n(\theta',\phi')}\right] d\Omega$

or $\quad C_{mn} = C_{nm} = \iint V_m^u(\theta',\phi') V_n^u(\theta',\phi') \cos(\phi_m-\phi_n+\psi_m(\theta',\phi')-\psi_m(\theta',\phi')) d\Omega$

To find the amplitude of the optimum weighting coefficients the partial derivative of Eq. (12) with respect to A_i is equated to zero yielding for the ith component

$$(13) \quad A_i \frac{N_i}{V_i} + \frac{B}{V_i} \sum_{r=1}^{N} A_n C_{ir} = \frac{\sum_i A_i^2 N_i + B \sum_m \sum_n A_m A_n C_{mn}}{\sum A_i V_i}$$

or the following system of N equations

$$(14) \quad \begin{aligned}
&A_1 \frac{N_1}{V_1(\theta_o,\phi_o)} + \frac{B}{V_1(\theta_o,\phi_o)} (A_1 C_{11} + A_2 C_{12} + A_3 C_{13} + \cdots) = K \\
&A_2 \frac{N_2}{V_2(\theta_o,\phi_o)} + \frac{B}{V_2(\theta_o,\phi_o)} (A_1 C_{21} + A_2 C_{22} + A_3 C_{23} + \cdots) = K \\
&A_3 \frac{N_3}{V_3(\theta_o,\phi_o)} + \frac{B}{V_3(\theta_o,\phi_o)} (A_1 C_{31} + A_2 C_{32} + A_3 C_{33} + \cdots) = K \\
&\cdots \\
&\cdots
\end{aligned}$$

where $$K = \frac{\sum A_i^2 N_i + B \sum \sum A_m A_n C_{mn}}{\sum A_i V_i}$$

Since only the relative values of A_i can be determined (i.e., multiplying all the A_i's by a constant will not change the SNR) the above system of equations can be solved. Alternatively the equations can be written more compactly in matrix notation as

(15) $$\left[[N] + B[C]\right][A] = K[V]$$

where

$$[A] = \begin{bmatrix} A_1 \\ A_2 \\ A_3 \end{bmatrix}$$ a column matrix

$$[V] = \begin{bmatrix} V_1(\theta_o,\phi_o) \\ V_2(\theta_o,\phi_o) \\ V_3(\theta_o,\phi_o) \\ \vdots \end{bmatrix}$$

$$[C] = \begin{bmatrix} C_{11} & C_{12} & C_{13} & \cdots \\ C_{21} & C_{22} & C_{23} & \cdots \\ C_{31} & C_{32} & C_{33} & \cdots \end{bmatrix}$$ a symmetric square matrix

$$[N] = \begin{bmatrix} N_1 & 0 & 0 & \cdots \\ 0 & N_2 & 0 & \cdots \\ 0 & 0 & N_3 & \cdots \end{bmatrix}$$ a diagonal matrix

Hence the formal solution of weighting values which maximize SNR for uniform background antenna noise is

(16) $$[A] = K\left[[N] + B[C]\right]^{-1}[V]$$ provided the inverse exists

D. Dipole Array Model

In order to quantitatively study the optimization of SNR a particular antenna array model was selected for analysis, namely, a linear array of half-wavelength dipoles placed a quarter-wavelength over a ground plane. This choice of study model was made for two reasons. First it is an antenna array commonly used in practice, and secondly it lends itself to mathematical analysis quite well.

For this model the assumption of uniform background noise is quite reasonable. For example, Fig. 2 shows the pattern of a single dipole element in the H-plane. In the E-plane the pattern is even more narrow so that the antenna collects nearly all of its power from a sector of space within $\pm 70^{o}$ from zenith. Figure A2 in Appendix I shows that at microwave frequencies the sky noise remains fairly constant over this sector. In addition the magnitude of background noise will be much less than the noise generated by the electronic components. For example a typical value of antenna temperature will be of the order of $10^{o}K$ while the effective noise temperature of say a transistor amplifier will be of the order of $300^{o}K$ (3 dB noise figure). The noise power is related to effective temperature by

$$P = kT_{eff}\,\Delta f$$

Thus for this particular model the noise from the array's environment is much less than from internally generated contributions.

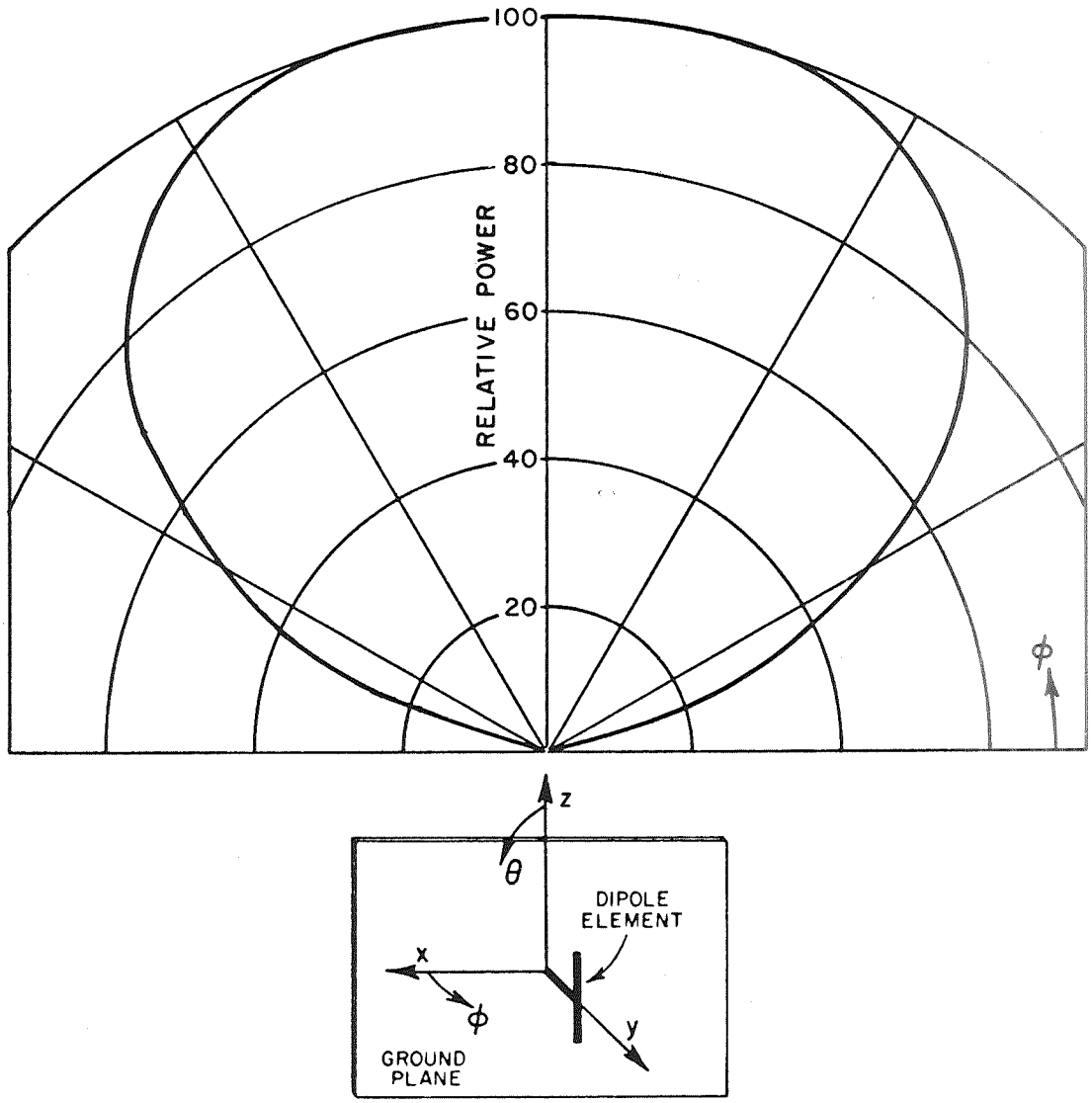

Fig. 2--Power pattern of 0.5λ dipole placed 0.25λ over ground plane ($\theta = 90^{o}$).

For this condition Eq. (16) yields

(17) $$[A] = K[N]^{-1}[V]$$

or

$$A_1 = K \frac{V_1}{N_1}$$

$$A_2 = K \frac{V_2}{N_2}$$
$$\vdots$$

That is, when the noise in each channel is uncorrelated each weighting coefficient should be made proportional to the rms value of signal voltage in that channel and inversely proportional to the noise power in the channel. It is interesting to point out that this particular example is analogous to the "optimum combiner" studied by others[9]. The corresponding value of optimum SNR is easily found from Eq. (17) as

$$\frac{S_o}{N_o} = \sum_{i=1}^{N} \frac{V_i^2}{N_i} = \frac{V_1^2}{N_1} + \frac{V_2^2}{N_2} + \cdots \tag{18}$$

or the optimum output SNR is simply the sum of the SNR's in each channel.

In order to evaluate the actual weighting coefficients and determine the optimum value of SNR it is necessary to calculate the voltage induced at each element due to an incident plane wave signal generated by some distant transmitter. A convenient method of analysis for this problem is the Z-parameter technique commonly used in circuit theory.* Figure 3 shows a transmitting antenna and an N element receiving array. Since everything inside the dotted line is linear, passive, and bilateral, the terminal voltages and currents at each terminal can be represented by a system of N + 1 linear equations of the form

*One of the first to use this approach for antenna problems was Silver in his book Microwave Antenna Theory and Design, Radiation Laboratory Series - McGraw Hill.

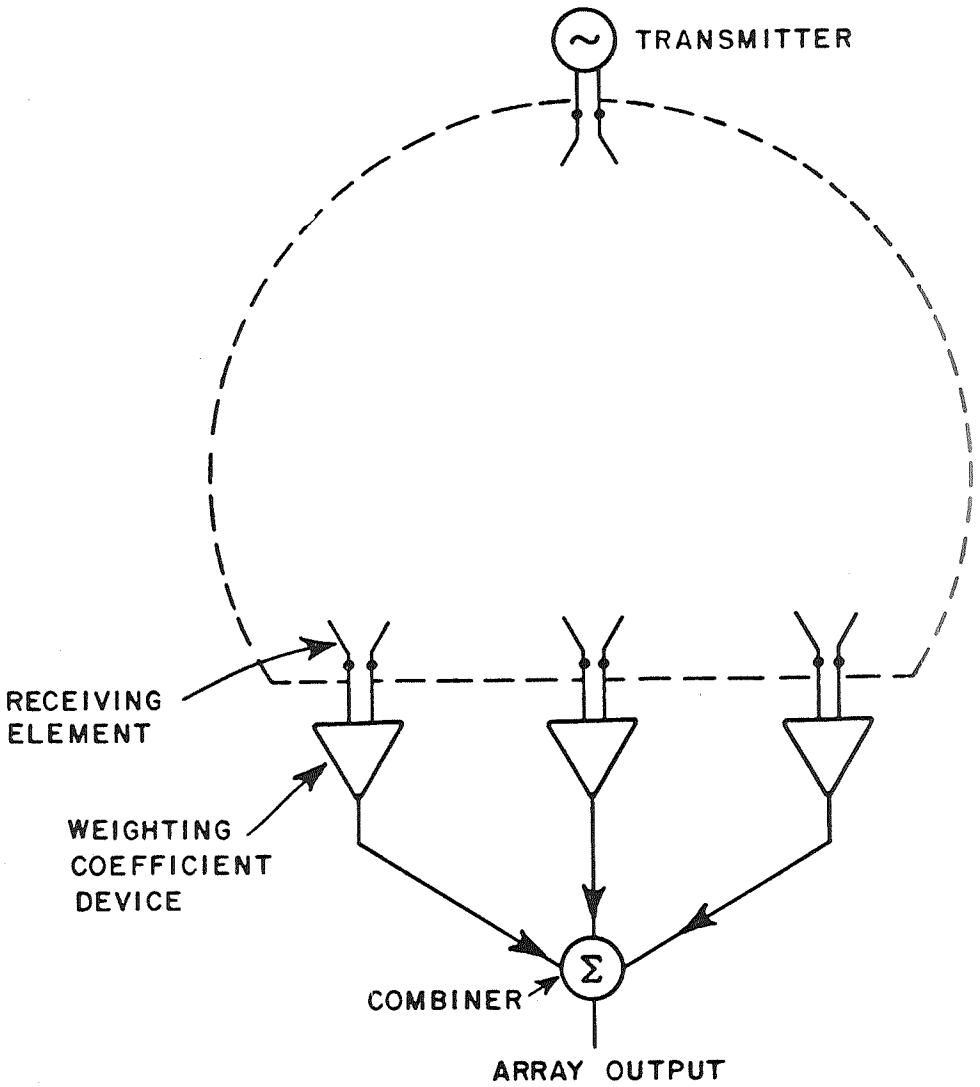

Fig. 3--Transmitter-receiver geometry.

$$
\begin{aligned}
v_0 &= Z_{00}I_0 + Z_{01}I_1 + Z_{02}I_2 + \cdots = -Z_{L1}I_0 \\
v_1 &= Z_{10}I_0 + Z_{11}I_1 + \cdots \qquad\quad = -Z_{L2}I_1 \qquad (19) \\
v_2 &= Z_{20}I_0 + Z_{21}I_1 + \cdots
\end{aligned}
$$

where

v_o = terminal voltage of transmitter

$v_i (i=1,N)$ = terminal voltage of the ith receiving element

$Z_{mn} = Z_{nm}$ mutual impedance between element m and n

z_{nn} = self impedance of the nth element with all other elements open circuited

Z_{Li} = load impedance at ith terminals

An alternate set of equations which completely describe the properties of a receiving array when a plane wave is incident on it can be expressed as:

$$\begin{aligned} v_1 &= V_1^{OC} + Z_{11}I_1 + Z_{12}I_2 + \cdots \\ v_2 &= V_2^{OC} + Z_{21}I_1 + \cdots \\ &\vdots \end{aligned} \tag{20}$$

where

V_i^{OC} is the open circuit voltage at terminals i with all other receiving elements also open circuited.

Note that the voltages and currents depend on the angle of arrival ($v_i(\theta_o)$, $V_i^{OC}(\theta_o)$, $I_i(\theta_o)$) of the incident plane wave and load impedance but the mutual impedances, or Z-parameters, are fixed constants for a given frequency and array geometry (element spacing, height over ground plane, etc.). Once the set of Z-parameters and open circuit voltages have been determined (see Appendix IV) it is possible to calculate the output SNR for all conditions of load impedance, scan angle, channel noise figure, weighting coefficient, etc.

Due to mutual coupling effects the terminal currents (and hence the voltages) and SNR in each channel will differ from element to element. For example Fig. 4 shows this variation of terminal currents, and Fig. 5 shows the variation of SNR for the case of equal channel noise in a 4 element array with 0.5λ spacing. It can be seen that 4 dB variations may exist between elements. Hence according to Eq. (17), it is necessary to adjust both the magnitude and phase of each weighting coefficient in order to achieve the optimum output SNR. It is interesting to note however that this optimum condition is only slightly better than simple coherent combination (adding the signals together in-phase without regard for amplitude). Figure 6 compares the optimum value of output SNR vs θ with that obtained by this uniform amplitude - inphase case. It can be seen that the improvement is typically less than 0.1 dB. This result is quite important because it shows that the considerably more complex system hardware required to achieve optimum SNR yields very little improvement over a relatively simple system (e.g., a phase lock scheme).

As the interelement spacing decreases the mutual coupling effects become more significant. For example Fig. 7 shows the variations in terminal currents as the angle of arrival changes when the element spacing is $.1\lambda$; Fig. 8 shows the corresponding variations of SNR in each channel. Even for this extreme case there is still little difference between optimum combining and uniform amplitude coherent combining (see Fig. 9).

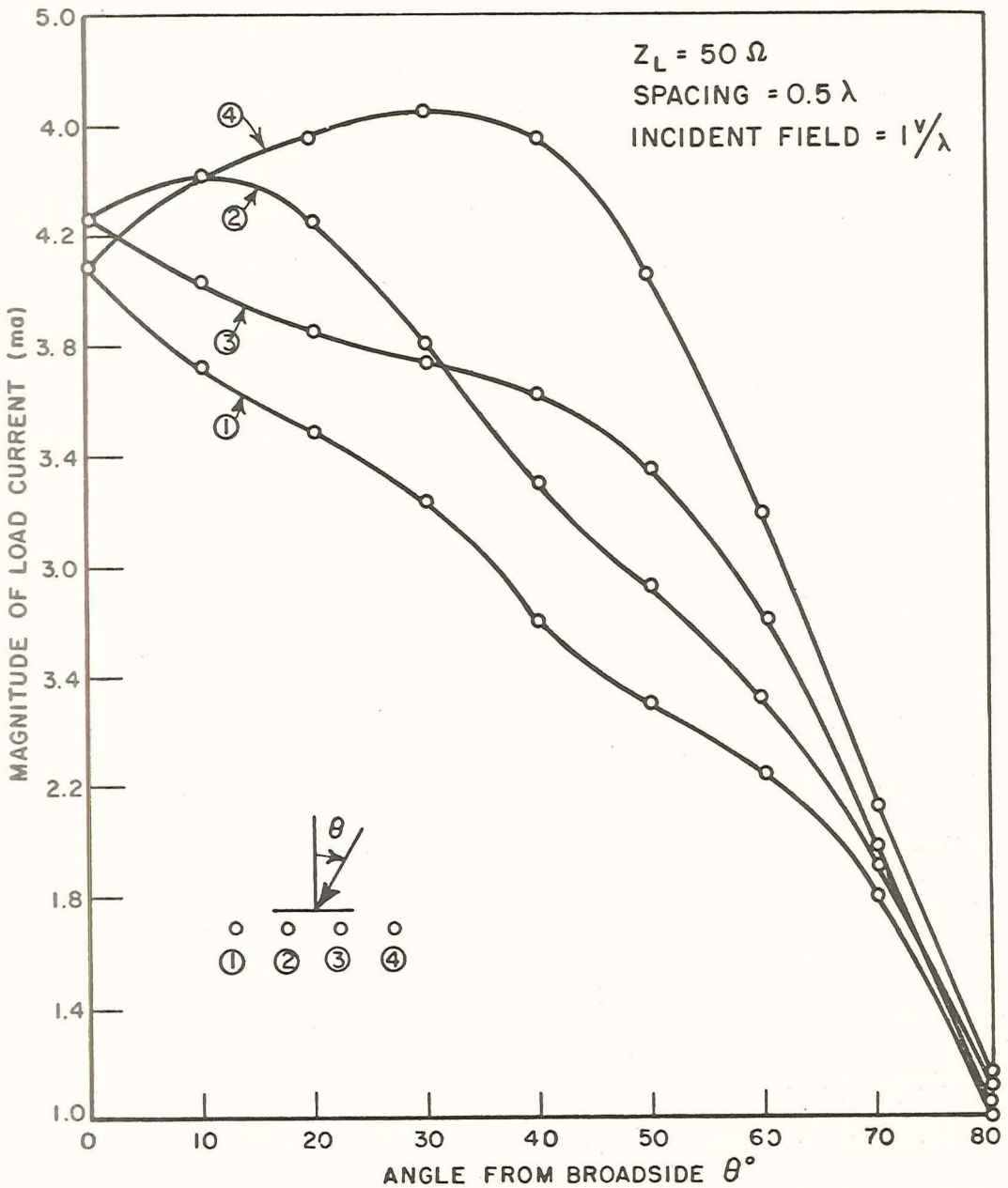

Fig. 4--Magnitude of element load currents vs angle of arrival.

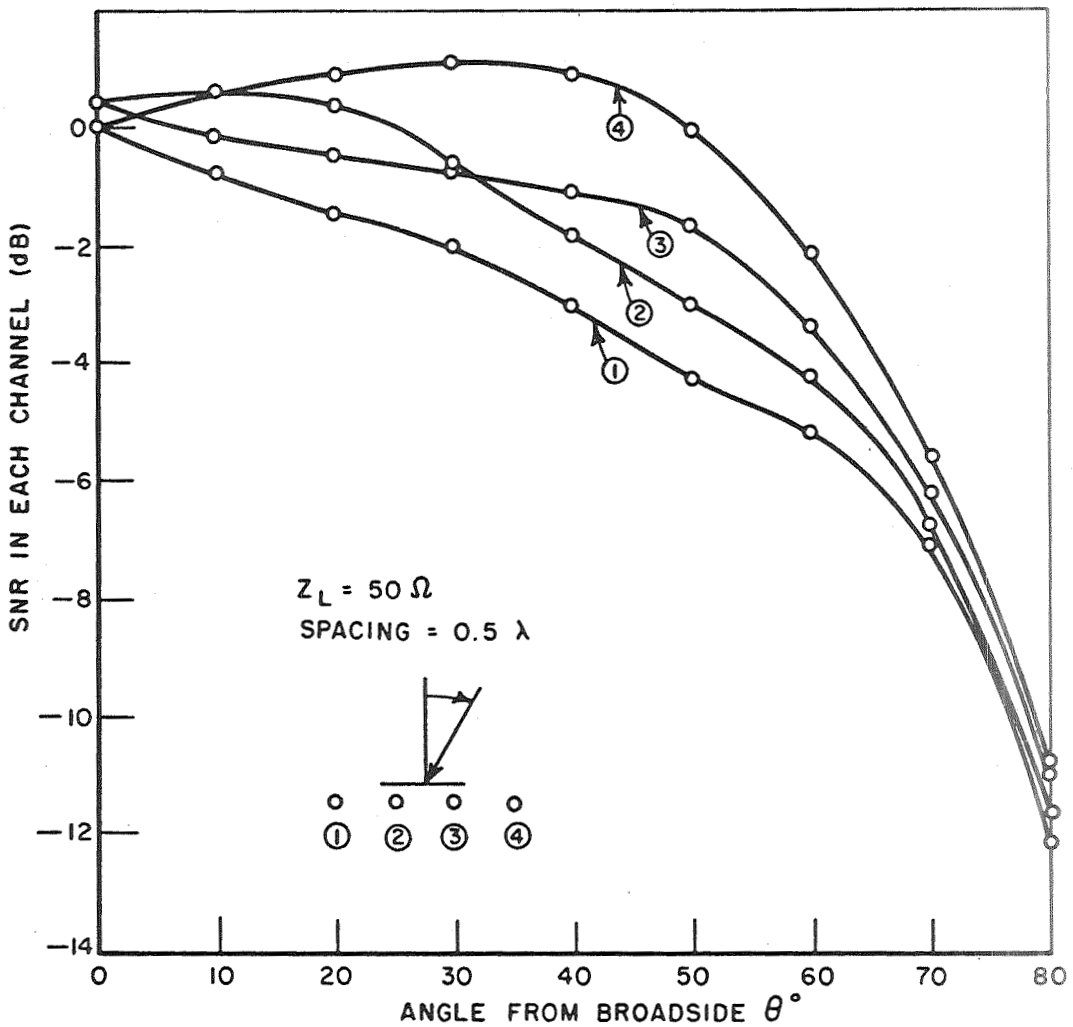

Fig. 5--Comparison of the SNR in each channel vs angle of arrival.

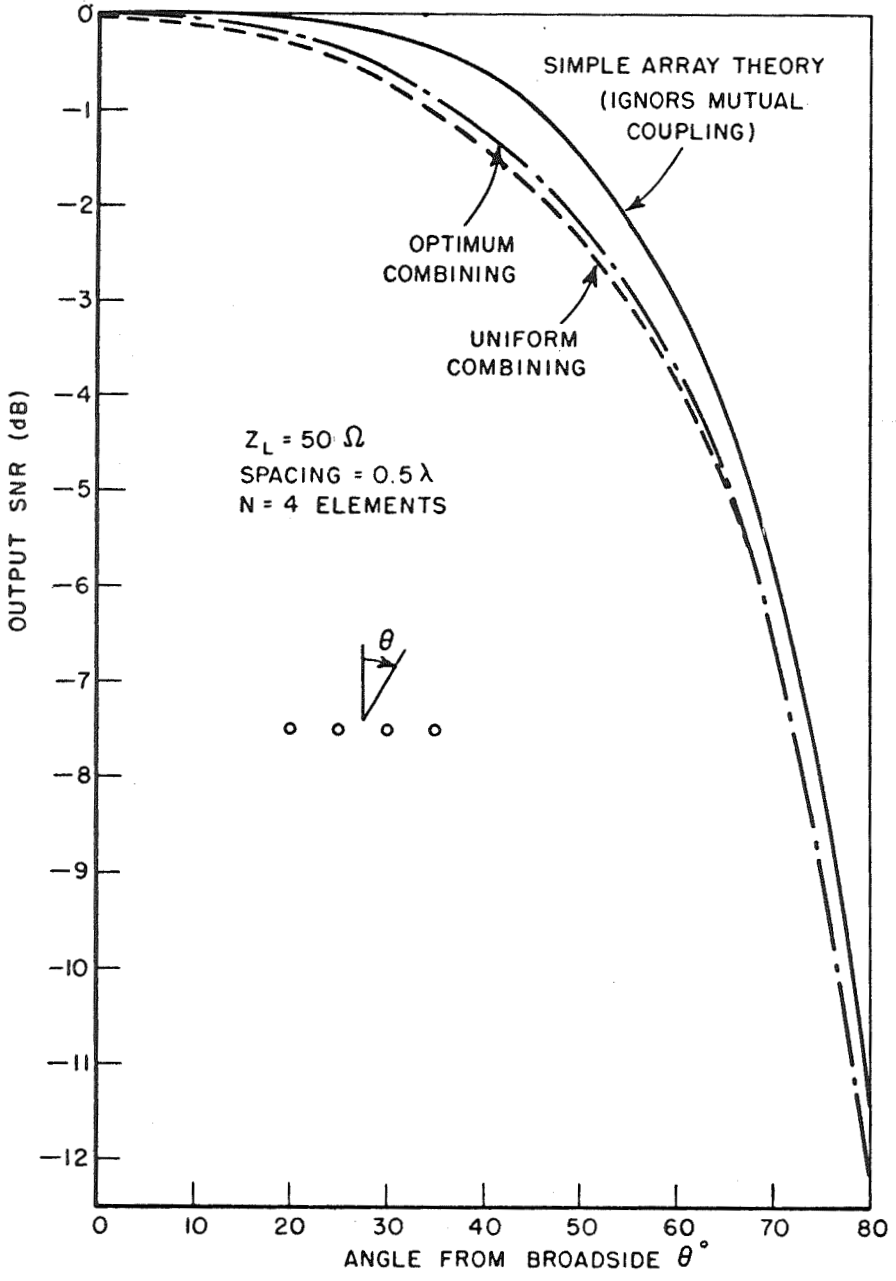

Fig. 6--Variation in output SNR vs angle of arrival.

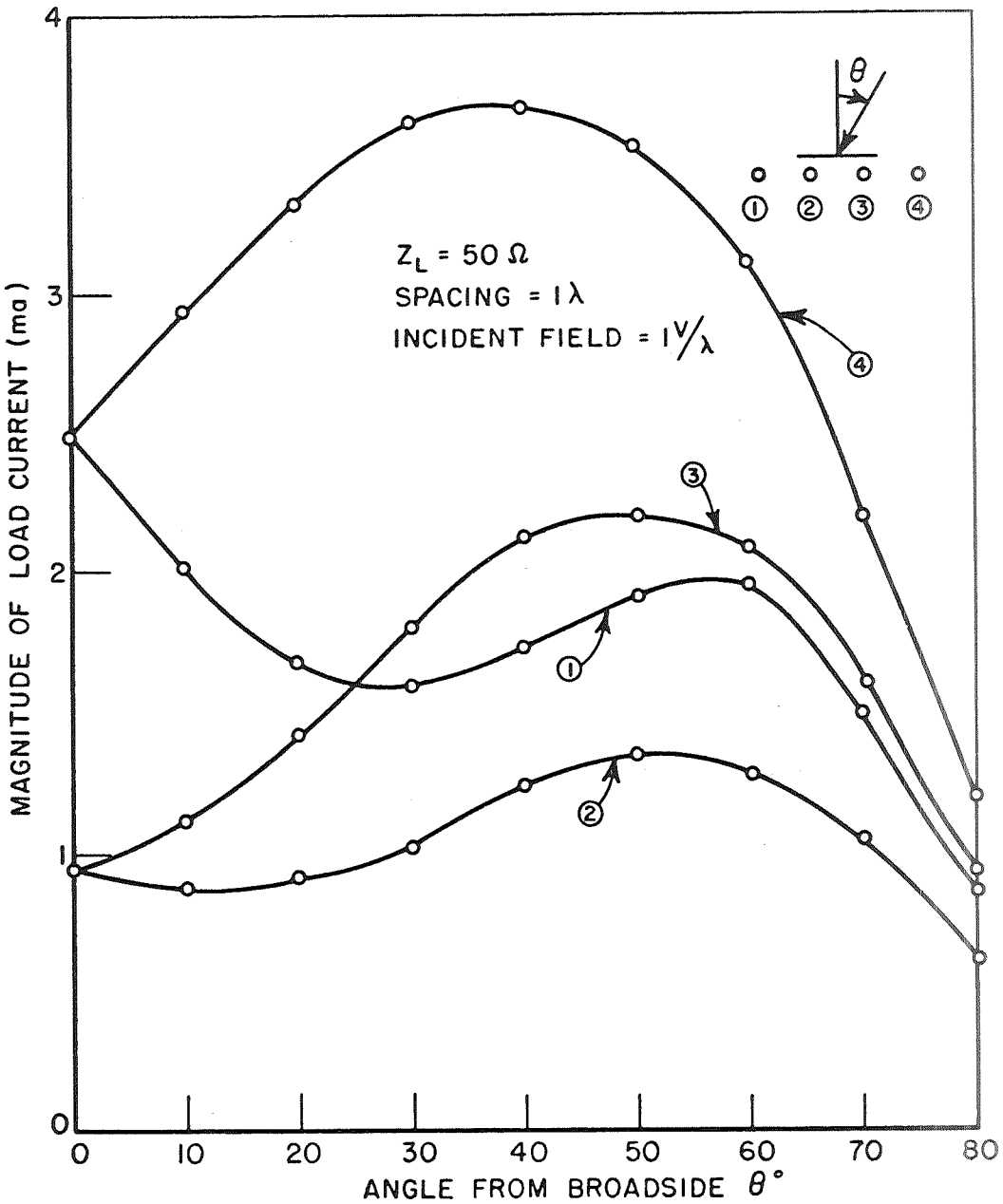

Fig. 7--Magnitude of element load currents vs angle of arrival.

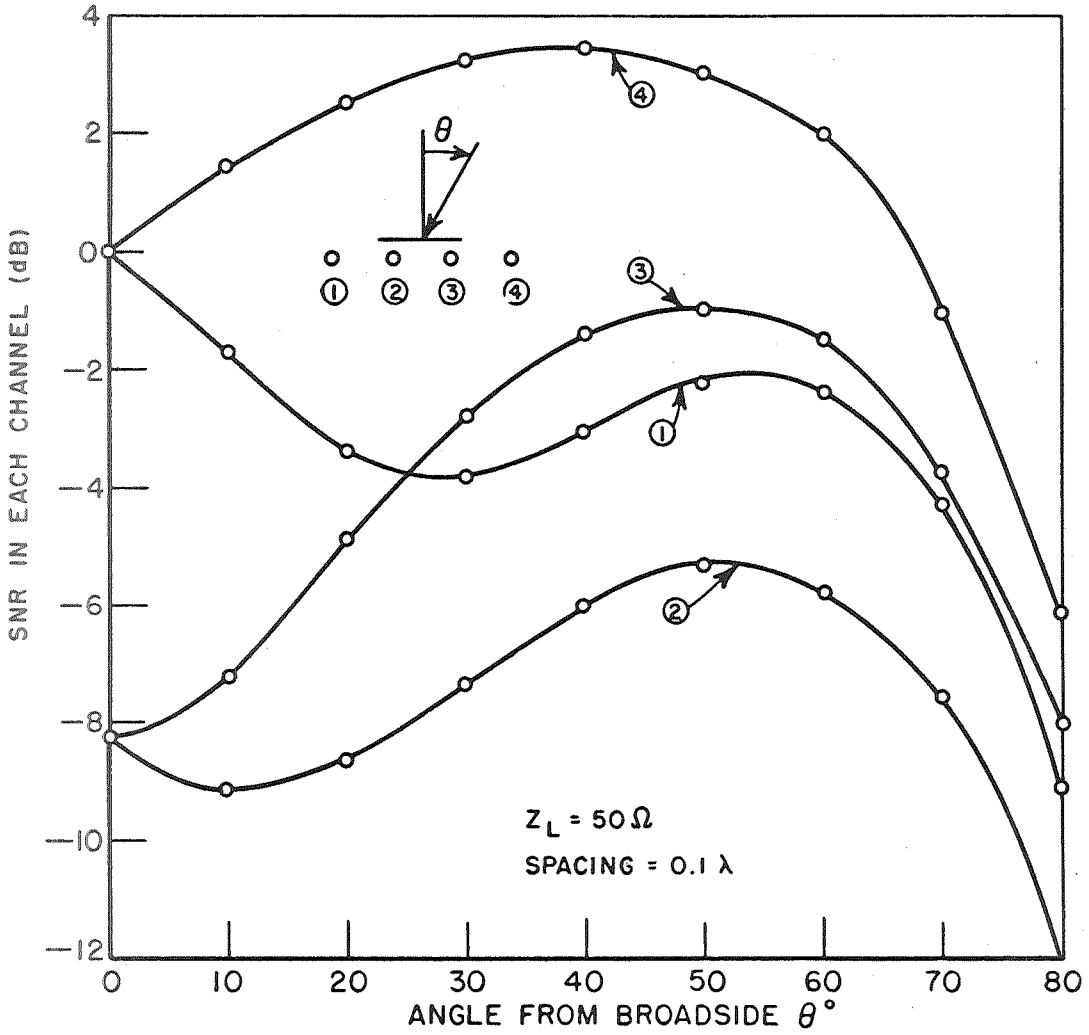

Fig. 8--Comparison of the SNR in each channel vs angle of arrival.

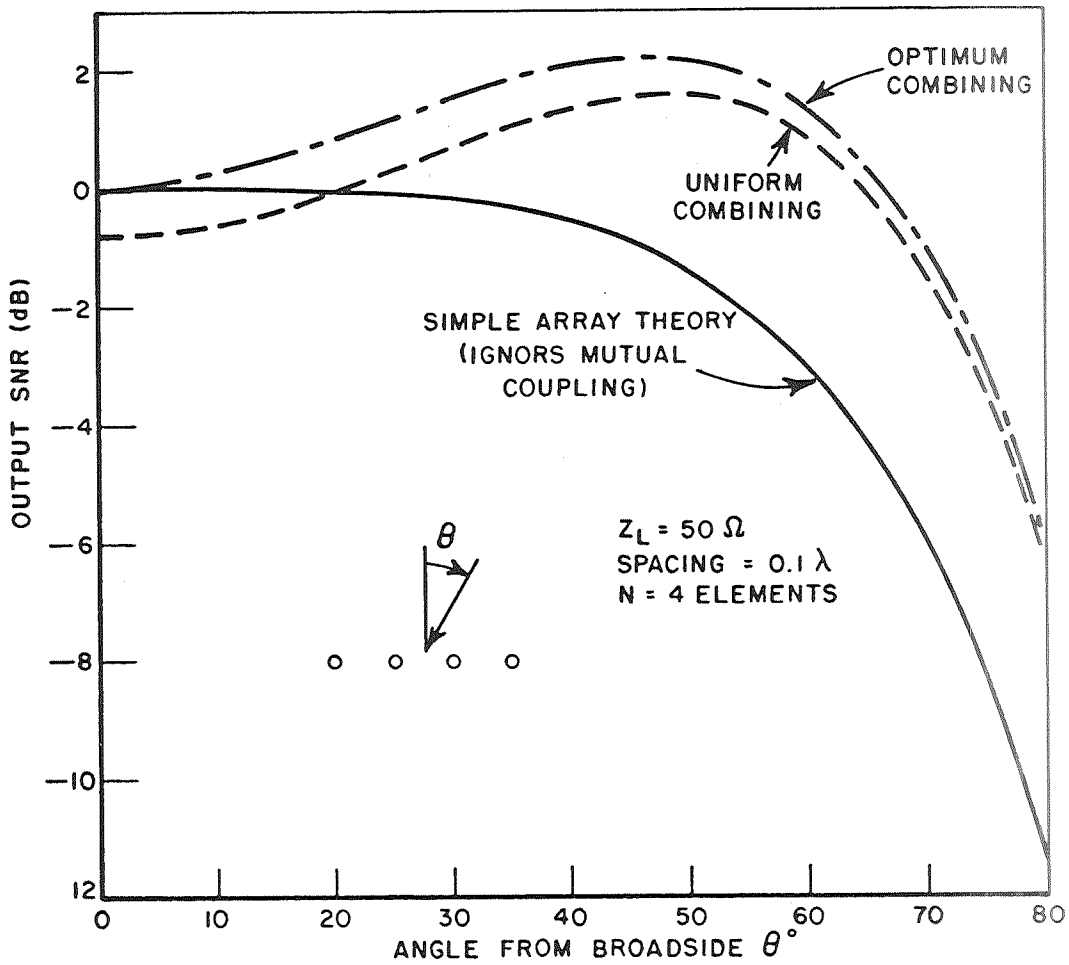

Fig. 9--Variation in output SNR vs angle of arrival.

As the number of elements increases the difference in SNR between these two processing schemes become less and less. This was verified by studying a 10 element array. In fact Floquets theorem can be used to show that this difference goes to zero as the number of elements becomes infinite.

The SNR curves shown in Fig. 6 and 9 have both been normalized to 0 dB at broadside since it was only intended to show degradation in SNR as the array was scanned. Actually for the particular load impedance case shown (50Ω) the broadside SNR for 0.1λ spacing was 6.9 dB below that for 0.5λ spacing. For a higher load termination of 10 KΩ there was essentially no difference in SNR from 10λ spacing to 0.1λ spacing, indicating very little structural scattering existed for the dipole array.

CHAPTER III
OPTIMIZATION FOR COHERENT INTERFERENCE

In the previous chapter the weighting coefficients which optimized output SNR were determined for an array operating in a uniform background noise environment with internally generated noise contributions. The array could be made adaptive by incorporating a phase lock loop to automatically set the phase, and feedback gain control to set the amplitude of each weight. In this chapter an adaptive array capable of rejecting coherent interference is discussed. This interference could be from unintentional sources, for example from nearby systems which just happen to be using the same frequency, or from hostile jamming sources.

The basic form of the adaptive array is shown in Fig. 10. The voltage at the terminals of each element is passed through a weighting device, for example an amplifier with controllable gain and phase. The weighted outputs of each element are then added to produce the array output $S(t)$. To make the array adaptive, $S(t)$ is compared with a reference signal $R(t)$, and the difference, the error signal $\varepsilon(t)$, forms the input to a feedback system that controls the weights w_i. The feedback is designed to adjust the weights so the mean-square value of $\varepsilon(t)$

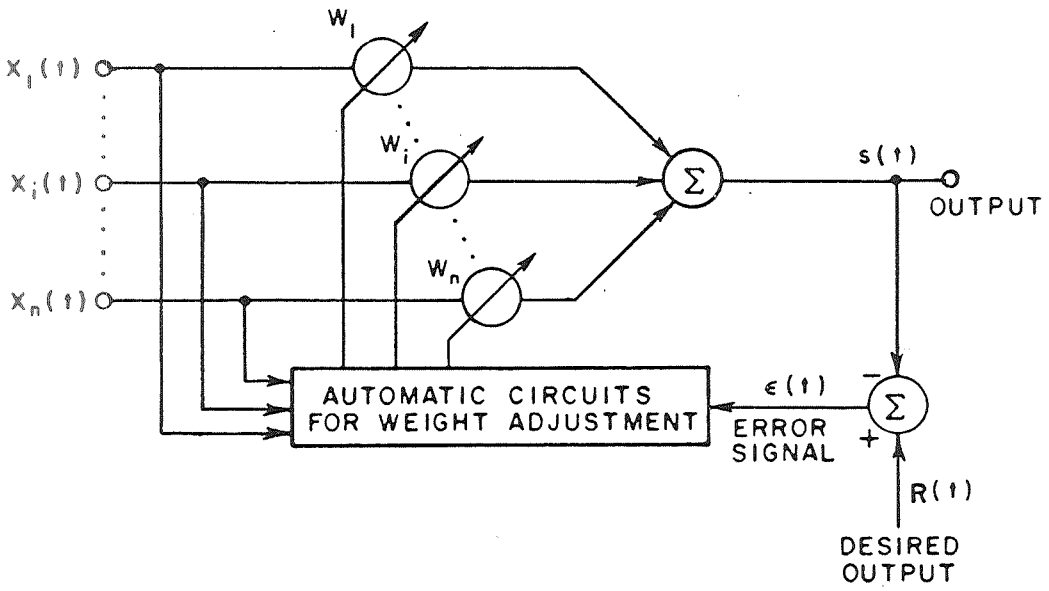

Fig. 10--Basic adaptive feedback system.

is minimized. This has the effect of forcing the output of the array S(t) to approximate the reference signal R(t) as closely as possible on a mean-square basis. Thus, any received signal that is not represented in R(t) appears as an error signal, and the feedback adjusts the weights to remove it from the output. The result, in antenna parlance, is a pattern null in the direction from which this signal comes. If the received signal is represented in R(t), the feedback retains this signal in the output (with amplitude and phase the same as R(t)). Thus, one can discriminate between "desired" and "undesired" signals (e.g., between a desired communication signal and an interfering signal) by means of what is used for the reference signal R(t).

The feedback concept discussed above was suggested by Widrow, et al.[8]. The work described here differs from their work, however, in several respects. First, we are interested mainly in the problem of interference rejection in radio communications. To treat this problem realistically, it must be assumed that the desired signal contains modulation components that are unknown at the receiver. Hence the reference signal R(t) cannot be made exactly equal to the desired signal, but can only approximate it in some sense. Some experiments in which the desired signal contains modulation components not present on the reference signal are described in Chapter IV. Widrow, et al. treat the case where the desired signal is known exactly at the receiver, so an exact replica can be used for the reference R(t). Second, the feedback system discussed here is a continuous, analog system. Widrow, et al., consider a digital, sampled-data feedback loop. Although this is only a minor difference, the problems of feedback loop stability, which are discussed in some detail in[8], arise only with a sampled loop. A continuous loop, based on the feedback algorithm discussed below, is stable for all gain settings. Third, the work reported here contains considerable experimental results, whereas the work in[8] is theoretical.

A. The LMS Feedback Algorithm

Assume for the moment that the weighting coefficients w_1, $\cdots$, w_N shown in Fig. 10 are real. That is, we ignore the possibility of varying the phase of each element. This represents no loss of generality since phase control can also be achieved with two real weighting coefficients for each channel. This will be discussed in more detail later on. The array output may then be written

$$(21) \qquad s(t) = \sum_{i=1}^{N} w_i x_i(t).$$

The error signal is

$$(22) \qquad \varepsilon(t) = R(t) - \sum_{i=1}^{N} w_i x_i(t),$$

and hence the squared error is

$$(23) \qquad \varepsilon^2(t) = R^2(t) - 2T(t) \sum_{i=1}^{N} w_i x_i(t) + \sum_{i=1}^{N} \sum_{j=1}^{N} w_i w_j x_i(t) x_j(t).$$

The mean-square error is thus:

$$(24) \qquad \overline{\varepsilon^2(t)} = \overline{R^2(t)} - 2 \sum_{i=1}^{N} w_i \, \overline{R(t) x_i(t)} + \sum_{i=1}^{N} \sum_{j=1}^{N} w_i w_j(t) \overline{x_i(t) x_j(t)}$$

where the bar indicates the time average. Equation (24) may be written more conveniently in matrix form as

$$(25) \qquad \overline{\varepsilon^2(t)} = \overline{R^2(t)} - 2W^T \Phi(x,R) + W^T \Phi(x,x) W$$

where w and (x,R) are column matrices,

$$W = \begin{pmatrix} w_1 \\ w_2 \\ \cdot \\ \cdot \\ \cdot \\ w_N \end{pmatrix}, \tag{26}$$

$$(x,R) = \begin{pmatrix} \overline{x_1(t)\ R(t)} \\ \overline{x_2(t)\ R(t)} \\ \cdot \\ \cdot \\ \cdot \\ \overline{x_N(t)\ R(t)} \end{pmatrix}, \tag{27}$$

(x,x) is an N x N matrix,

$$(x,x) = \begin{pmatrix} \overline{x_1(t)\ x_1(t)} & \overline{x_1(t)\ x_2(t)} & \cdots & \overline{x_1(t)\ x_N(t)} \\ \overline{x_2(t)\ x_1(t)} & & & \cdot \\ \cdot & & & \cdot \\ \cdot & & & \cdot \\ \cdot & & & \cdot \\ \overline{x_N(t)\ x_1(t)} & \cdots & & \overline{x_N(t)\ x_N(t)} \end{pmatrix} \tag{28}$$

and W^T denotes the transpose of W.

It may be seen from Eq. (24) or (25) that $\overline{\varepsilon^2(t)}$ is a quadratic function of the weights. Thus, if it is assumed that $\overline{x_i(t)\ x_j(t)}$ and $\overline{x_i(t)\ R(t)}$ are constant, the surface obtained by plotting $\overline{\varepsilon^2(t)}$ versus

the weights is a bowl-shaped surface, as illustrated in Fig. 11 for the case of two weights. (The case where $\overline{x_i(t)\, x_j(t)}$ and $\overline{x_i(t)\, R(t)}$ change with time* may be viewed as a motion of the bowl.) The quadratic nature of Eq. (24) is important, because it indicates that the bowl has a well-defined minimum, and furthermore it has only one minimum. Thus, saddle-points or relative minima are not possible.

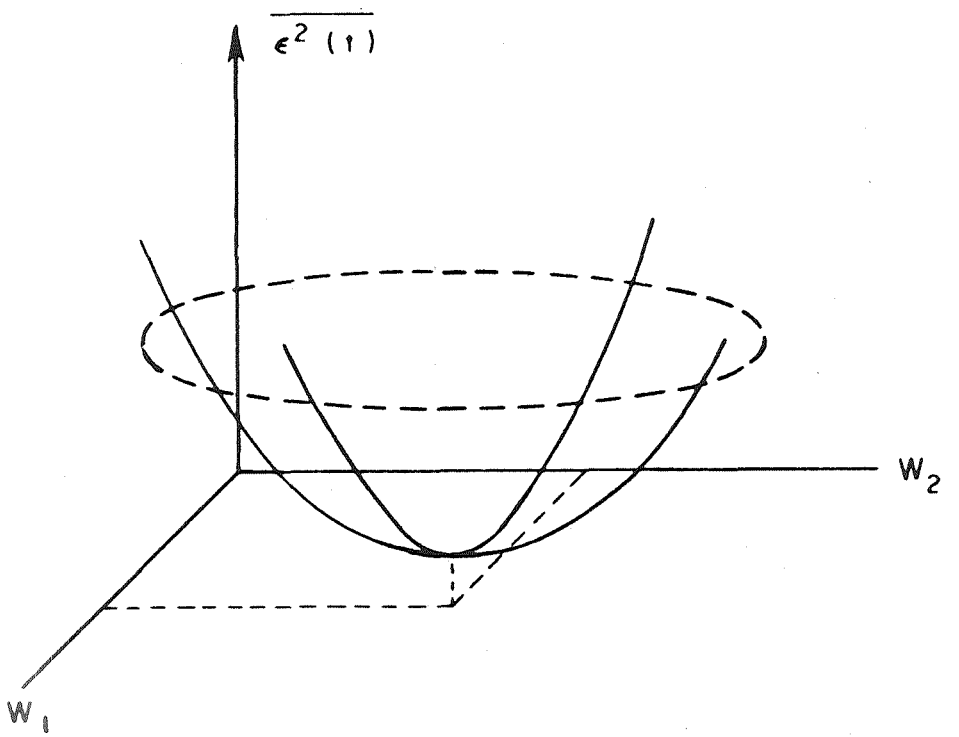

Fig. 11--The error surface.

*These time averages are understood to be taken over an interval long compared with the fluctuations of $x_i(t)$ and $R(t)$, but still finite, so gradual changes in the characteristics of the signals result in time-changing averages.

It is clear on physical grounds that the extremum of the bowl is a minimum, not a maximum, since the error can be made arbitrarily large by a suitable setting of the weights. The value of the weight vector giving minimum $\overline{\varepsilon^2(t)}$, denoted by $w_{opt.}$, may be found by setting

$$\nabla_w(\overline{\varepsilon^2}) = 0, \tag{29}$$

where ∇_w denotes the gradient with respect to w. Since

$$\nabla_w(\overline{\varepsilon^2}) = -2\Phi(x,R) + 2\Phi\ (x,x)\ w, \tag{30}$$

then

$$\Phi(x,x)w_{opt.} = \Phi(x,R) \tag{31}$$

or

$$w_{opt.} = \Phi(x,x)^{-1}\ \Phi(x,R), \tag{32}$$

where it is assumed that $\Phi(x,x)$ is nonsingular so its inverse $\Phi(x,x)^{-1}$ exists. If the weight vector w is set equal to $w_{opt.}$, the resulting minimum mean-square error is found from Eq. (25) to be

$$\overline{\varepsilon^2_{min}} = \overline{R^2(t)} - \Phi^T(x,R)\ \Phi^{-1}(x,x)\ \Phi(x,R). \tag{33}$$

This result may be used to rewrite Eq. (25) in the form

$$\overline{\varepsilon^2(t)} = \overline{\varepsilon^2_{min}} + (w-w_{opt.})^T\ \Phi(x,x)\ (w-w_{opt.}), \tag{34}$$

which places the quadratic dependence of $\overline{\varepsilon^2(t)}$ on the weights w_i clearly in evidence. Finally, it may be seen that the "bowl" does not necessarily have its principle axes oriented parallel to the

w_i-axes. A coordinate system whose axes do lie parallel to the principle axes may be defined by the relation:

$$(35) \qquad w - w_{opt.} = R\ell$$

where R is an N x N rotation matrix of elements r_{ij}:

$$(36) \qquad R = \begin{pmatrix} r_{11} & r_{12} & \cdots & r_{1N} \\ \vdots & & & \\ & & & \\ r_{N1} & & \cdots & r_{NN} \end{pmatrix}$$

and ℓ is an N-element column matrix whose elements ℓ_i are the "normal coordinates" of the bowl:

$$(37) \qquad \ell = \begin{pmatrix} \ell_1 \\ \vdots \\ \\ \ell_N \end{pmatrix}$$

Substituting Eq. (35) into Eq. (34) gives

$$(38) \qquad \overline{\varepsilon^2(t)} = \overline{\varepsilon^2_{min}} + \ell^T \left[R^T \Phi(x,x) R\right] \ell$$

and when R is chosen so $R^T \Phi(x,x)R$ is diagonal,

$$(39) \qquad R^T \Phi(x,x) R = \Lambda = \begin{pmatrix} \lambda_1 & 0 & 0 & \cdots \\ 0 & \lambda_2 & 0 & \cdots \\ 0 & 0 & . & \\ . & . & . & \\ . & . & . & \\ . & . & & \lambda_N \end{pmatrix}$$

then the ℓ_i are normal coordinates. Since the $\overline{\varepsilon^2(t)}$ surface has a minimum for $w = w_{opt.}$, the eigenvalues λ_i are nonnegative. The fact that $\lambda_i \geq 0$ may also be shown directly from $\Phi(x,x)$.

The justification for using minimum mean-square error as the criterion for optimizing array performance will now be discussed. In general, the output from the array consists of three types of contributions: a desired signal, an undesired interfering signal, and random noise. One may write

$$S(t) = \alpha S_d(t) + \beta S_u(t) + \gamma n(t) \tag{40}$$

where

$S_d(t)$ = a desired signal

$S_u(t)$ = an undesired or interfering signal

$n(t)$ = random noise

and where α, β, and γ are constants representing the combined effect of the weights w_i on these signals. Assume for the moment that the waveform of the desired signal is known exactly at the receiver. Then if the reference signal $R(t)$ is set equal to a replica of the desired signal,

$$R(t) = S_d(t) \tag{41}$$

the error signal becomes

$$\varepsilon(t) = R(t) - S(t) = (1-\alpha)\, S_d(t) - [\beta S_u(t) + \gamma n(t)] \tag{42}$$

where the terms $S_d(t)$, $S_u(t)$ and $n(t)$ are assumed uncorrelated, so the cross-product terms, such as $\overline{S_d(t)\ S_u(t)}$, are zero. Thus, to minimize $\overline{\varepsilon^2(t)}$, the sum of $(1-\alpha)^2\ \overline{S_d^2(t)}$ and $\beta^2\ S_u^2(t) + \gamma^2\ n^2(t)$ must be minimized. In general terms, this quantity will be minimum if α is nearly unity and β^2 and γ^2 are as small as possible. But this condition is constraining the power in the desired signal to be constant. Stated another way, minimizing $\overline{\varepsilon^2}$ is equivalent to maximizing the signal-to-noise ratio, where "noise" is interpreted as including the interference.

This argument, although generally correct, does overlook certain limitations. First, in practice one cannot set $R(t) = S_d(t)$ because the exact form of the desired signal is unknown at the receiver. However, in many cases $R(t)$ can be made to approximate $S_d(t)$ in some sense. For example, when $S_d(t)$ is a signal with amplitude modulation, it is possible to use the carrier component of $S_d(t)$ for $R(t)$ and still obtain suitable operation (as will be seen in the experiments described later). The presence of the sideband components in $S_d(t)$ increases the minimum mean-square error $\overline{\varepsilon^2_{min}}$, but minimizing $\overline{\varepsilon^2}$ still corresponds to maximizing signal-to-noise ratio.

A second limitation is that the above arguments may be oversimplified for very low signal-to-noise ratios in the elements. At low SNR's, the array may not tend to constrain $\alpha \cong 1$, if the $S_d(t)$ term contributes only negligibly to $\varepsilon^2(t)$. Thus for low SNR conditions, minimum $\overline{\varepsilon^2}$ may no longer correspond to maximum SNR. However, for most cases, minimizing $\overline{\varepsilon^2}$ is equivalent to maximizing SNR.

B. Relationship between SNR and LMS Error

Using the above definition of noise it is possible to obtain an expression for SNR when the weighting coefficients are adjusted to yield minimum squared error. Again let the total voltage X_i which appears at the input of the ith amplifier consist of three components,

$$X^i = X_d^i + X_u^i + X_n^i$$

where X_d^i = desired component in the ith channel

X_u^i = undesired component in the ith channel

X_n^i = random noise in ith channel

or in matrix notation

(44) $$[X]=[X_d]+[X_u]+[X_n]$$

where

$$[X]=\begin{bmatrix} X^1 \\ X^2 \\ X^3 \end{bmatrix}$$ a column matrix

$$[X_d]=\begin{bmatrix} X_d^1 \\ X_d^2 \\ X_d^3 \end{bmatrix}$$

similarly for X_u and X_n.

The total output power is then

$$P_o = \frac{1}{T}\int_0^T \left(\sum_i X^i\right)^2 dt \tag{45}$$

or

$$P_o = W^T \overline{XX^T} W$$

Substituting the expression (Eq. (32)) for W which minimizes mean squared error yields

$$\begin{aligned} P_o &= [\Phi(X,X)\Phi(X,R)]^T \overline{XX^T} [\Phi^{-1}(X,X)\ \Phi(X,R)] \\ &= \Phi^T(X,R)\ \Phi^{-1^T}(X,X)\ \overline{XX^T}\ \Phi^{-1}(X,X)\ \Phi(X,R) \\ &= \Phi^T(X,R)\ \Phi^{-1}(X,X)\ \overline{XX^T}\ \Phi^{-1}(X,X)\ \Phi(X,R) \end{aligned} \tag{46}$$

which contains both signal and noise.

The desired signal component is

$$S_o = \Phi^T(X,R)\ \Phi^{-1}(X,X)\ X_d X_d^T\ \Phi^{-1}(X,X)\ \Phi(X,R). \tag{47}$$

The noise component consisting of both undesired signals plus random noise is

$$N_o = \Phi^T(X,R)\ \Phi^{-1}(X,X)\ (X_u X_u^T + X_n X_n^T)\ \Phi^{-1}(X,X)\ \Phi(X,R) \tag{48}$$

so that the output SNR is given by

$$SNR = \frac{S_o}{N_o} = \frac{\Phi^T(X,R)\ \Phi^{-1}(X,X)\ X_d X_d^T\ \Phi^{-1}(X,X)\ \Phi(X,R)}{\Phi^T(X,R)\ \Phi^{-1}(X,S)(X_u X_u^T + X_n X_n^T)\ \Phi^{-1}(X,X)\ \Phi(X,R)} \tag{49}$$

which can also be expressed in terms of autocorrelation and cross-correlation functions as

$$(50) \quad SNR = \frac{\Phi^T(X,R)\ \Phi^{-1}(X,X)\ \Phi(X_d,X_d)\ \Phi^{-1}(X,X)\ \Phi(X,R)}{\Phi^T(X,R)\ \Phi^{-1}(X,X)(\Phi(X_u,X_u) + \Phi(X_n,X_n))\ \Phi^{-1}(X,X)\ \Phi(X,R)}$$

where

$$\Phi(X_d,X_d) = \begin{pmatrix} \overline{X_d^1 X_d^1} & \overline{X_d^1 X_d^2} & \cdots \\ \overline{X_d^2 X_d^1} & \overline{X_d^2 X_d^2} & \cdots \\ \cdot & \cdot & \cdot \end{pmatrix}$$

Similar relationships are obtained for $\Phi(X_u,X_u)$ and $\Phi(X_n,X_n)$.

Unfortunately Eq. (50) is so formidable it gives little insight into the actual behavior of SNR as a function of the other parameters. In order to quantitatively show the effect of undesired and random noise signals a particular example, namely a two element array, was investigated. For this case (see Fig. 10)

$$(51) \quad \begin{aligned} X_1 &= A\cos(\omega_d t + \phi_1) + B\cos(\omega_u t + \theta_1) + n_1(t) \\ X_2 &= A\sin(\omega_d t + \phi_1) + B\sin(\omega_u t + \theta_1) + n_1(t-\tau) \\ X_3 &= A\cos(\omega_d t + \phi_2) + B\cos(\omega_u t + \theta_2) + n_2(t) \\ X_4 &= A\sin(\omega_d t + \phi_2) + B\sin(\omega_u t + \theta_2) + n_2(t-\tau) \end{aligned}$$

where

X_1, X_3 = direct component of total voltage in element 1 and 2 respectively

X_2, X_4 = quadrature component of total voltage in element 1 and 2 respectively

A, B = amplitude of desired and undesired signal

ϕ_i, θ_i = phase of desired and undesired signal in element i

τ = time delay corresponding to $\lambda/4$ or 90^o at ω_d

The reference signal is assumed to be at the same frequency as the desired signal, i.e., $A_r \cos \omega_d t$.

Four weighting coefficients and four values of X_i are required for a two element array in order to allow both amplitude and phase control. After a considerable amount of matrix algebra the final expression for SNR is then

(52)

$$SNR = \frac{2A^2(C_1 - C_2)^2}{(C_1-C_2)^2[B^2(1+\cos\theta)+2\overline{n^2}]- (C_1-C_2)[2C_3B^2\sin\theta]+C_3[B^2(1-\cos\theta)+2\overline{n^2}]}$$

where

$$C_1 = \frac{A^2}{2} + \frac{B^2}{2} + \overline{n^2}$$

$$C_2 = \frac{A^2}{2} + \frac{B^2}{2} \cos\theta$$

$$C_3 = \frac{B^2}{2} \sin\theta$$

$$\theta = \theta_2 - \theta_1$$

A broadside signal ($\phi_1 = \phi_2$) has been assumed with equal random noise ($\overline{n_1^2} = \overline{n_2^2} = \overline{n^2}$) in each channel.

Figure 12 is a 3 dimensional plot showing the response of output SNR to an undesired signal incident upon the array with variable amplitude and phase parameters. Initially no undesired signal is present (B = 0) and only random noise corresponding to a 10 dB signal

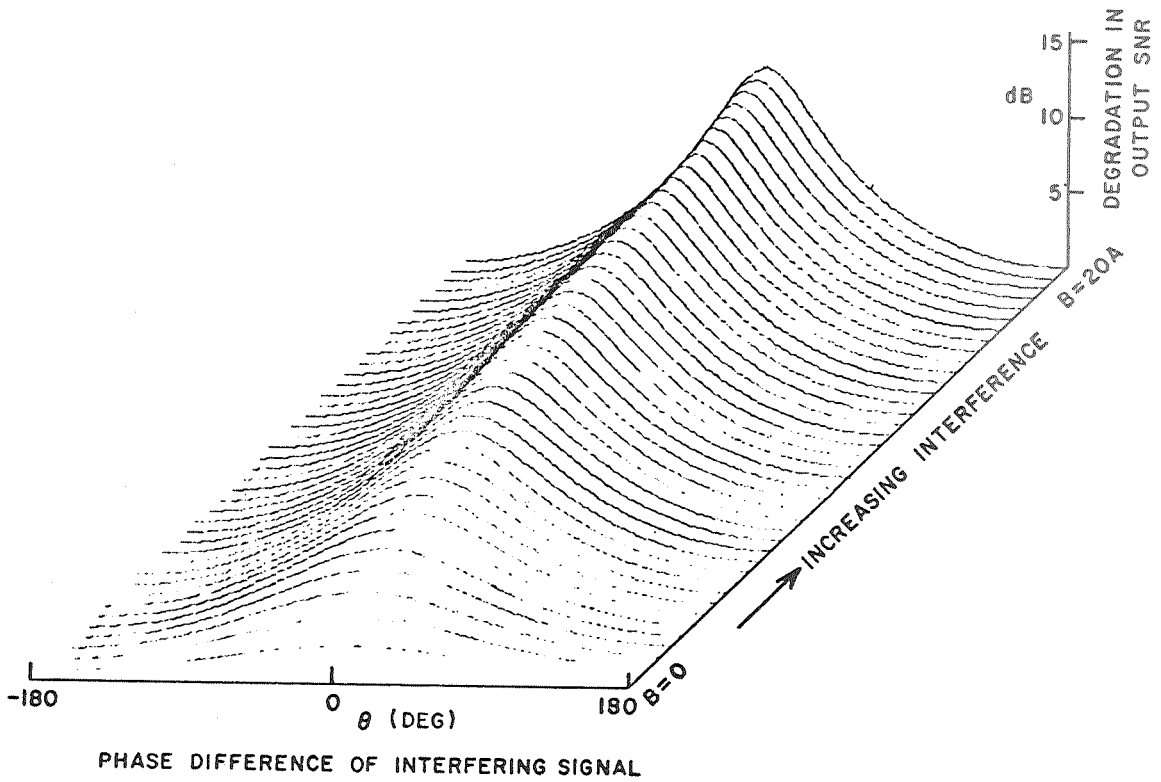

Fig. 12--SNR degradation due to coherent interference (LMS algorithm).

to noise ratio is present in each channel. As the undesired or jamming signal is increased to a value 13 dB higher than the desired signal Fig. 12 shows how this initial SNR condition is degraded. At $\theta = \pm 180^{o}$ (endfire for a $\lambda/2$ spaced array) there is no degradation, i.e., the interference can be completely rejected. At $\theta = 0^{o}$ (broadside condition) no signal processing improvement is possible since the desired signal is also coming from this direction, i.e., rejecting the undesired signal would also reject the desired signal and no improvement would be gained. For

comparison Fig. 13 shows the performance of a conventional phased array (pointed at the desired signal) under the same conditions. It can be seen that the LMS error criteria gives superior performance for all values of θ except 0^0 where no improvement is possible, and $\theta = \pm 180^0$ the particular angle where the phased array has an antenna pattern null in the direction of the interference.

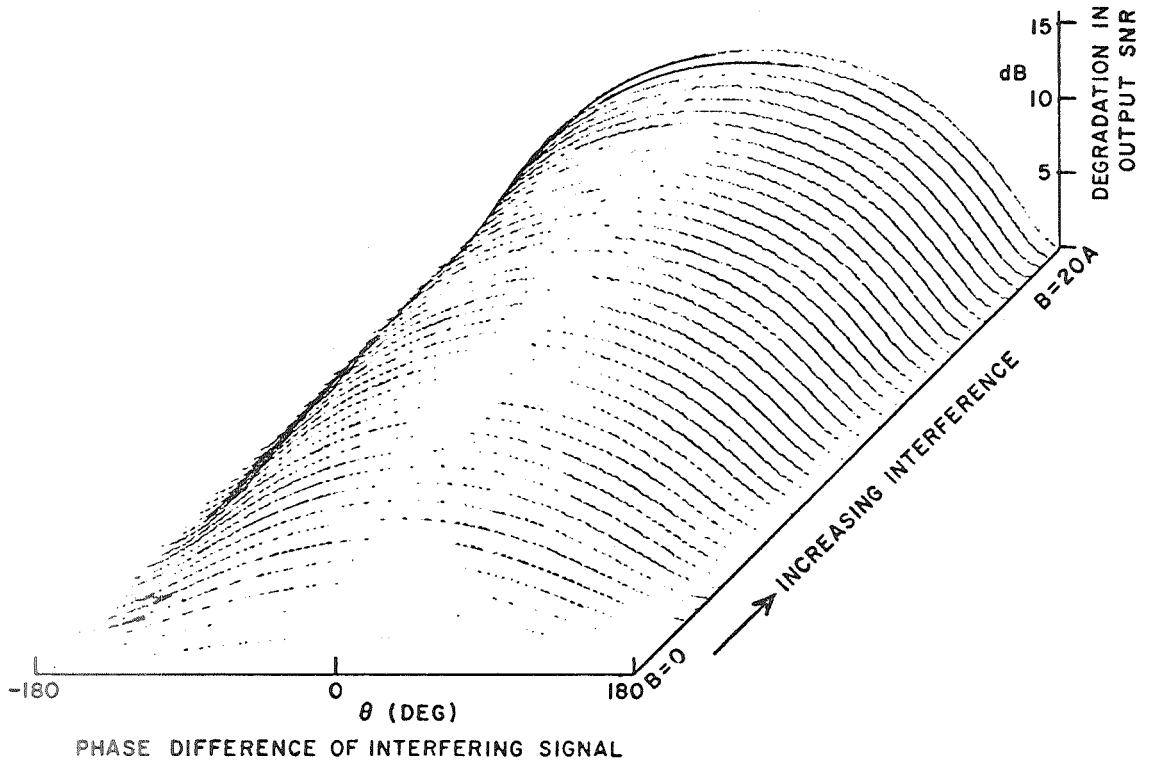

Fig. 13--SNR degradation due to coherent interference (conventional phased array).

C. The Steepest Descent Optimization

Now consider the method by which the weights are to be set equal to their optimum values. One approach is to measure the quantities $\overline{x_i(t)\, x_j(t)}$ and $\overline{x_i(t)\, R(t)}$ for all i,j, and thus determine the matrices $\Phi(x,x)$ and $\Phi(x,R)$. $\phi(x,x)^{-1}$ may then be computed, and the optimum weights evaluated by means of Eq. (32). From a practical standpoint, this approach is not appealing, because of the difficulty in measuring $\Phi(x,x)$ and computing $\Phi^{-1}(x,x)$, especially if the number of elements is large. Furthermore, the object is to build an adaptive array, so that, for example, changes in the angle of arrival of the interfering signal will be automatically "tracked" by the weight settings. To adapt to such changes by the above method would require that the measurement of $\phi(x,x)$ and $\phi(x,T)$ and the computation of $\phi(x,x)^{-1}$ be repeated periodically.

A more attractive alternative is to use the feedback algorithm suggested in [8]. This feedback rule is based on a steepest descent minimization of ε^2 (not $\overline{\varepsilon^2}$). Specifically, each weight w_i is to be adjusted according to the rule:

$$\frac{dw_i}{dt} = k_s \nabla_{w_i} [\varepsilon^2(t)] \tag{53}$$

where $\nabla_{w_i}[\varepsilon^2(t)]$ denotes the ith component of the gradient of $\varepsilon^2(t)$ with respect to the weight vector w, and k_s is a negative constant. Since the gradient measures the sensitivity of $\varepsilon^2(t)$ to each of the weights, the feedback rule states that a given weight w_i will be changed at a rate proportional to the sensitivity of the $\varepsilon^2(t)$ surface

to that weight. The gradient of a surface is a vector in the maximum uphill direction, so $k_s \nabla_N [\varepsilon^2(t)]$ points in the maximum downhill direction. Hence this is a steepest-descent algorithm, and it has also been referred to as the LMS algorithm.

Evaluating the gradient gives

$$\nabla_{w_i} [\varepsilon^2(t)] = 2\varepsilon(t)\, \nabla_{w_i} [\varepsilon(t)] \tag{54}$$

and from Eq. (22),

$$\nabla_{w_i} [\varepsilon(t)] = -x_i(t). \tag{55}$$

Hence the feedback rule becomes

$$\frac{dw_i}{dt} = -2k_s x_i(t)\, \varepsilon(t) \tag{56}$$

or in integral form

$$w_i(t) = w_i(0) - 2k_s \int_{t'=0}^{t} x_i(t')\, \varepsilon(t')dt' \tag{57}$$

This feedback may be instrumented as shown in Fig. 14, which shows one loop of the system.

So far it has been assumed that the weighting coefficients in the array are real, so that only the amplitudes of the signals $x_i(t)$ are adjusted. Actually, it is necessary to adjust the phase of each signal $x_i(t)$ as well, to make use of the full flexibility available in the pattern. Phase control can be achieved by splitting the signal from each element into an in-phase component and a quadrature

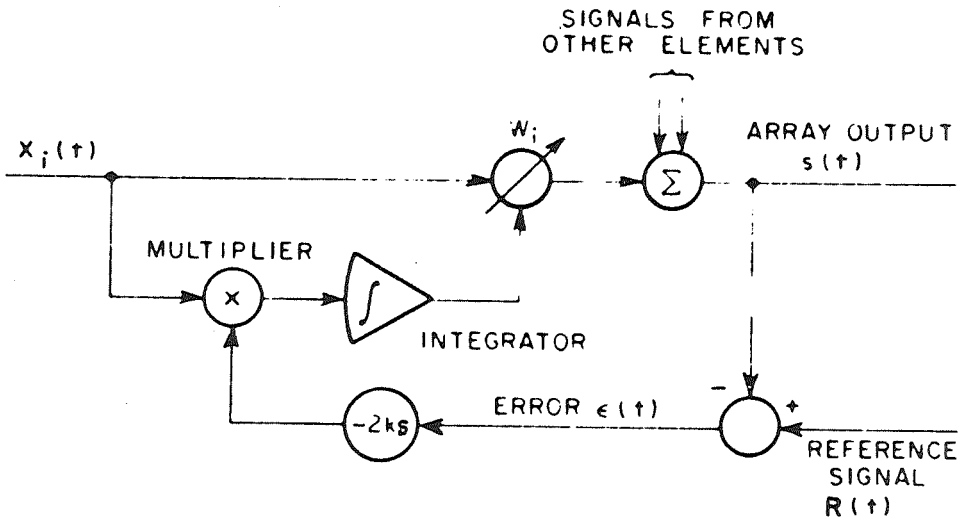

Fig. 14--Basic feedback algorithm.

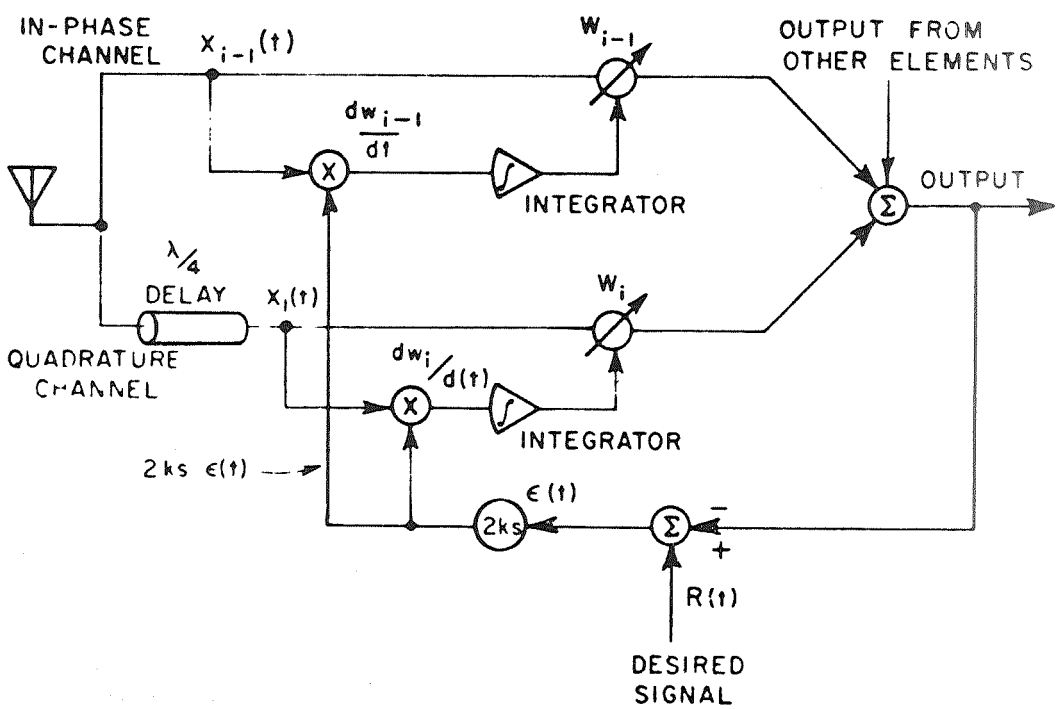

Fig. 15--Feedback circuit for each element.

component and then adjusting each with a real weighting coefficient, as shown in Fig. 15. The signal is used directly for the in-phase component, and is delayed one quarter wavelength* to produce the quadrature component. Independent control of the two weights is then equivalent to control of both magnitude and angle.

*The system to be described in Chapter IV is relatively narrowband (3 MHz bandwidth at an IF center frequency of 65 MHz) and the delay required was one-quarter wavelength at 65 MHz.

CHAPTER IV
EXPERIMENTAL RESULTS

In this chapter some experimental results of the adaptive array discussed in Chapter III are discussed. The measurements are presented here to demonstrate the correctness of the principles upon which the LMS algorithm are based, and to demonstrate that the physical implementation is well within present state of the art technology. The measured results should not be interpreted as either basic limitations or best possible values, but merely typical results which could be obtained rather easily.

A. Description of Equipment

The Processing Units

Two signal processing units based on the feedback scheme shown in Fig. 15 were designed and built. Figure 16 shows a photograph of one of these units. Figure 17 shows the various electronic functions in this unit in more detail. The signal from the element is split into an inphase channel and a quadrature channel, as discussed above. Each channel is then split again into two parallel paths, one to provide positive gain and the other negative gain. To achieve a full 360^{o} phase control in the unit requires both the in-phase channel and the quadrature channel to be capable of having either positive or negative gain. In practice, this is most easily accomplished by

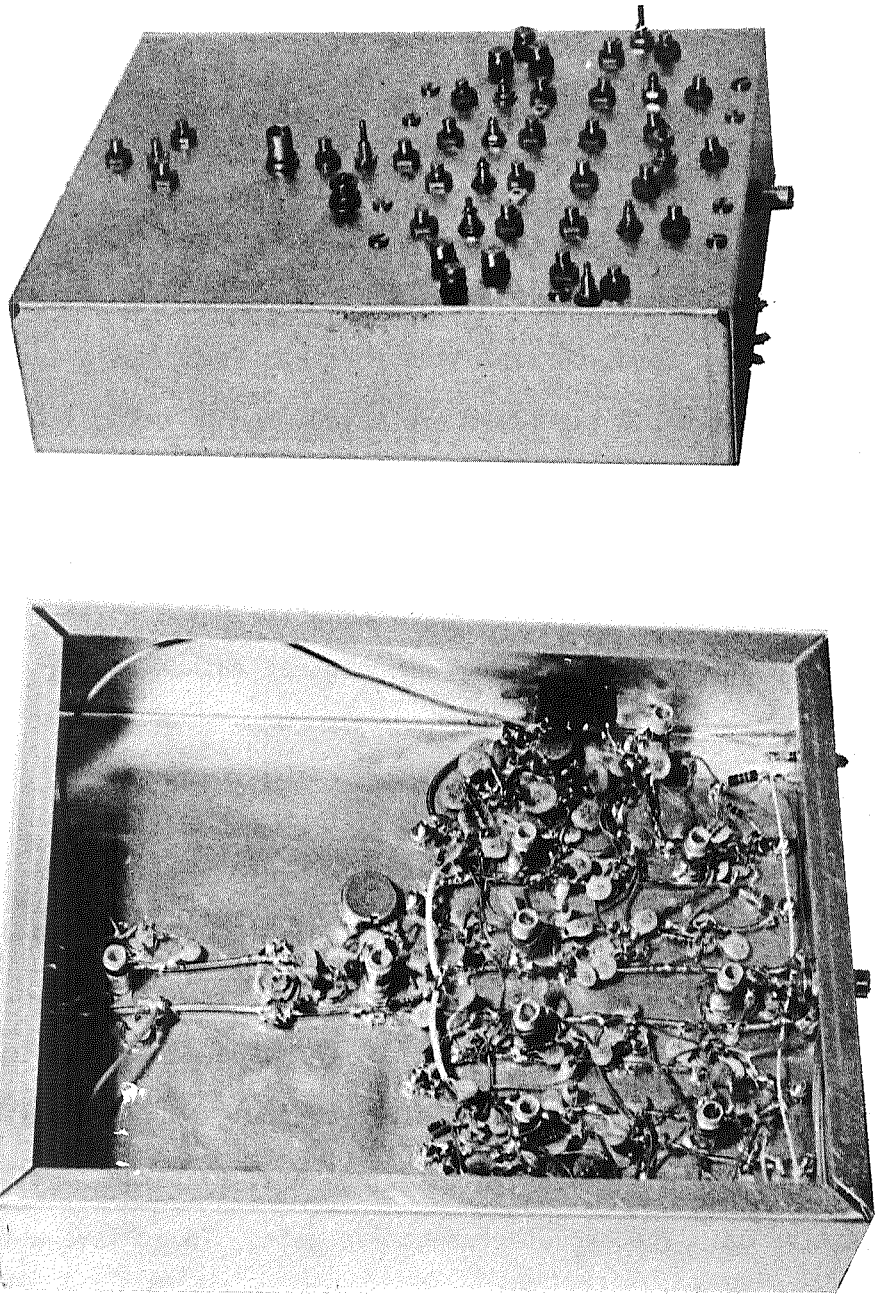

Fig. 16--Electronics unit for one element.

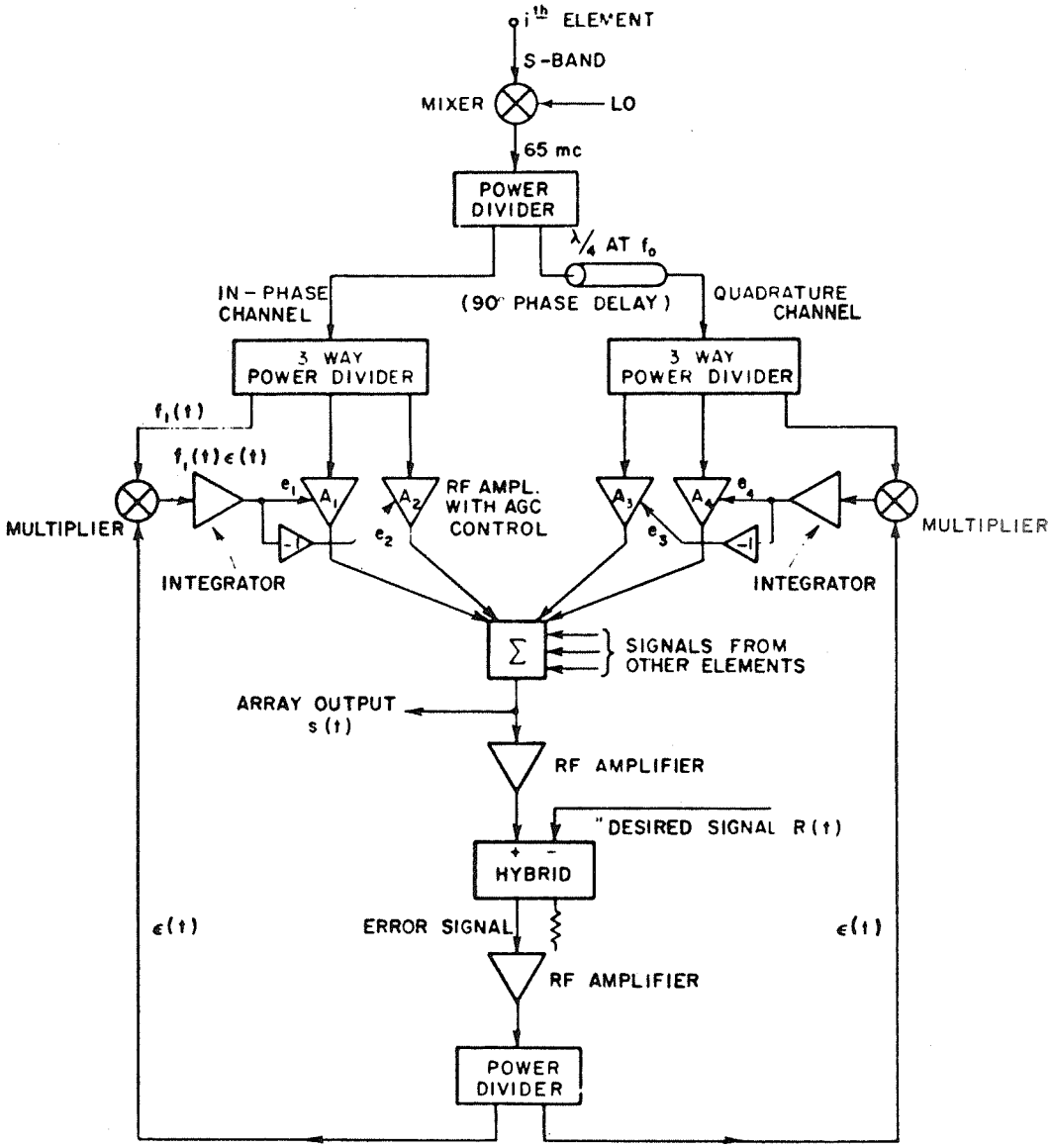

Fig. 17--Adaptive processing unit.

using two amplifiers "back-to-back", one with positive gain and the other with negative gain.

The amplifiers used were dual-gate field effect transistors (FET's), which were found to be superior to integrated circuit AGC amplifiers or current controlled diode attenuators with regard to cross-modulation, linearity and phase stability*. In addition, FET amplifiers have the helpful property that the input impedance at the control gate is essentially infinite, so it is possible to "freeze" the weighting coefficients in the array by simply disconnecting the control voltages.

The processing units operate at a center frequency of 65 MHz with an RF bandwidth of approximately 3 MHz. A complete schematic of the processing units is shown in Appendix III.

Figure 18 shows some experimentally measured gain curves for one of the "back-to-back" amplifiers. The plot shows the RF output voltage from the amplifiers as a function of the control voltage, for various input signal levels. Although the curves are not completely linear at lower power levels, the performance was acceptable.

B. Description of Measured Results

In this section the results of several experiments performed on a two-element adaptive array, using the processing units described above, are given.

*The phase shift of the amplifiers should not change as the gain is adjusted. In practice, it was found that with FET's the phase shift could be held to within 10^{o} over a 25 dB range of gain control.

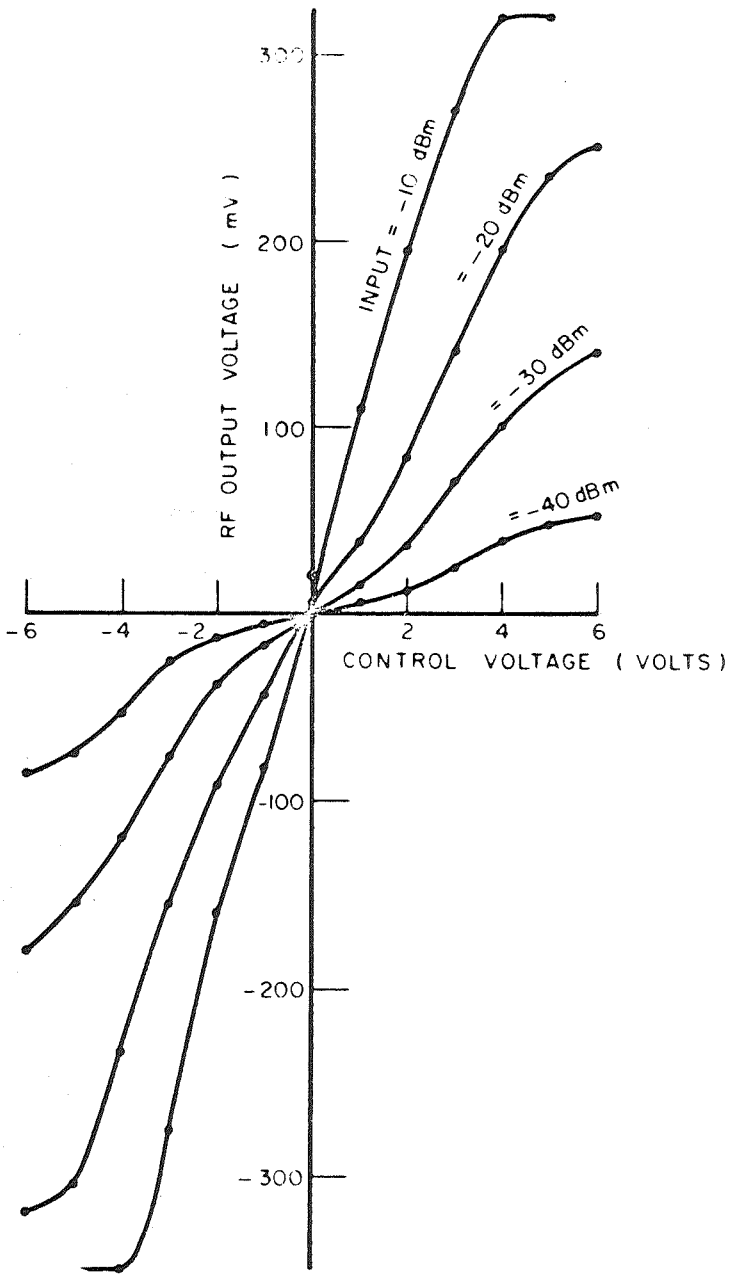

Fig. 18--Amplifier gain characteristic.

i. Phase Tracking

First, consider the following experiment. An unmodulated signal is fed into both processing units and also into the reference signal port. The adaptive feedback should then adjust both the amplitude and phase of the output signal until they match those of the reference signal (it must minimize the error). Figure 19 shows the measured difference in phase and amplitude between the array output and the reference signal as the phase difference between the two elements is varied over a 360^{o} range. (This is equivalent to varying the angle of arrival of the signal.) It is seen that the phase error varied between -5^{o} and 9^{o} and the amplitude ratio varied over a range of -0.5 dB to +0.4 dB.

ii. Amplitude Tracking

Next, Fig. 20 shows the results of an experiment in which the amplitude of the signal was varied, while the reference signal was held constant. The curve shows the amplitude of the error signal $\varepsilon(t)$, relative to the reference signal amplitude. (The lower the error, the better the array processing units are performing.) It may be seen that the error was maintained 20 dB or more below the reference over a range of input signal levels of approximately 23 dB.

C. Interference Rejection

Next we discuss a number of experiments dealing with the interference rejection capability of the array. As discussed above, any signal not represented in the reference signal R(t) contributes directly to the error signal, and the feedback system adjusts the weights to minimize it.

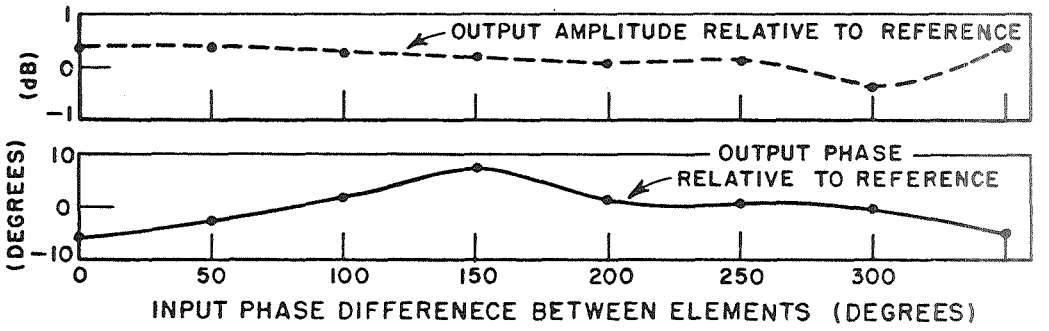

Fig. 19--Response of output amplitude and phase to input phase changes.

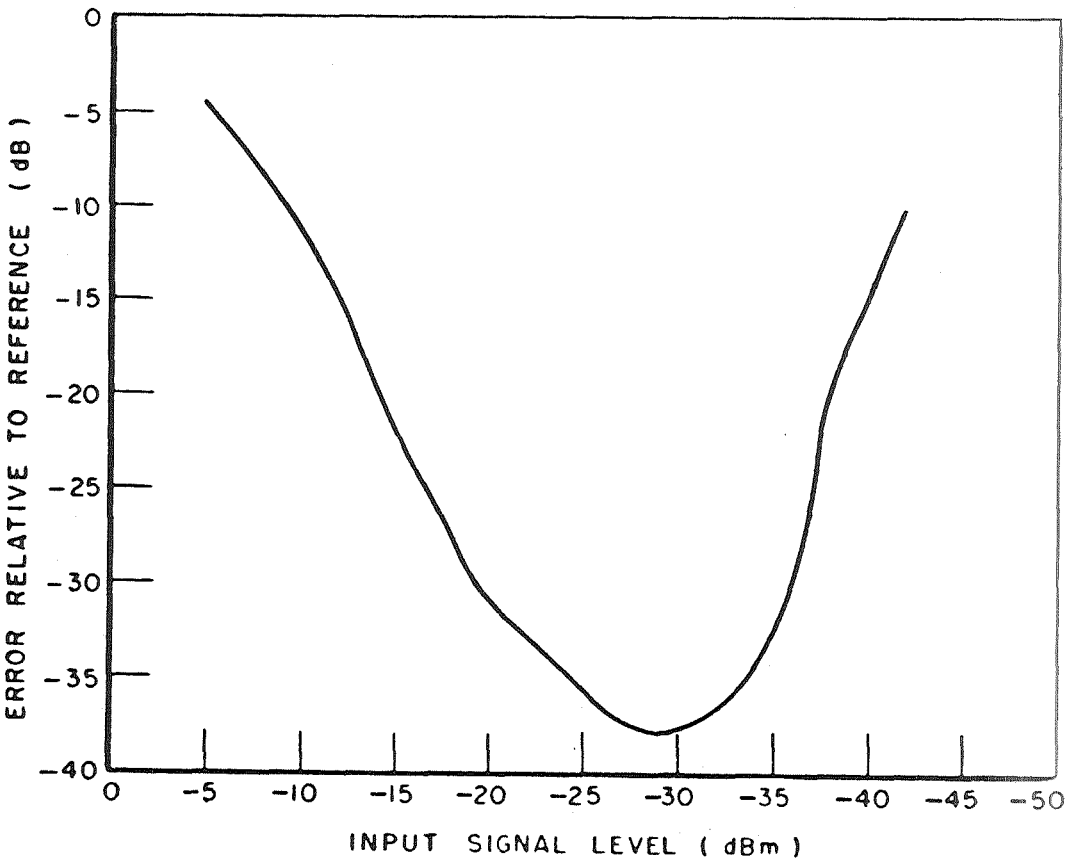

Fig. 20--Error level vs signal level.

The first experiment involved a simulated test of interference rejection by the array. Two CW signals were injected directly into the processing units (i.e., no actual antenna elements were used). The signals were separated 10 kHz in frequency. First, one of them was injected with equal phase on each processing unit, corresponding to a desired signal arriving from broadside. This signal was also used for the reference signal R(t). The weighting coefficients were allowed to adapt, and the final values were noted and used to compute the pattern labelled "before adaptation" in Fig. 21. Next, a second signal (an interfering signal) was also injected, with an electrical phase angle between the units corresponding to a signal incident from 40^{o} off broadside with half-wavelength spacing between elements. After this signal was turned on, the weighting coefficients changed to new values. These values were then used to compute the second pattern, labelled "after adaptation" in Fig. 21. It may be seen how the adaptive feedback causes the antenna to form a null on the interfering signal.

The second experiment performed was a measurement of the improvement in the ratio of desired signal power to interfering signal power at the output of the array due to the adaptive feature. First, a desired signal arriving from broadside was injected in the array. After the weighting coefficients reached their final values, they were frozen and the interfering signal was turned on. The ratio of desired signal power to interfering signal power at the output of the array was measured. The array coefficients were then allowed to readapt, and after they reached their new final values, the ratio of the powers of the desired and interfering signals was again measured. This ratio is

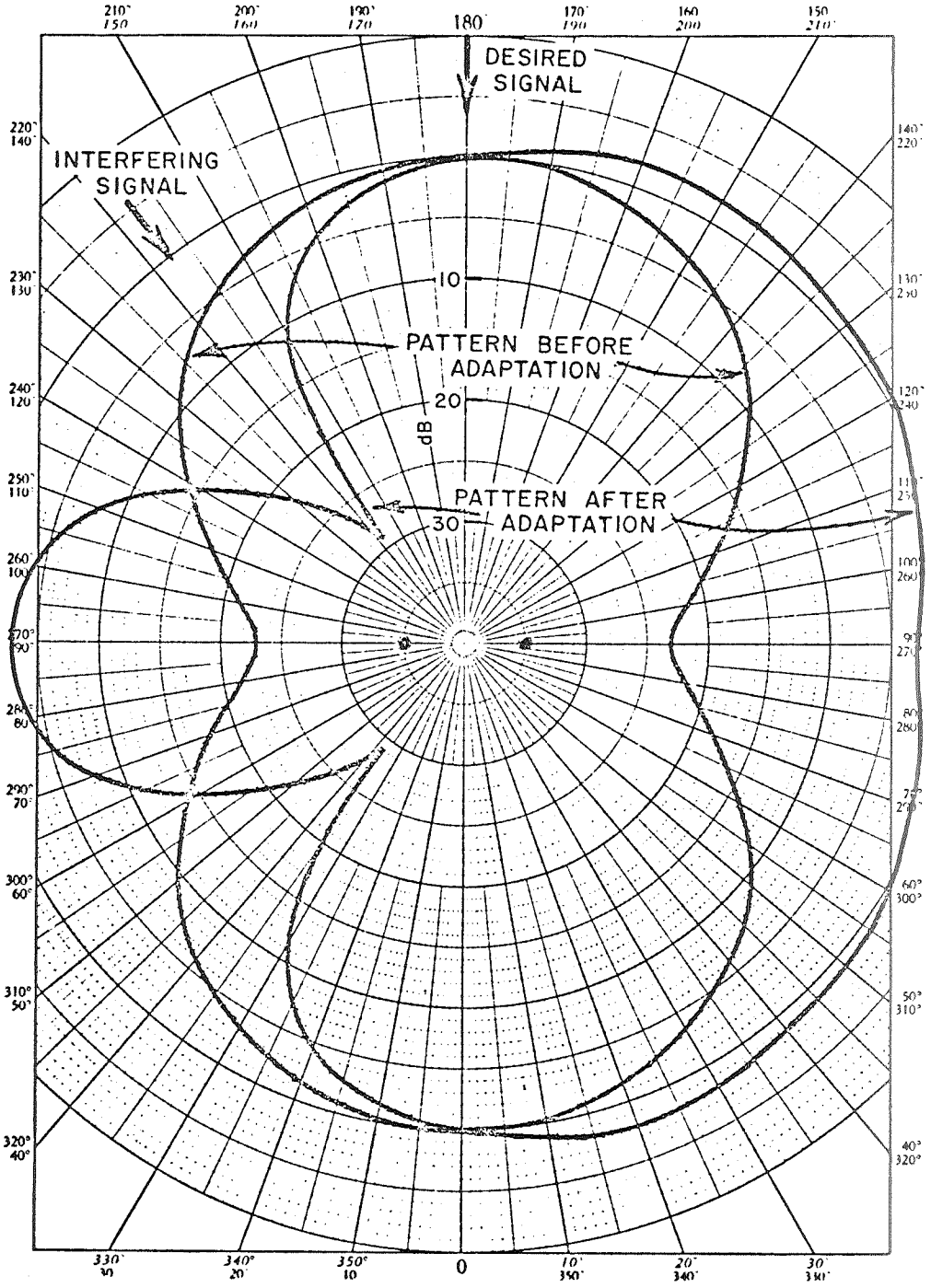

Fig. 21--Patterns before and after adaptation.

called adaptivity. That is,

$$\text{Adaptivity} = \frac{\frac{D}{I} \text{ after adaptation}}{\frac{D}{I} \text{ before adaptation}}$$

where

D = desired signal power

I = interfering signal power

Figure 22 shows the adaptivity in dB versus the electrical phase angle difference between elements for the interfering signal. The desired signal arrived from broadside (in phase in both elements) for the entire curve. The adaptivity is shown for five different interfering signal power levels at the input to the array. For all curves (except the 0 dB one) the interfering signal power is higher than that of the desired signal. The type of feedback used (see Eq. (57)) has the property that it tends to hold the error signal at a relatively constant level, regardless of the power level of the interfering signal.* This property projects into the adaptivity curves in Fig. 22. When the interfering signal power is increased 5 dB, the error signal remains constant, so the adaptivity increases 5 dB.

For the case where the interfering signal power is 20 dB higher than the desired signal power, the processing units have been driven beyond their linear limits and the units no longer operate properly.

*The feedback loop for each element is a Type I (coupled) loop with loop gain proportional to the signal intensity squared. See Section D below.

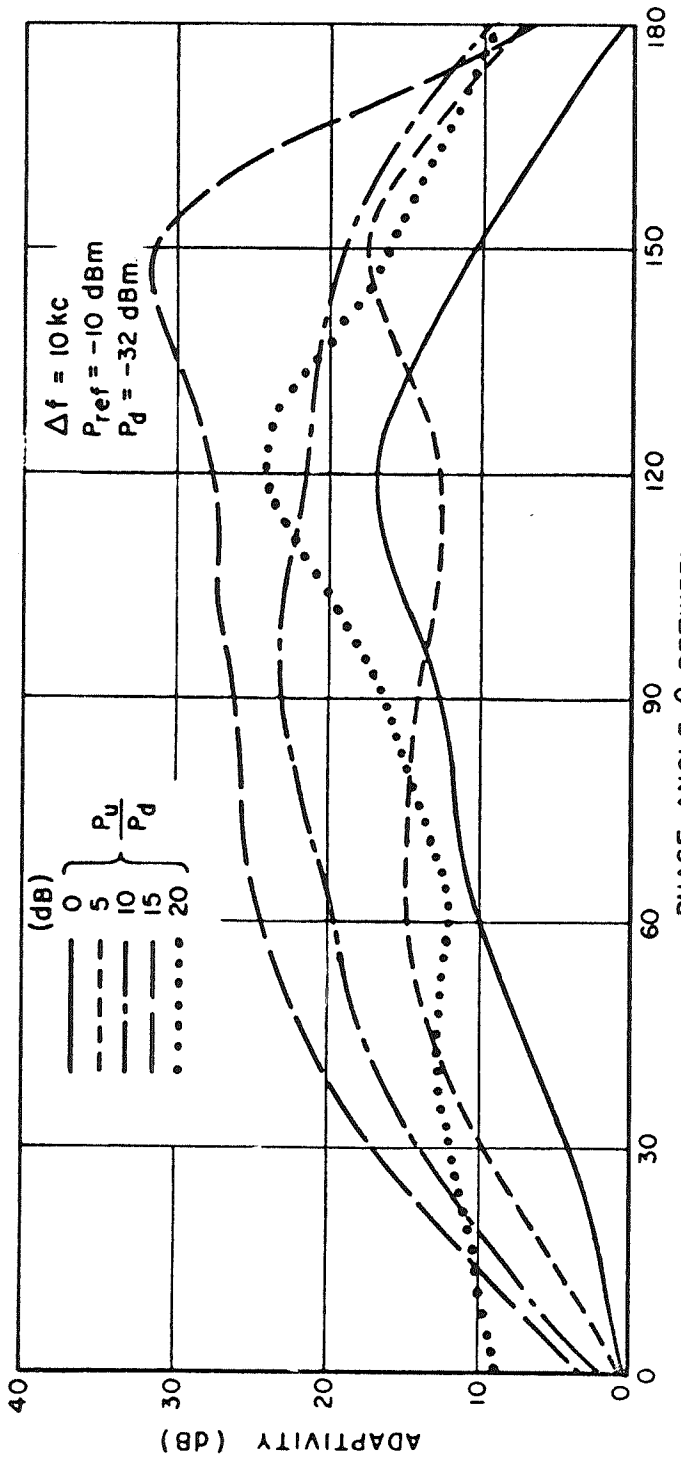

Fig. 22--Adaptive array improvement over 2 element phased array.

It is noted that the adaptivity drops to zero at both ends of the curve, where the electrical phase angle between the interfering signal in the two elements approaches 0^{o} or 180^{o}. Near 180^{o}, this result is simply due to the fact that the array pattern, when maximized for broadside, has a null in the endfire direction anyway. That is, a desired signal incident from broadside results, in the absence of interference, in a pattern with a null in the endfire direction. When the interference is then turned on, it is already in a null, so the adaptive feedback makes very little change. This results in a measured adaptivity of nearly zero, but it represents no real limitation to array performance.

The drop in adaptivity near 0^{o}, on the other hand, represents the actual limitation in the system. This end of the curve defines how close the interfering signal can come to the desired signal in space and still be nulled out.

These curves show that 10 dB improvement of signal-to-interference ratio is quite easily achieved in such an array for most interference angles, and 30 dB is even possible under some conditions. Furthermore, this improvement is based on only two elements, and one may hope to do better with more elements.

Next we consider some interference rejection experiments in which actual antenna elements were used, and antenna patterns were taken on a pattern recorder. The antennas used were a pair of $\lambda/4$ monopoles*

---

*λ is the wavelength.

spaced $\lambda/2$ apart on a rectangular ground plane. The patterns were recorded at 2.1 gHz. Each element was connected directly to a mixer, where the frequency was converted to 65 mHz and put into the two processing units. A common local oscillator fed both mixers.

In Fig. 23, a single desired signal illuminates the antenna from the direction shown. The weighting coefficients were allowed to adapt, and were then frozen. With the weights frozen, the pattern was run, and Fig. 23 shows the result.

In Fig. 24, the experiment was the same as for Fig. 23, except that now the array weighting coefficients were allowed to adapt as the pattern recorder turned. In this case the weighting coefficients were varying as the recorder turned, and the pattern beam tracked the signal, resulting in an "omnidirectional" pattern.

In Figs. 25, 26, and 27, both a desired signal and an interfering signal illuminated the antenna. The weights were allowed to adapt and were then frozen. The patterns shown in the figures were run with the weights fixed. These patterns show three different sets of incidence angles for the desired and interfering signals. It may be seen how the adaptive feedback forced a null in the direction of the interfering signal.

Finally, Fig. 28 shows the depth of the null on the interfering signal as a function of its angle of arrival, when the desired signal remains at broadside. (This is not an instantaneous pattern, but a plot of null depth.)

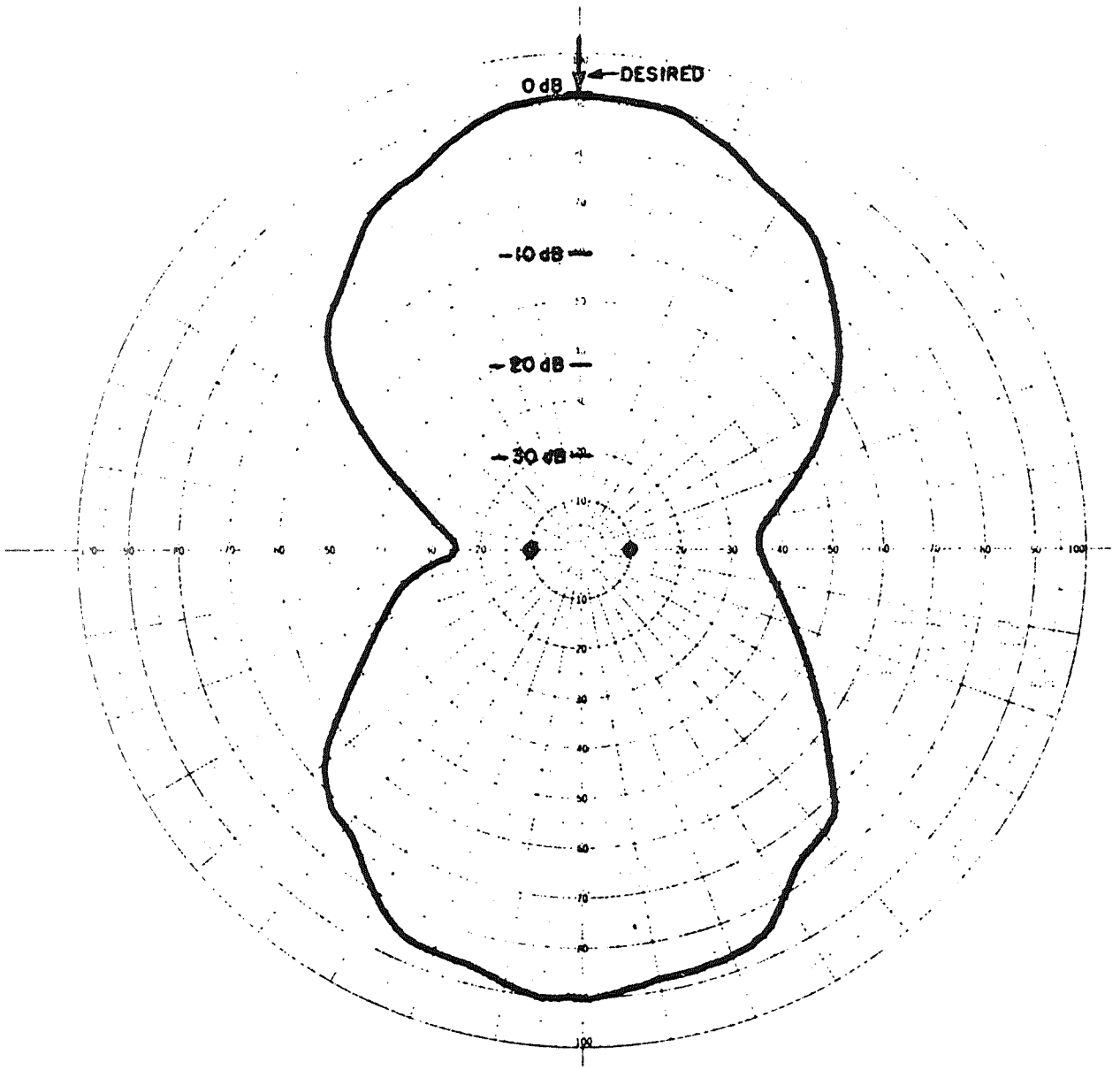

Fig. 23--Adaptive antenna pattern; desired signal only.

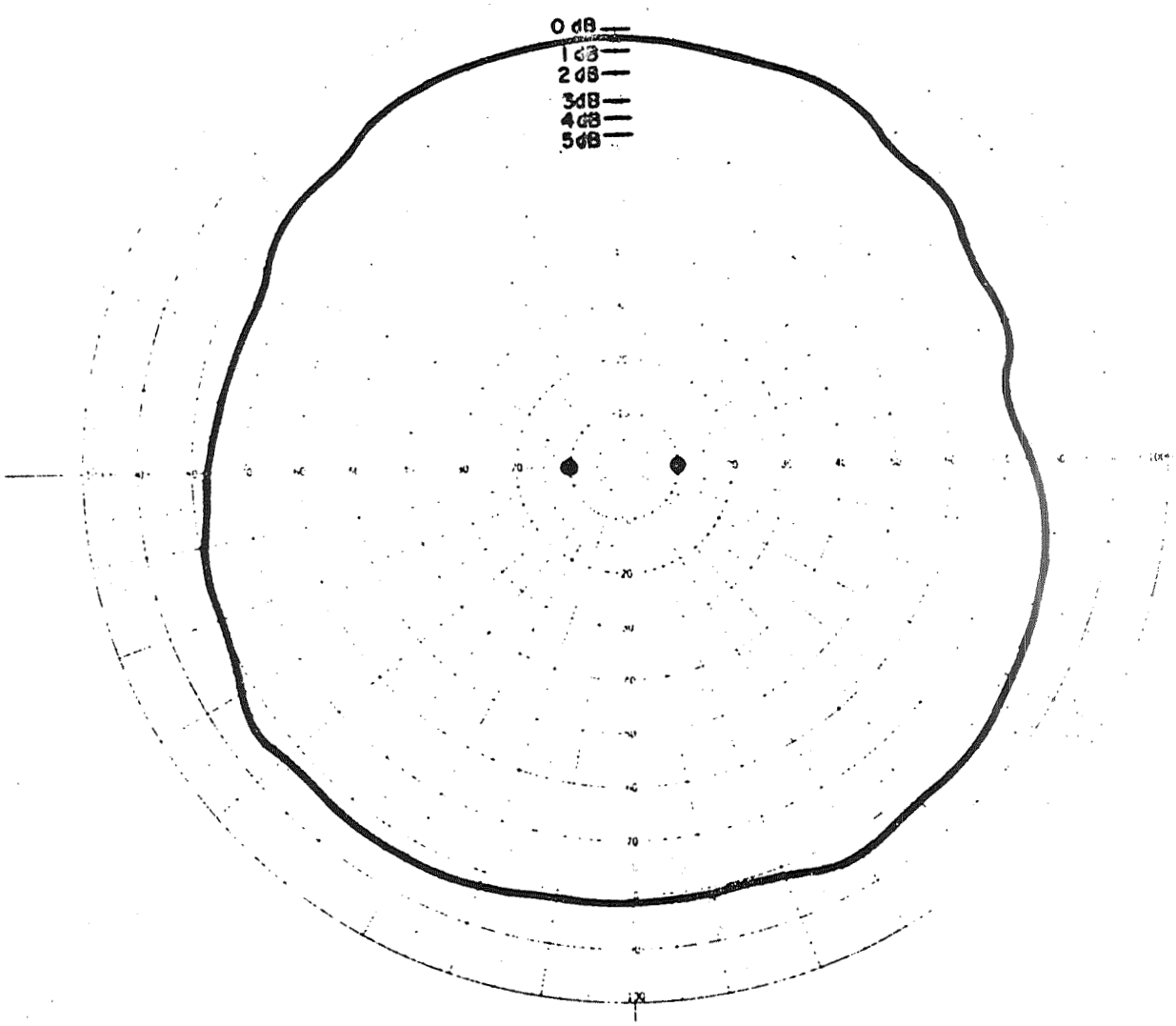

Fig. 24--Adaptive antenna pattern; desired signal tracked.

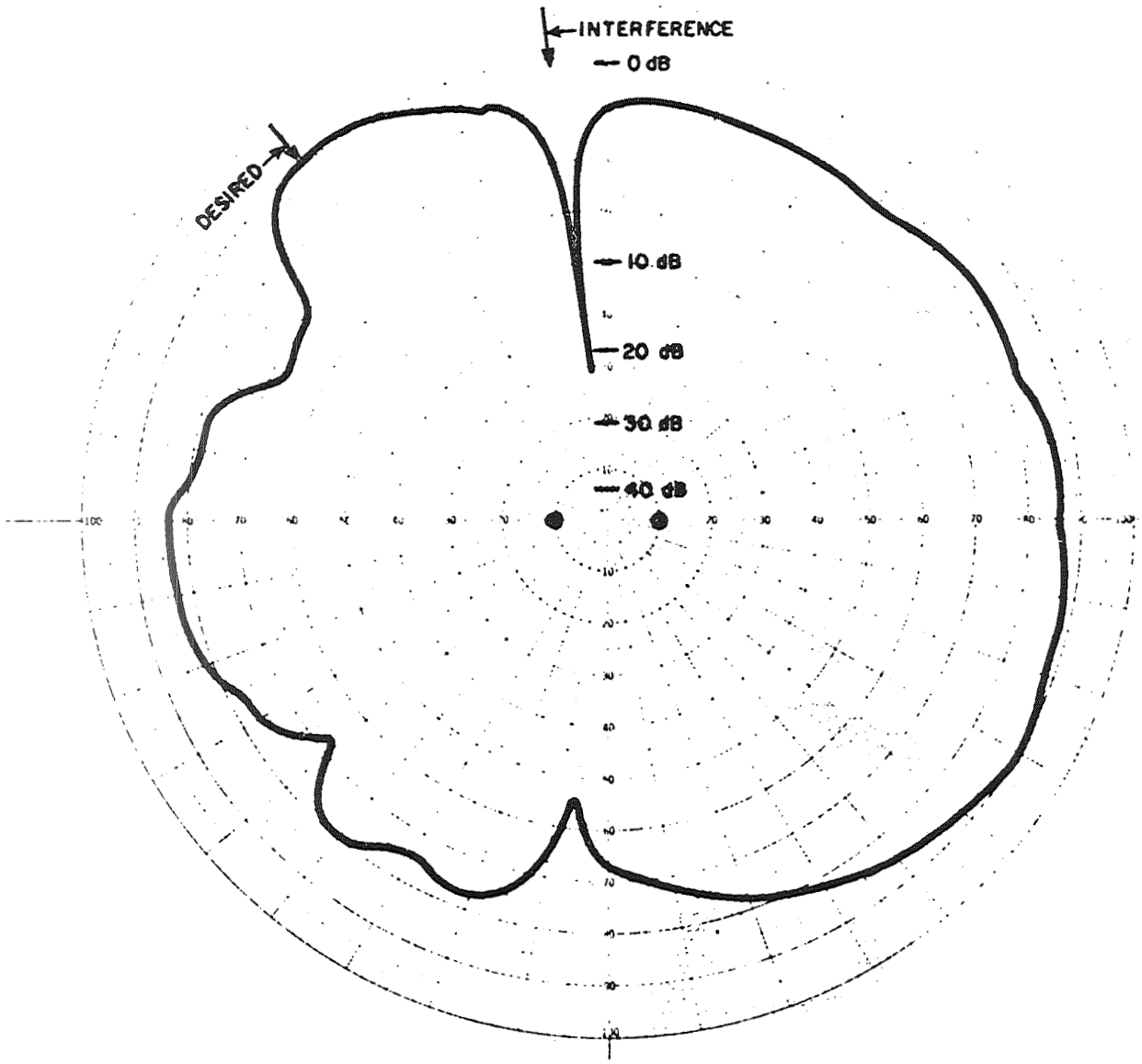

Fig. 25--Adaptive antenna pattern; desired signal plus interference.

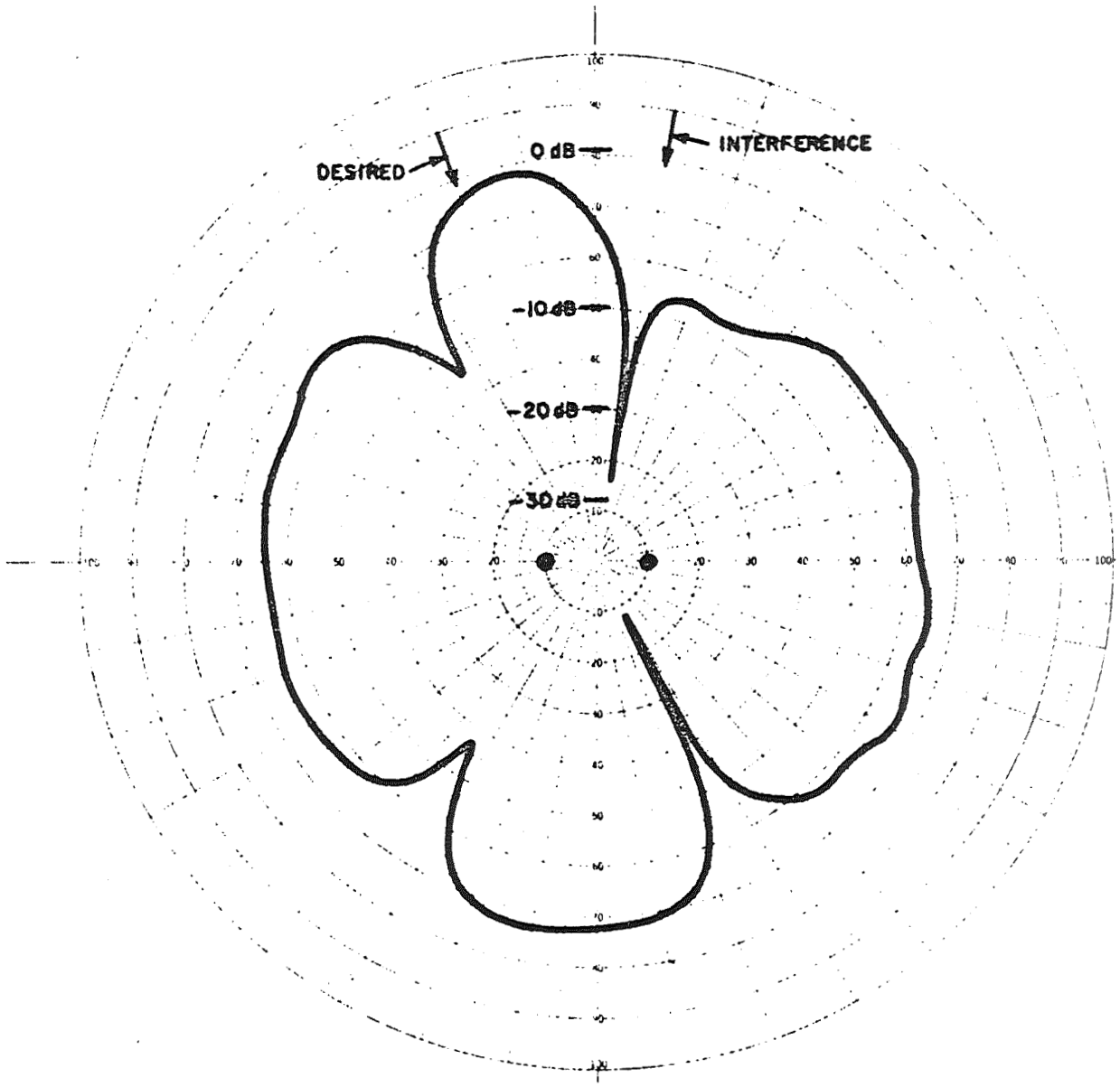

Fig. 26--Adaptive antenna pattern; desired signal plus interference.

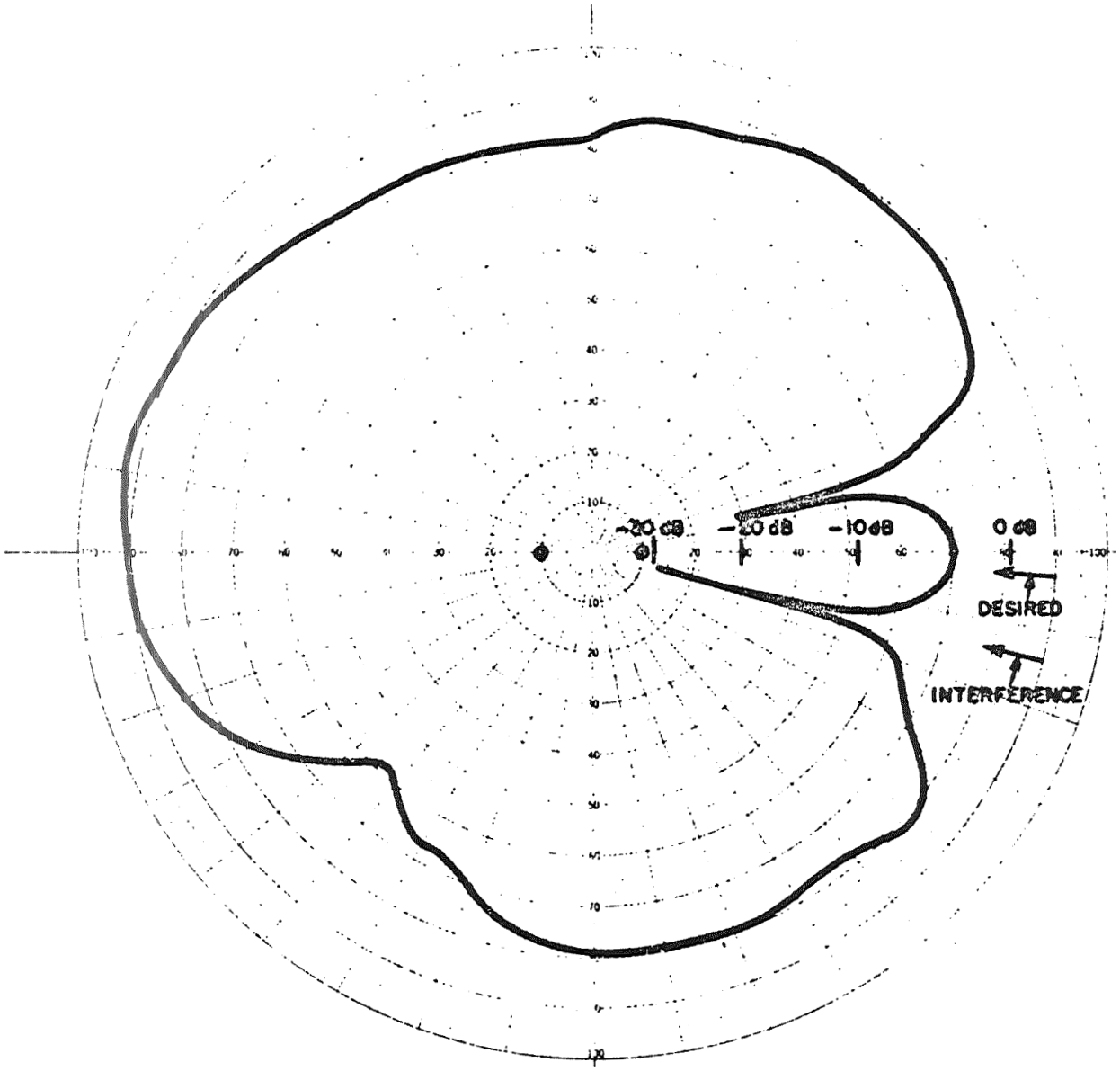

Fig. 27--Adaptive antenna pattern; desired signal plus interference.

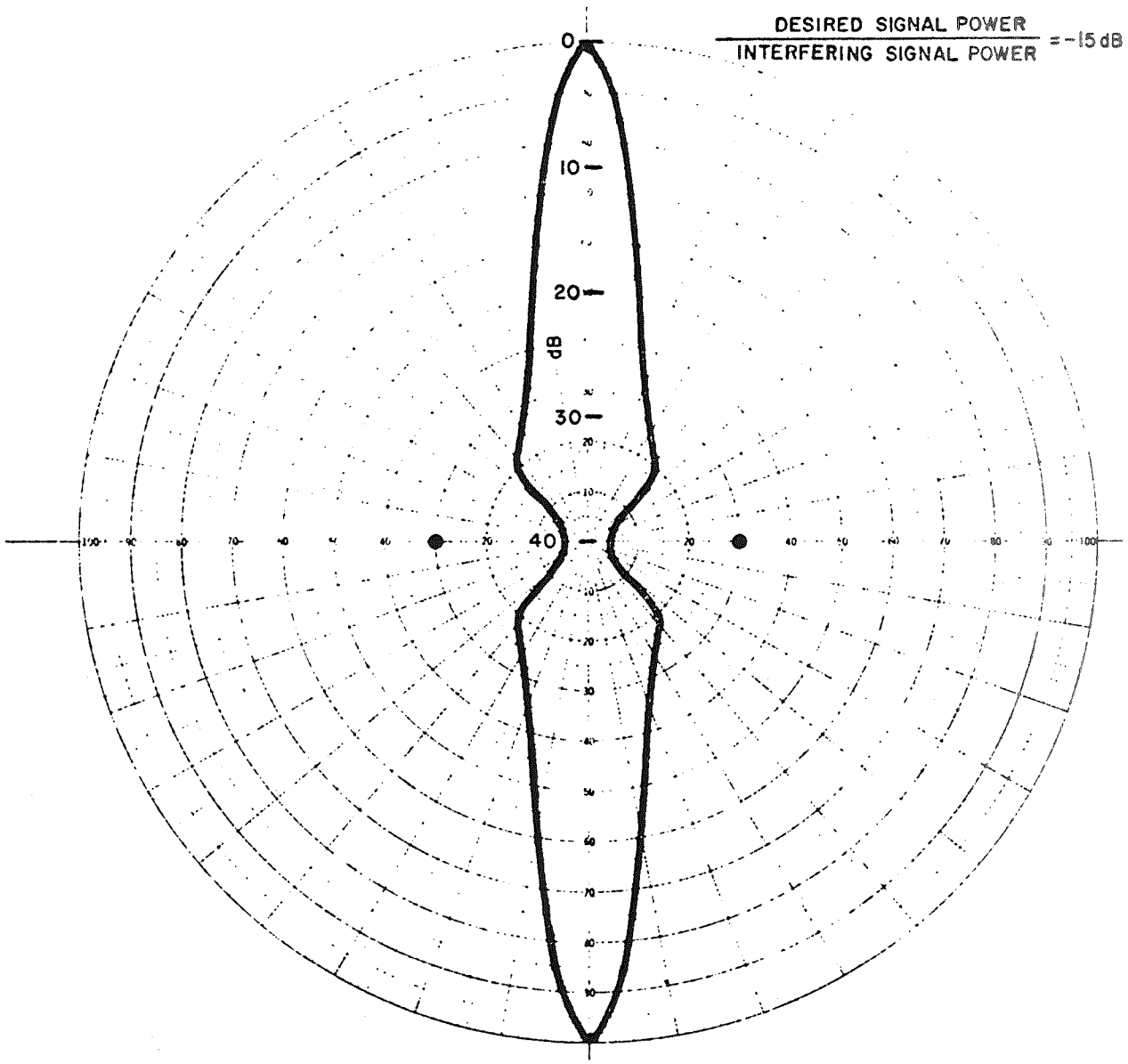

Fig. 28--Depth of interference null.

D. Speed of Response

To study the transient behavior of the weighting coefficients, one may examine the differential equations which they satisfy. Since

$$\frac{dw_i}{dt} = k_s x_i(t)\, \varepsilon(t), \tag{58}$$

and

$$\varepsilon(t) = R(t) - \sum_{j=1}^{N} w_j x_j(t), \tag{59}$$

we find

$$\frac{dw_i}{dt} = k_s x_i(t) \left[R(t) - \sum_{j=1}^{N} w_j x_j(t)\right], \tag{60}$$

or

$$\frac{dw_i}{dt} + k_s x_i(t) \sum_{j=1}^{N} x_j(t) w_j = k_s x_i(t)\, R(t). \tag{61}$$

Written in matrix form, this is

$$\frac{dw}{dt} + k_s\, X\, w = k_s\, Rx, \tag{62}$$

where w is defined in Eq. (26),

$$X = \begin{pmatrix} x_1(t)\,x_1(t) & x_1(t)\,x_2(t) & \cdots & x_1(t)\,x_N(t) \\ x_2(t)\,x_1(t) & \cdots & & \cdot \\ \cdot & & & \cdot \\ \cdot & & & \cdot \\ \cdot & & & \cdot \\ x_N(t)\,x_1(t) & \cdots & & x_N(t)\,x_N(t) \end{pmatrix} \tag{63}*$$

*Note that $\phi(x,x) = \overline{X}$, $\phi(x,R) = \overline{R(t)x}$.

and

$$(64)^* \qquad x = \begin{pmatrix} x_1(t) \\ x_2(t) \\ \cdot \\ \cdot \\ \cdot \\ x_N(t) \end{pmatrix} .$$

Unfortunately, Eq. (62) is a system of differential equations for which no method of constructing a general solution is known. For the special case where there is only one weight, say w_1, Eq. (62) becomes

$$(65) \qquad \frac{dw_1}{dt} + k_s x_1^2(t) w_1 = k_s R(t)\, x_1(t).$$

A general solution for this equation is easily obtained by use of an integrating factor, with the result

$$(66) \qquad w(t) = e^{-\int k_s x_1^2(t)dt} \left\{ \int k_s x_1(t) R(t) e^{\int k_s x_1^2(t)dt}\, dt + C \right\}$$

where C is a constant of integration. But when more than one weight is involved, no general solution for the system (62) can be constructed. There are certain special cases, of course, where the system can be solved. For example, if the matrix X is constant, a solution is easily found. Or, if the signals happen to be such that the product of the matrices X and dX/dt commutes, then a matrix integrating factor can be used to construct a solution analogous to Eq. (66). However, these

---

*Note that $\phi(x,x) = \overline{X}$, $\phi(x,R) = \overline{R(t)x}$.

cases do not appear to correspond to a meaningful set of signals in the adaptive array problem.

Other approaches to solving the system (62) are of course possible. The equations can be solved on an analog computer or a digital computer. Various techniques for obtaining approximate analytical solutions, such as series solutions or perturbation techniques, seem promising.

One important case which can be analyzed is the response of a single signal processing unit to the introduction of a desired signal or an abrupt change in its amplitude or phase.

For this case $x_1(t) = A \cos(\omega_d t + \phi) \quad t \geq 0$

$x_2(t) = A \sin(\omega_d t + \phi) \quad t \geq 0$

$R(t) = A_r \cos \omega_d t$

where A = amplitude of voltage at the input of the signal processor due to an incident signal

ϕ = phase of this voltage relative to reference.

Equation (62) then becomes

$$(68) \qquad \begin{bmatrix} \frac{dw_1}{dt} \\ \frac{dw_2}{dt} \end{bmatrix} + \begin{bmatrix} a & 0 \\ 0 & a \end{bmatrix} \begin{bmatrix} w_1 \\ w_2 \end{bmatrix} = b \begin{bmatrix} \cos \phi \\ \sin \phi \end{bmatrix}$$

where $a = k_s \frac{A^2}{2}$

$b = k_s \frac{A A_n}{2}$

or

$$\frac{dw_1}{dt} + aw_1 = b \cos$$

$$\frac{dw_2}{dt} + aw_2 = b \sin \quad .$$

A solution can easily be found, for example by variation of parameters, as

$$w_1 = \frac{b}{a}(1-e^{-at})\cos\phi = \frac{A_r}{A}\left(1-e^{\frac{-k_s A^2}{2}}\right)\cos\phi$$

(69)

$$w_2 = \frac{b}{a}(1-e^{-at})\sin\phi = \frac{A_r}{A}\left(1-e^{\frac{-k_s A^2}{2}}\right)\sin\phi$$

where it has been assumed that $w_1(0) = w_2(0) = 0$.

It can be seen that both w_1 (the direct component) and w_2 (the quadrature component) have the same time constant and differ only in their final value. The inverse square dependence of this time constant ($2/k_s A^2$) on input signal amplitude can be seen in Fig. 29A, an analog computer solution of Eq. (69) for various A. The larger the A the smaller the time constant, or alternatively the faster the system response. The effect of phase changes can be seen in Fig. 29B, also an analog computer result. Initially an input signal with $\phi = 0$ is turned on and the processor is allowed to reach a final value. At time t = 6 seconds an abrupt phase jump of 90^o is made in the input signal and the signal processor is again allowed to reach a steady state condition.

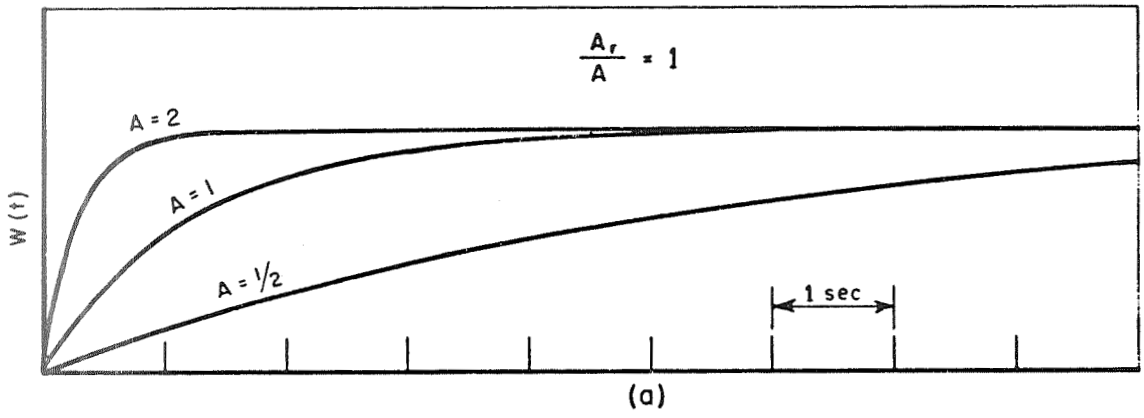

Fig. 29A--Relationship between system response and signal amplitude.

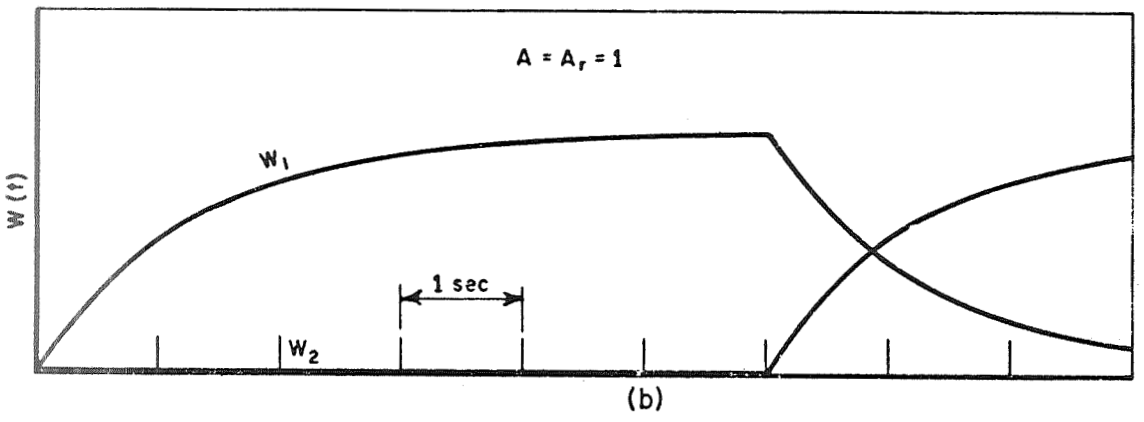

Fig. 29B--Response of system to phase changes.

The actual physical implementation of the algorithm was based on a slightly modified version of Eq. (62). The pure integrator, having Laplace transform 1/s was replaced by a transfer function $1/(s+\alpha)$ to assure stability for high signal to noise conditions. This can be understood by considering, for example, a two element array with only a desired signal present. Suppose the signal arrives from the broadside direction with electrical phase equal to the reference, i.e.,

let $X_1 = X_3 = A \cos \omega_d t$

$X_2 = X_4 = A \sin \omega_d t$

$R = A_r \cos \omega_d t$

Then a correct solution for the weights w which yield zero error is

$$w_1 = w_3 = \frac{1}{2}\frac{A_r}{A}$$
$$w_2 = w_3 = 0. \tag{70}$$

However the slightest difference or unbalance in the two elements together with the infinite dc gain of the integrator may cause an equally correct but highly undesirable solution of the form:

$$w_1 = \frac{1}{2}\frac{A_r}{A} + k_1 t + k_2 t^2 + k_3 t^3 + \cdots$$

$$w_3 = \frac{1}{2}\frac{A_r}{A} - k_1 t - k_2 t^2 - k_3 t^3 - \cdots \tag{71}$$

$$w_2 = w_4 = 0$$

t = time k's are arbitrary constants.

For this solution the weighting coefficients also produce zero error but increase in magnitude without bound until the electronic components saturate and the system is no longer able to function correctly. This type of behavior is shown in Fig. 30, the result of an analog computer simulation of Eq. (62) for the example discussed above. Replacing the ideal integrator by a network with transfer function $1/s+\alpha$, having a dc gain of $1/\alpha$, eliminates this diverging weighting coefficient phenomenon. Note that this condition only occurs for very high SNR cases. The presence of internally generated system noise for example will force a solution of the type given in Eq. (70).

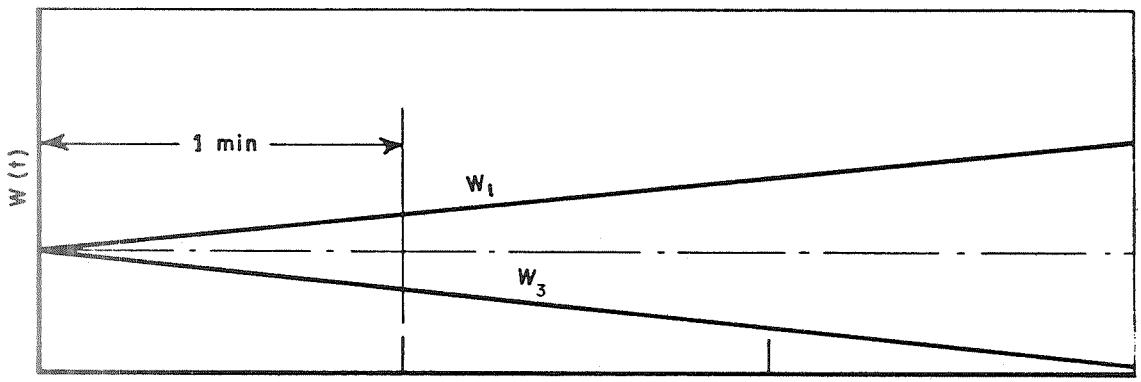

Fig. 30--Diverging weighting coefficients for pure integration and high SNR.

Certain general conclusions about time response are possible. When this system is viewed as a problem in feedback control, it is clear that the response time of the system depends on the amplitudes of both the desired and interfering signals, because of the

$x_i(t)\ x_j(t)$ terms in the differential equations. Stated another way, the feedback loop has a gain constant proportional to the square of the signals $x_i(t)$. Hence the larger the signals $x_i(t)$, the tighter the loops. This is the reason that the error signal amplitude is approximately independent of the input signal level, as we previously remarked. In a linear feedback loop, a larger input signal would imply a larger steady state error. But for this loop, a larger input results in a tighter loop, with the result that the error stays constant.

Figure 31 shows a measured transient response of one of the weighting coefficients in the array. This curve is a typical result, and has a time constant of approximately 20 milliseconds.

E. Experiments with Modulated Signals

Next we consider some experiments where the signals in the array contain modulation but the reference signal is unmodulated. For a desired signal having amplitude modulation of the form

$$S(t) = a(t) \cos \omega_o t = A_o [1 + 2k_m \cos \omega_m t] \cos \omega_o t, \tag{72}$$

and a reference signal of the form

$$R(t) = A_r \cos \omega_o t, \tag{73}$$

the mean-square error $\overline{\varepsilon^2(t)}$ is found to be

$$\overline{\varepsilon^2(t)} = \frac{1}{2} (A_r - A_o)^2 + (A_o k_m)^2 \tag{74}$$

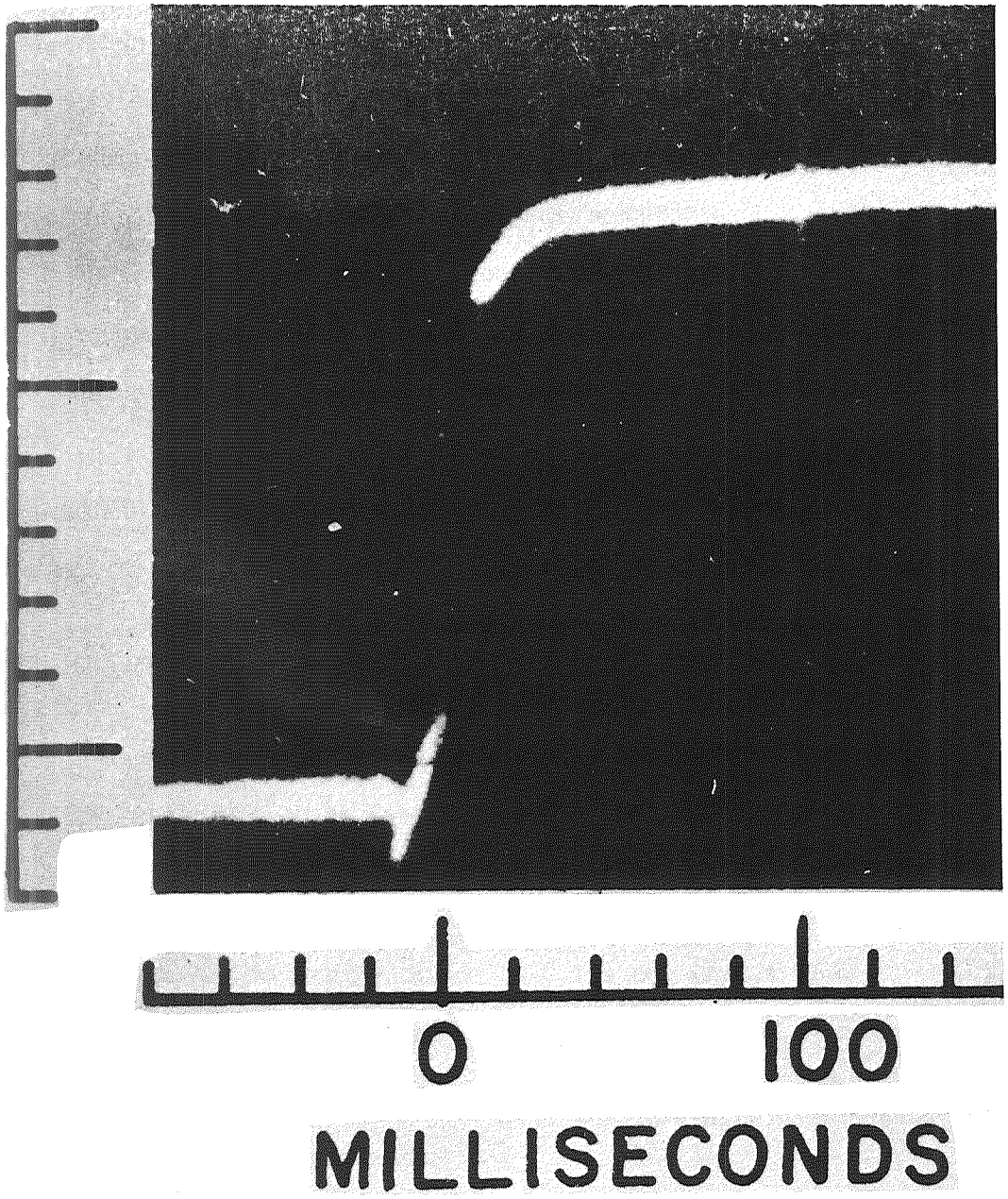

Fig. 31--Time response of weighting coefficient.

The value of A_o giving least $\overline{\varepsilon^2(t)}$ may be found by setting

$$\frac{2\varepsilon^2(t)}{A_o} = 0, \tag{75}$$

which yields

$$A_o = \frac{A_r}{1 + 2k_m^2} \tag{76}$$

Hence the minimum mean-square error criterion does not force the carrier component of the AM signal to be equal to the reference signal carrier. Instead the carrier of the AM signal is suppressed relative to the reference carrier, by an amount dependent on the modulation factor k_m.

Figure 32 compares this calculated suppression with the results measured on the processing units, for two different signal levels. For $k_m = 0$, A_o should be equal to A_r and no suppression should occur. For $k_m = \frac{1}{2}$ (100% modulation) $A_o = 2/3\ A_r$ and the carrier of the signal should be about 3.5 dB lower than the reference signal. The experimental results shown in Fig. 32 agree reasonably well with this.

Next, we consider the interference rejection properties of the array with modulated signals. Figures 33-35 show photographs taken of the trace of a spectrum analyzer connected to the output of the array. In Fig. 33, the desired signal consists of a carrier component and two sidebands separated 50 kHz from the carrier. The carrier of the desired signal was used for the reference signal (that is, the reference signal did not contain the modulation components). A CW interfering signal was added 10 KHz below the

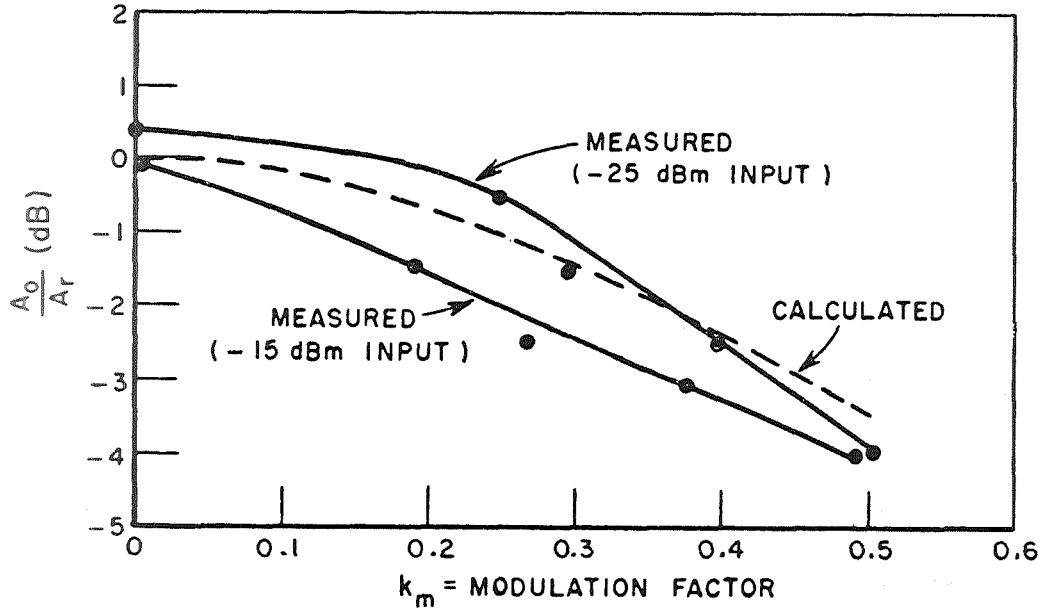

Fig. 32--Effect of modulation on desired signal.

carrier of the desired signal. The top photo shows the output spectrum before the weighting coefficients are allowed to adapt, and the bottom curve shows it after adaptation. It may be seen how the interference is removed from the output by the adaptive feedback. In Figs. 33-35, the spectrum analyzer has a linear voltage scale. In Fig. 33, the interfering signal has approximately 4 times the voltage of the desired signal carrier, or 16 times the power.

Figure 34 shows a case in which both the desired signal and the interfering signal are modulated. The desired signal has sidebands 50 kHz from the carrier, and the carrier alone is also used for the reference signal, as before. The interference has a carrier approximately 8 kHz below the carrier of the desired signal, and modulation

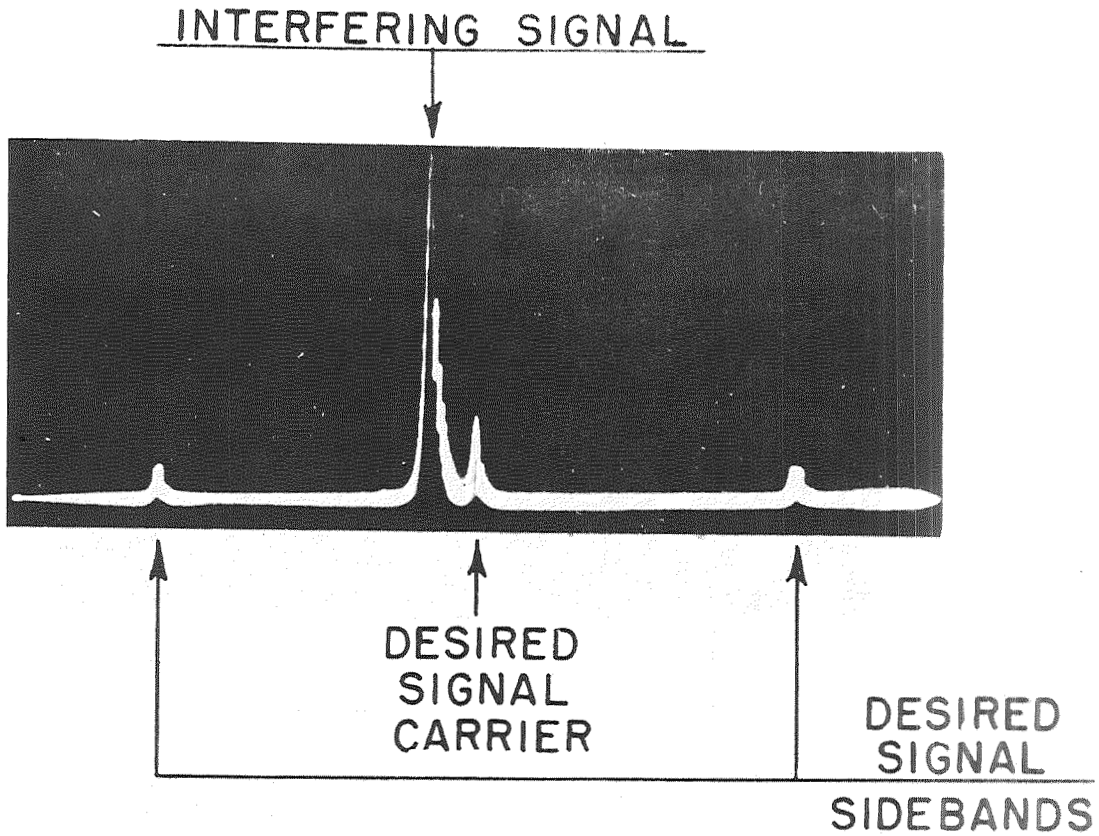

(a) BEFORE ADAPTATION

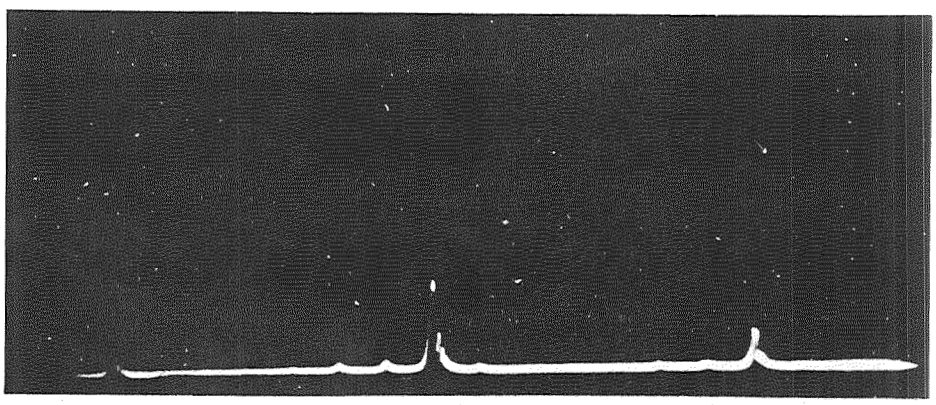

(b) AFTER ADAPTATION

Fig. 33--Adaptive rejection of interfering signal.

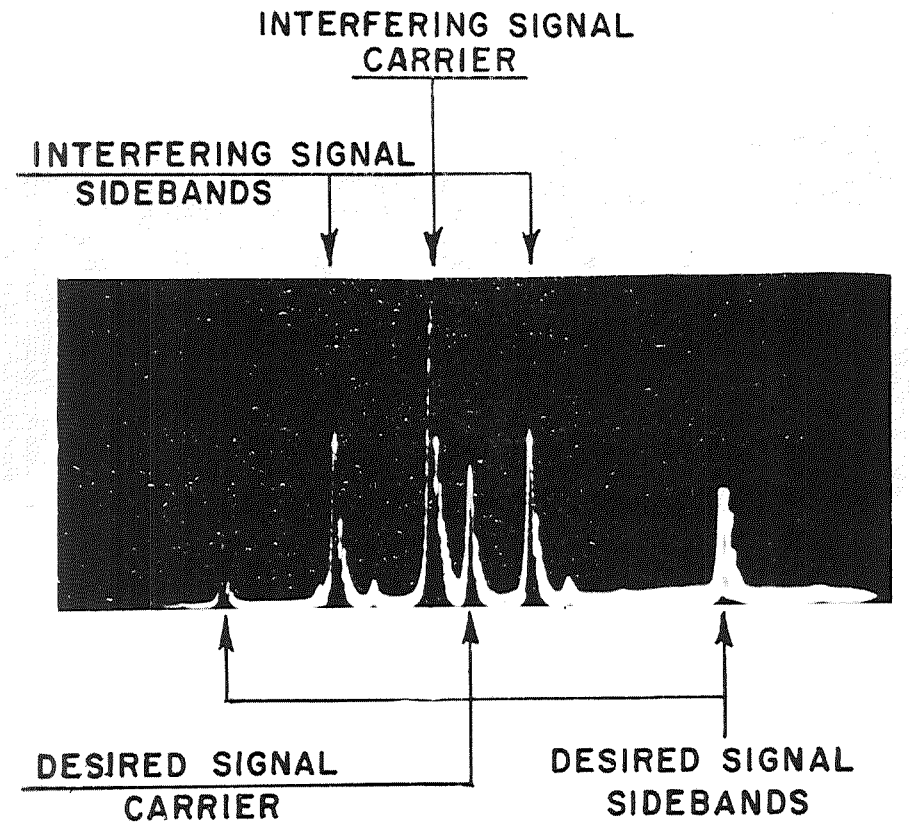

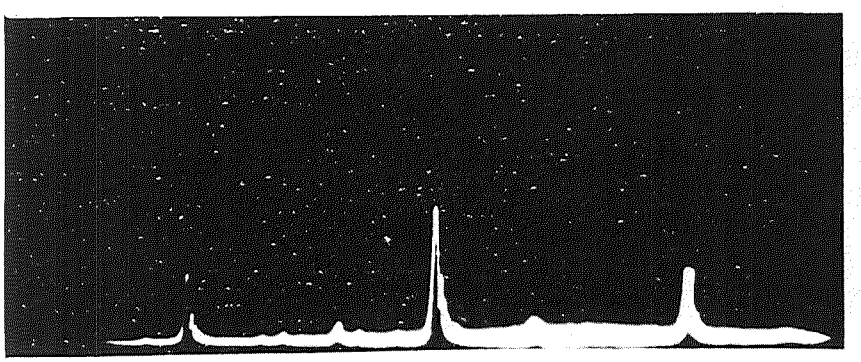

Fig. 34--Adaptive rejection of interfering signal.

sidebands 20 kHz each side of the carrier. The pictures again show the spectra before and after adaptation.

Finally, Fig. 35 shows a case involving noise modulation on the interfering signal. Photo (a) shows the spectrum of the desired signal alone. (The carrier of the desired signal was used for the reference signal.) Photo (b) shows the output from the array when the interference is added, but before adaptation. Photo (c) shows the output again after adaptation.

The photograph in Fig. 35 appears blurred because the spectrum analyzer is approaching the limit of its frequency resolution capability. In order to determine how close in frequency the interfering signal could be to the desired signal and still be rejected, a Collins 75S2 receiver was used to obtain the spectra of Figs. 36 through 38. This receiver was able to resolve 65 MHz signals separated by 1 KHz.

Figure 36 shows the typical results obtained when the interference is outside the information band. Figure 37 shows the performance when a modulated interfering signal is inside the information band. Finally Fig. 38 shows the capability of the system to reject an undesired signal only 1 KHz away from the desired carrier. It is expected that the interference would be rejected as long as the frequency separation between the desired and interfering signals is more than the feedback loop bandwidth; this was about 50 Hz for the measurements reported here. For a particular system this bandwidth is chosen as a compromise between desired

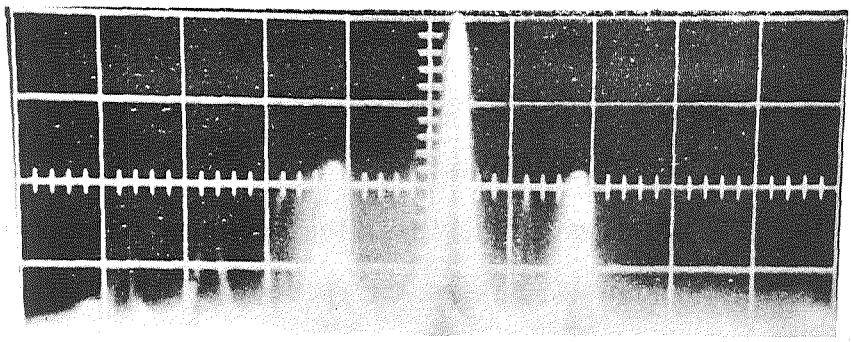

(a) SPECTRUM OF DESIRED SIGNAL

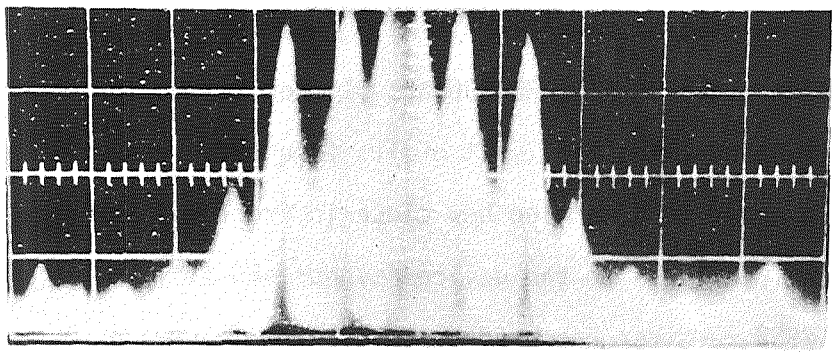

(b) ARRAY OUTPUT SPECTRUM BEFORE ADAPTATION
(DESIRED) SIGNAL PLUS INTERFERING SIGNAL

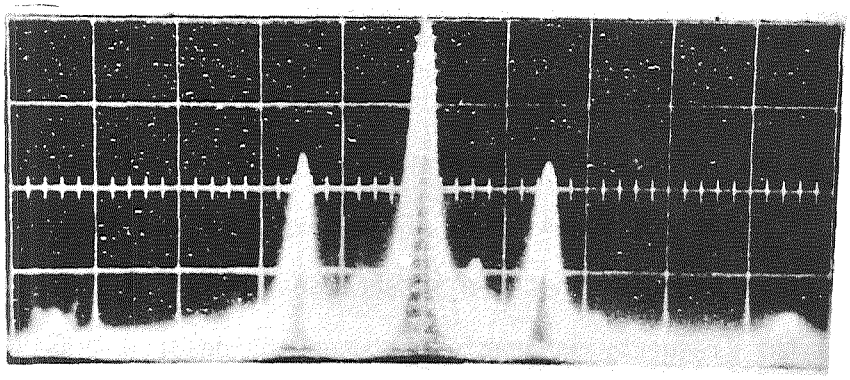

(c) ARRAY OUTPUT SPECTRUM AFTER ADAPTATION
(DESIRED) SIGNAL PLUS INTERFERING SIGNAL

Fig. 35--Adaptive rejection of interfering signal.

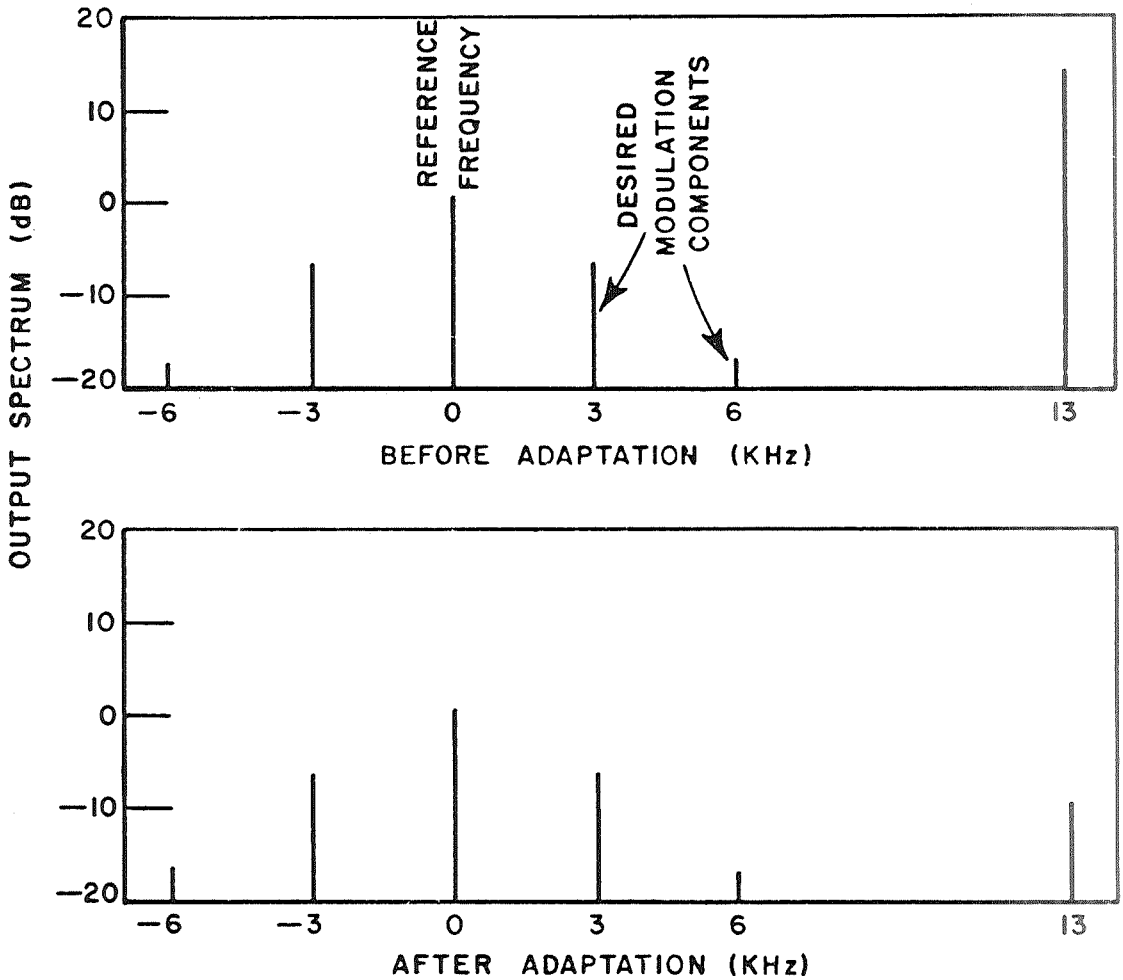

Fig. 36--Improvement in interference rejection over a conventional phased array (interference outside information bandwidth).

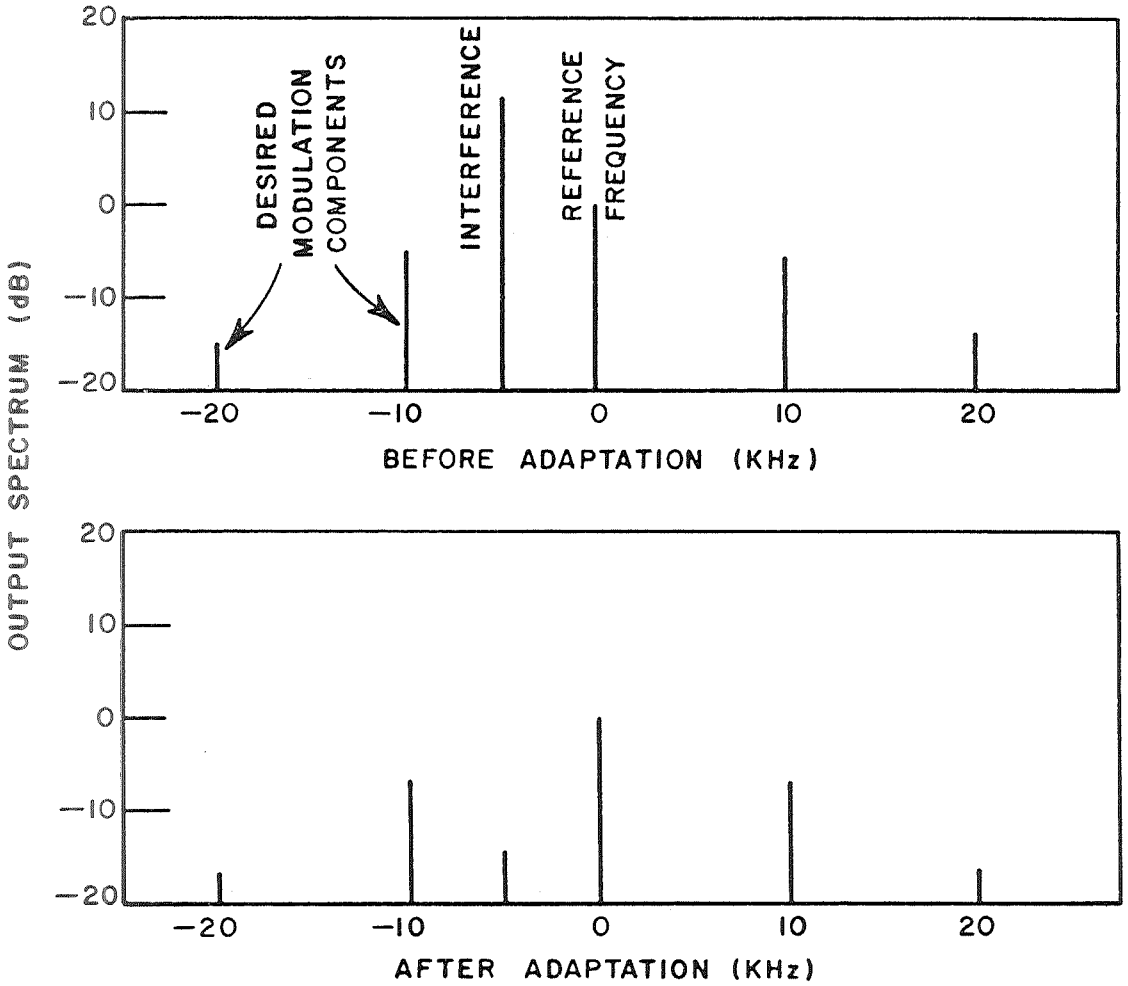

Fig. 37--Improvement in interference rejection over a conventional phased array (interference inside information bandwidth).

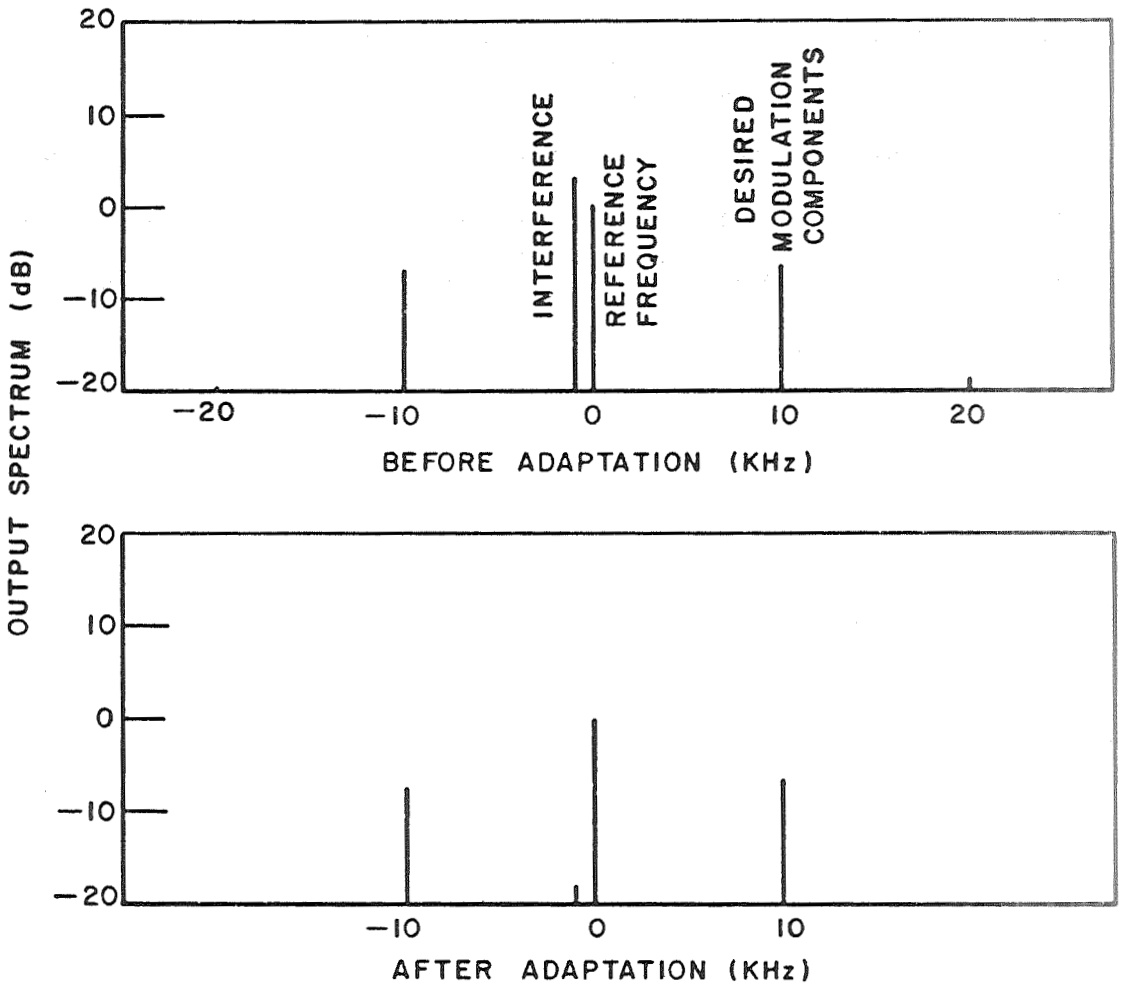

Fig. 38--Improvement in interference rejection over a conventional bandwidth).

speed of response, minimum frequency offset between desired and interfering signals, and maximum frequency offset between the desired carrier and reference signal.

The manner in which the adaptive feedback cleans out the interference in these tests is very impressive, and it is clear that these antennas have considerable potential for applications where interference rejection is needed.

CHAPTER V
CONCLUSIONS

This report has shown how it is possible to improve the output SNR of receiving arrays with signal processing techniques.

In Chapter II the element weighting coefficients (amplitude and phase) which maximize SNR were derived for the case of uniform background sky noise plus internally generated noise. A particular array model, dipoles over a ground plane, was analyzed in detail to show the effect of such phenomena as mutual coupling. In particular it was shown that this optimum SNR was only slightly better than that which could be obtained by a much simpler technique of uniform amplitude-coherent combining (i.e., phase locking).

In Chapter III the case of coherent jamming signals was considered. A signal processing scheme based on a feedback algorithm determined by a steepest descent minimization of error was described. It was shown that this is equivalent to maximizing output SNR for many cases. The array was found to be capable of automatically tracking a desired signal, while automatically rejecting an interfering signal.

In Chapter IV experimental verification of the theory described in Chapter III was presented.

A number of experiments were performed on a two-element S-band array, including

(1) measurements of the ability of the processing units to track phase and amplitude of the desired signal (Figs. 19 and 20),

(2) measurements of the "adaptivity" of the array (Figs. 21 and 22),

(3) measurements of antenna patterns obtained with interference present (Figs. 23-27),

(4) measurements of the transient response of the system (Fig. 31), and

(5) measurements of the interference rejection capabilities with modulated signals (Figs. 33-38).

The tests described show that these antennas have considerable potential for applications where interference rejection is needed. The signal processing equipment is straightforward and can be constructed with readily available components.

APPENDIX I
BACKGROUND SKY NOISE

This appendix presents some additional information about the background sky noise and antenna temperature concept which was discussed earlier in Chapter II.

All objects above zero degrees Kelvin emit electromagnetic radiation. The amount of radiation emitted can be calculated quite accurately by using the Rayleigh-Jeans low frequency approximation to Planck's law of radiation. Planck's law for a blackbody radiator is given by the equation

$$J = \frac{2hf^3}{c^2} \Delta f \left[\frac{1}{\epsilon^{\frac{hf}{kT}} - 1} \right] \frac{\text{watts}}{\text{m}^2 - \text{sterad}} \tag{77}$$

where

J = emitted power per unit area of its surface per unit solid angle

c = velocity of light = 3×10^8 meters/sec

h = 6.623×10^{-34} joule-sec (Planck's const)

k = 1.38×10^{-23} joule/^{o}K (Boltzmann's const)

T = thermometric temperature of the radiating body in degrees Kelvin

Δf = incremental bandwidth.

The Rayleigh-Jeans approximation then makes use of the fact that $hf << kT$ for temperatures above a few degrees Kelvin in the microwave region, to provide a much simpler expression for emitted power. The exponential term can be expanded into a power series; only the first two terms need be retained so that

$$(78) \qquad J = \frac{2hf^3}{c^2}\,\Delta f\left[\frac{1}{\frac{hf}{kT}}\right] = \frac{2k^2kT\Delta f}{c^2} = \frac{2kT\Delta f}{\lambda^2} \quad \frac{\text{watts}}{\text{m}^2 - \text{sterad}} \,.$$

It is now necessary to relate the power emitted by an object to the power received at the terminals of a single antenna. Consider an ideal antenna which has a very small uniform beamwidth Ω_{ant} steradians and no other side or back lobes. The small beam area of the antenna assures that the object will present a constant temperature to the antenna. If the blackbody object is at T_o degrees Kelvin then the power received at the terminals of the antenna is:

$$(79) \qquad P_{ant} = \frac{1}{2} J A_{em} \Omega_{ant}$$

A_{em} is the maximum effective collecting aperture of the antenna and is given by

$$(80) \qquad A_{em} = \frac{\lambda^2}{4\pi} D_{max} = \frac{\lambda^2}{4\pi} \text{ [maximum directivity]} \,.$$

The factor of ½ is due to the assumed randomness of polarization of the emitted radiation, so that only half the incident power will be absorbed by the antenna. Thus

$$(81) \qquad P_{ant} = \frac{1}{2}\left[\frac{2kT\Delta f}{\lambda^2}\right] A_{em}\,\Omega_{ant}.$$

Using the expression for A_{em} and cancelling

$$(82) \qquad P_{ant} = k\,T_o\Delta f.$$

Since the standard definition of antenna temperature T_a is given by $P_{ant} = k\,T_a\Delta f$, the antenna temperature at the receiving terminals of the ideal antenna is exactly equal to the physical temperature of the blackbody radiator.

Since blackbody radiators are rarely encountered in practice it is necessary to introduce the concept of equivalent brightness temperature of a real body. The equivalent brightness or apparent radiometric temperature (T_{eq}) of any body is defined as the temperature of an ideal blackbody situated at the same position as the original body and emitting the same radiation intensity to the point of observation. The power density from a real body is then

$$J = \frac{2kT_{eq}}{\lambda^2}\,\Delta f\,\frac{\text{watt}}{\text{m}^2 - \text{sterad}}\,.$$

Returning again to the relationship between the antenna temperature and the effective brightness temperature, consider an ideal antenna (refer to Fig. A1) which has only a single pencil beam, described by its normalized antenna pattern function $f(\theta',\phi')$. Assuming that the object under observation is large enough so that its equivalent temperature is constant over the area covered by

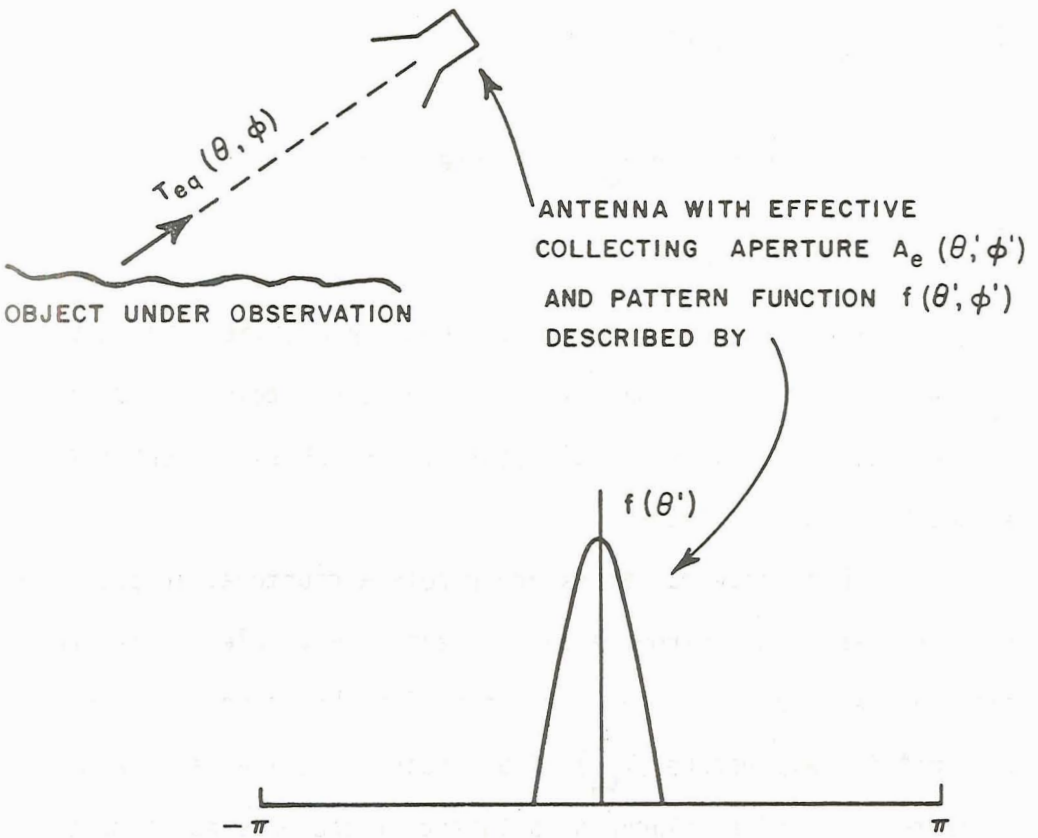

Fig. A1--Antenna description.

the antenna beam, the power received at the terminals of the antenna is

$$(84) \quad P_{ant} = \frac{J(\theta,\phi)}{2} \iint A_e(\theta',\phi')d\Omega = 2kT_{eq}(\theta,\phi) \frac{\Delta f A_{em}}{2\lambda^2} \iint f(\theta',\phi')d\Omega$$

but

$$(85) \quad A_{em} = \frac{D_{max}\lambda^2}{4\pi} = \frac{\lambda^2}{\iint f(\theta',\theta')d\Omega}$$

so that one obtains $P_{ant} = kT_{eq}(\theta,\phi)\,\Delta f$ and the equivalent brightness

temperature of the body is equal to the antenna temperature of an ideal antenna.

It must be realized, however, that in practice antennas do not have the ideal pattern assumed above, but in fact accept some radiation from every direction. For this case the equivalent brightness temperature is related to the antenna temperature by*

$$(87)\quad T_{ant}(\theta_o) = \frac{\int_0^{2\pi}\int_0^{\pi} T(\theta)\, f(\theta',\phi') \sin\theta'\, d\theta'\, d\phi'}{\int_0^{2\pi}\int_0^{\pi} f(\theta',\phi') \sin\theta'\, d\theta'\, d\phi'}$$

or more generally the antenna temperature is the weighted average of all radiometric temperatures where

---

*In fact, Eq. (87) should be replaced by

$$(86)\quad T_{ant}(\theta_o) = \frac{\sum_{i=1}^{2}\int_0^{2\pi}\int_0^{\pi} T_i(\theta) f_i(\theta',\phi') \sin\theta'\, d\theta'\, d\phi'}{\sum_{i=1}^{2}\int_0^{2\pi}\int_0^{\pi} f_i(\theta',\phi') \sin\theta'\, d\theta'\, d\phi'}$$

where $f_1(\theta',\phi')$ is the antenna pattern measured with the design polarization and $T_1(\theta)$ is the temperature of radiation impinging on the antenna with that polarization; $f_2(\theta',\phi')$ is the antenna pattern for polarization state orthogonal to the design polarization and $T_2(\theta)$ is the incident radiation of corresponding polarization. In practice the cross polarized term is small for a well designed antenna, and contributes only a degree or two to T_{ant}.

$T_{ant}(\theta_o)$ is the antenna temperature in the direction θ_o

$T(\theta)$ is the radiometric temperature distribution

$f(\theta',\phi')$ is the normalized antenna power pattern function which acts as the weighting function

$\sin\theta' \, d\theta' \, d\phi'$ is the element of solid angle.

The above discussion has been concerned with a single antenna but the results apply equally well for an array of antennas if that system is passive, lossless, and reciprocal. For this case $f(\theta',\phi)$ would be the power pattern function of the entire array rather than the pattern of a particular antenna element.

If the array is lossy, non-reciprocal, or contains active devices, such as amplifiers, then the appropriate expression for output power due to sky noise is

$$P_N = \iint B(\theta,\phi) \, A_e(\theta',\phi') d\Omega \tag{88}$$

where

$B(\theta,\phi)$ is the brightness or power density per solid angle in the direction θ,ϕ

$A_e(\theta',\phi')$ is the effective receiving aperture of the array in the direction θ',ϕ'

In practice it is quite difficult to determine the actual values of brightness or radiometric temperature to use in these expressions for output noise power. There are, however, several sky and surface models whose radiometric temperature can be predicted.

Sky Model

In the microwave region almost all of the atmospheric radiation is due to oxygen and water vapor absorption. The percentage of oxygen in the atmosphere remains almost constant as a function of time but the water vapor content may have a seasonal variation of twenty to one; hence the radiometric temperature of the sky is not a constant, but if the pressure, temperature, and water vapor are known the attenuation per unit length and hence the radiometric temperature can be computed using formulas derived by Van Vleck.[10]

The most commonly used model for determining sky temperature distributions is to assume a planar earth; for this case the path length over which absorption occurs is proportional to the secant of the angle from zenith. This assumption of a plane earth gives good accuracy for angles less than about 80^{o} from zenith.

A convenient form for determining the sky temperature as a function of angle is given by Wulfsberg[11]

$$(89)\quad T_{sky}(\theta) = (1-\alpha_o^{\text{secant }\theta})\, T_m$$

where

α_o is fractional transmission of atmosphere at zenith (θ=0)

T_m is the mean absorption temperature, which for clear sky conditions can be expressed as $T_m = 1.2\, T_{ground} - 50^{o}K$.

Extensive experimental measurements of sky temperature at several microwave frequencies have been made by Air Force Cambridge Laboratories[11] under various meteorological conditions

and the results agree quite well with calculations based on this simple model.

Smooth Surfaces

Another model which can be analyzed quite easily is the very smooth surface. Consider an antenna looking at a smooth planar surface at some angle of incidence θ_o. For terrestrial surfaces the transmissibility is zero so that the radiometric temperature is composed of two components, radiation which is emitted by the surface, and radiation from the atmosphere which is reflected by the surface.

The radiometric temperature can then be computed from the reflection coefficient since

$$T_{rv} = |\dot{r}_v|^2 T^v_{sky}(\theta) + (1 - |\dot{r}_v|^2)T_g \tag{90}$$

$$T_{rh} = |\dot{r}_h|^2 T^h_{sky}(\theta) + (1 - |\dot{r}_h|^2)T_g \tag{91}$$

where

$\dot{r}_v \dot{r}_h$ = reflection coefficient for vertical and horizontal polarization

T_{rv}, T_{rh} = vertically and horizontally polarized components of radiometric temperature

$T^v_{sky}(\theta_o), T^h_{sky}(\theta_o)$ = vertically and horizontally polarized components of radiometric sky temperature in direction θ_o

T_g = thermodynamic temperature of object.

$$\dot{r}_h = \frac{\dot{\mu}\cos\theta_o - \mu_o\sqrt{\omega^2\dot{\mu}\dot{\varepsilon} - k_o^2\sin^2\theta_o}}{\dot{\mu}\cos\theta_o + \mu_o\sqrt{\omega^2\dot{\mu}\dot{\varepsilon} - k_o\sin^2\theta_o}}$$

(92)

$$\dot{r}_v = \frac{\dot{\varepsilon}k_o\cos\theta_o - \varepsilon_o\sqrt{\omega^2\dot{\mu}\dot{\varepsilon} - k_o^2\sin^2\theta}}{\dot{\varepsilon}k_o\cos\theta_o + \varepsilon_o\sqrt{\omega^2\dot{\mu}\dot{\varepsilon} - k_o^2\sin^2\theta}}$$

where

$\dot{r}_h$ = complex reflection coefficient for horizontal polarization

$\dot{r}_v$ = complex reflection coefficient for vertical polarization

$\dot{\mu}$ = complex permeability of object

$\dot{\varepsilon}$ = complex dielectric constant of object

μ_o = free space permeability

ε_o = free space permittivity

$k_o^2 = \omega^2\mu_o\varepsilon_o$.

A case of particular interest is when the object is non-magnetic, that is $\mu = \mu_o$. Under this condition the radiometer equations for a smooth surface reduce to

$$T_{rh} = \left|\frac{\cos\theta_o - \sqrt{\varepsilon_r - \sin^2\theta_o}}{\cos\theta_o + \sqrt{\varepsilon_r - \sin^2\theta_o}}\right|^2 T^h_{sky}(\theta_o) + \left[1 - \left|\frac{\cos\theta_o - \sqrt{\varepsilon_r - \sin^2\theta_o}}{\cos\theta_o + \sqrt{\varepsilon_r - \sin^2\theta_o}}\right|^2\right] T_g$$

(93)

$$T_{rv} = \left|\frac{\varepsilon_r\cos\theta_o - \sqrt{\varepsilon_r - \sin^2\theta_o}}{\varepsilon_r\cos\theta_o + \sqrt{\varepsilon_r - \sin^2\theta_o}}\right|^2 T^v_{sky}(\theta_o) + \left[1 - \left|\frac{\varepsilon_r\cos\theta_o - \sqrt{\varepsilon_r - \sin^2\theta_o}}{\varepsilon_r\cos\theta_o + \sqrt{\varepsilon_r - \sin^2\theta_o}}\right|^2\right] T_g$$

where $\varepsilon_r = \frac{\dot{\varepsilon}}{\varepsilon_o}$ relative dielectric constant.

It is interesting to note that the reflection coefficient for vertical polarization is zero when $\tan \theta = \sqrt{\varepsilon_r}$ (Brewster's angle) and for this particular angle the radiometric temperature should be exactly equal to the thermal temperature of the object.

Figures A2 and A3 show some typical calculated and measured results for the sky model and the smooth surface model.

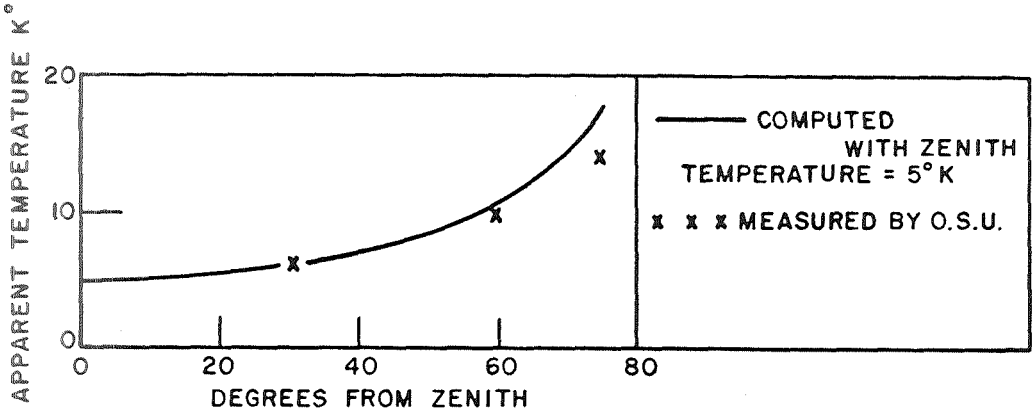

Fig. A2--X band sky profile.

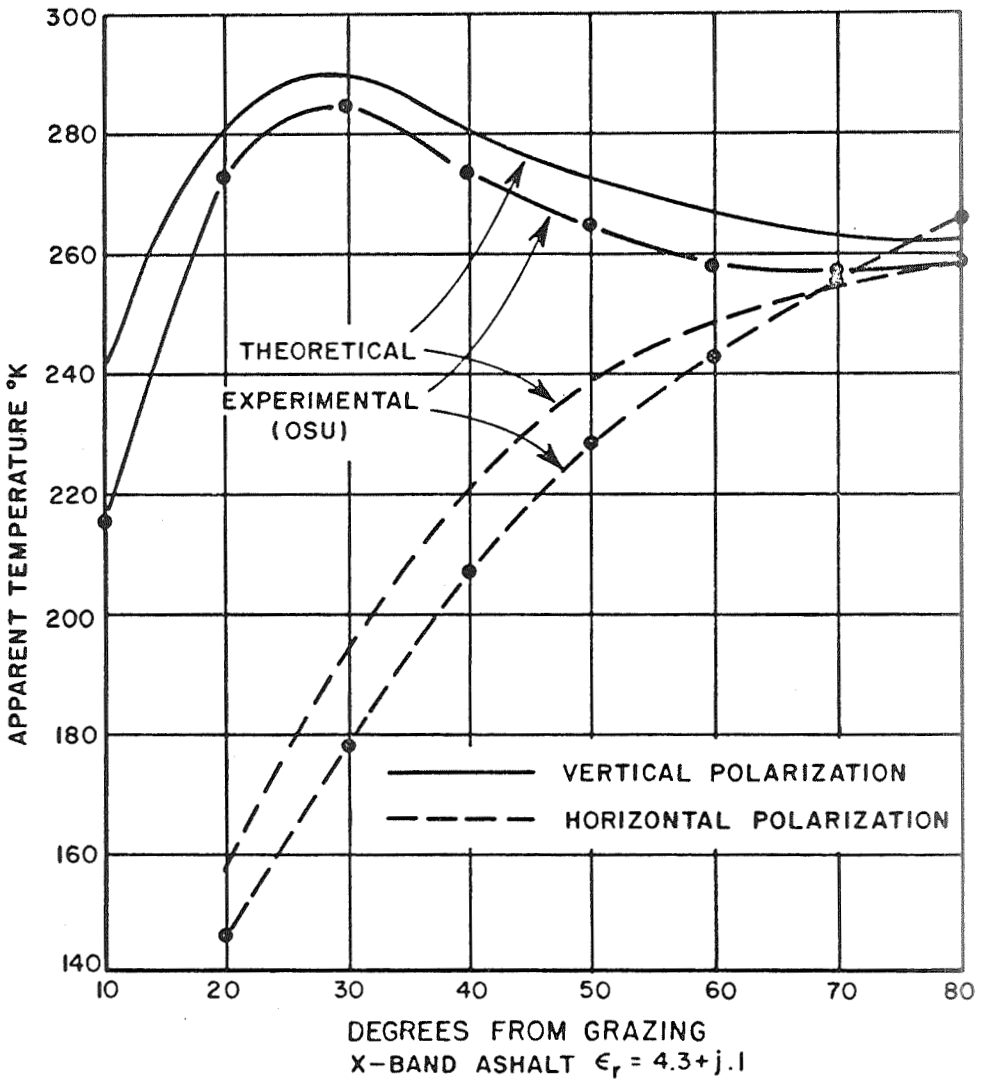

Fig. A3--X band asphalt.

APPENDIX II
ARRAY IMPEDANCE

This appendix contains some additional comments about array impedance. It was pointed out in Chapter II that one set of parameters which gave a complete description of the receiving array performance was the set of open circuit voltages plus the mutual impedance matrix. This matrix consists of the self impedance Z_{ii} of each element and the mutual impedance Z_{ij} between the ith and jth element. For a specified frequency and array geometry (i.e., element type, spacing, etc.) these impedances are constant. That is, they are independent of load termination and angle of arrival of the incident wave. For completeness tables 1 through 4 present a list of these impedances computed (see Appendix IV) for several interelement spacings, number of elements, and dipole diameters.

Another system of parameters which form a complete set for the description of the receiving properties of the array is the Thevenin equivalent circuit. Figure A4 shows this circuit representation; here E_i represents a voltage generator and Z^{TH}_i represent the Thevenin impedance of the ith element. The procedures required to evaluate these parameters can be seen by considering a two element array.

TABLE 1

Mutual impedances for half-wavelength dipoles placed quarter-wavelength over a ground plane.

I	J	R(I,J)	X(I,J)
1.0000000	1.0000000	115.4478111	68.2558241
	(a/λ = 0.007)		
1.0000000	1.0000000	90.2554493	73.0602198
	(a/λ = 0.000001)		
1.0000000	1.0000000	114.1435442	71.0355806
1.0000000	2.0000000	3.7978095	-45.3746324
1.0000000	3.0000000	-9.7650292	17.2897501
1.0000000	4.0000000	7.0951781	-7.6637405
2.0000000	2.0000000	113.4529676	73.7050257
2.0000000	3.0000000	4.3404632	-46.2369814
2.0000000	4.0000000	-9.7650372	17.2897396
3.0000000	3.0000000	113.4529581	73.7050266
3.0000000	4.0000000	3.7978113	-45.3746357
4.0000000	4.0000000	114.1435194	71.0355635
	(0.5λ SPACING, a/λ = 0.007)		
1.0000000	1.0000000	90.0107689	73.2942381
1.0000000	2.0000000	11.3742318	-32.9435415
1.0000000	3.0000000	-9.6041082	9.2256449
1.0000000	4.0000000	5.6664523	-3.4311553
2.0000000	2.0000000	89.8296089	73.5404062
2.0000000	3.0000000	11.4600917	-32.9991550
2.0000000	4.0000000	-9.6041104	9.2256366
3.0000000	3.0000000	89.8296022	73.5404387
3.0000000	4.0000000	11.3742332	-32.9435444
4.0000000	4.0000000	90.0107574	73.2942991
	(0.5λ SPACING, a/λ = 0.000001)		
1.0000000	1.0000000	107.8230095	41.7797103
1.0000000	2.0000000	106.6896753	-4.3821549
1.0000000	3.0000000	87.3056936	-44.5983925
1.0000000	4.0000000	55.6918511	-65.9761267
2.0000000	2.0000000	119.7950525	26.9127176
2.0000000	3.0000000	112.6154957	-13.2782221
2.0000000	4.0000000	87.3057003	-44.5984011
3.0000000	3.0000000	119.7950506	26.9126925
3.0000000	4.0000000	106.6896753	-4.3821793
4.0000000	4.0000000	107.8229961	41.7796679
	(0.1λ SPACING, a/λ = 0.0007)		

TABLE 2

Mutual impedances for half-wavelength dipoles placed quarter-wavelength over a ground plane

I	J	R(I, J)	X(I,J)
1.0000000	1.0000000	114.0536451	70.9792128
1.0000000	2.0000000	3.9505562	-45.3052120
1.0000000	3.0000000	-10.0413766	17.2312865
1.0000000	4.0000000	7.6412933	-7.7723015
1.0000000	5.0000000	-5.4416318	3.9705002
1.0000000	6.0000000	3.9196656	-2.2301445
1.0000000	7.0000000	-2.8944118	1.3548515
1.0000000	8.0000000	2.1891521	-0.8818871
1.0000000	9.0000000	-1.6807685	0.6105804
1.0000000	10.0000000	1.2741199	-0.4310103
2.0000000	2.0000000	113.1976137	73.6291971
2.0000000	3.0000000	4.7907727	-46.2081203
2.0000000	4.0000000	-10.6087363	17.5983424
2.0000000	5.0000000	8.0226188	-7.9411390
2.0000000	6.0000000	-5.7048934	4.0567622
2.0000000	7.0000000	4.1049795	-2.2799471
2.0000000	8.0000000	-3.0226901	1.3886070
2.0000000	9.0000000	2.2647576	-0.9074702
2.0000000	10.0000000	-1.6807677	0.6105825
3.0000000	3.0000000	112.6930933	73.8353157
3.0000000	4.0000000	5.0842679	-46.2514472
3.0000000	5.0000000	-10.7890786	17.5980396
3.0000000	6.0000000	8.1379451	-7.9309945
3.0000000	7.0000000	-5.7781882	4.0478979
3.0000000	8.0000000	4.1446416	-2.2762228
3.0000000	9.0000000	-3.0226897	1.3886085
3.0000000	10.0000000	2.1891447	-0.8819038
4.0000000	4.0000000	112.5347490	73.8216057
4.0000000	5.0000000	5.1751134	-46.2308631
4.0000000	6.0000000	-10.8415928	17.5822306
4.0000000	7.0000000	8.1638591	-7.9228923
4.0000000	8.0000000	-5.7781867	4.0478968
4.0000000	9.0000000	4.1049795	-2.2799351
4.0000000	10.0000000	-2.8944106	1.3548520
5.0000000	5.0000000	112.4876642	73.8047285
5.0000000	6.0000000	5.1961714	-46.2220569
5.0000000	7.0000000	-10.8415962	17.5822222
5.0000000	8.0000000	8.1379448	-7.9309895
5.0000000	9.0000000	-5.7048933	4.0567632
5.0000000	10.0000000	3.9196651	-2.2301507
6.0000000	6.0000000	112.4876595	73.8047276
6.0000000	7.0000000	5.1751179	-46.2308669
6.0000000	8.0000000	-10.7890872	17.5980217
6.0000000	9.0000000	8.0226234	-7.9411142
6.0000000	10.0000000	-5.4416298	3.9704917
7.0000000	7.0000000	112.5347385	73.8216057
7.0000000	8.0000000	5.0842732	-46.2514338
7.0000000	9.0000000	-10.6087303	17.5983367
7.0000000	10.0000000	7.6412986	-7.7722755
8.0000000	8.0000000	112.6930571	73.8352871
8.0000000	9.0000000	4.7907779	-46.2081084
8.0000000	10.0000000	-10.0413858	17.2312651
9.0000000	9.0000000	113.1975718	73.6291752
9.0000000	10.0000000	3.9505682	-45.3052006
10.0000000	10.0000000	114.0535746	70.9791937

(0.5 λ SPACING, $a/\lambda = 0.007$

TABLE 3

Mutual impedances for half-wavelength dipoles placed quarter-wavelength over a ground plane

I	J	R(I,J)	X(I,J)
1.0000000	1.0000000	90.0059433	73.2886896
1.0000000	2.0000000	11.3828173	-32.9356408
1.0000000	3.0000000	-9.6220664	9.2147846
1.0000000	4.0000000	5.7129207	-3.4257744
1.0000000	5.0000000	-3.5914099	1.5770701
1.0000000	6.0000000	2.4220351	-0.8405679
1.0000000	7.0000000	-1.7294828	0.4973517
1.0000000	8.0000000	1.2909504	-0.3182062
1.0000000	9.0000000	-0.9967629	0.2166791
1.0000000	10.0000000	0.7871012	-0.1546112
2.0000000	2.0000000	89.8145847	73.5294914
2.0000000	3.0000000	11.4909278	-32.9853501
2.0000000	4.0000000	-9.6804985	9.2271054
2.0000000	5.0000000	5.7479261	-3.4287584
2.0000000	6.0000000	-3.6142225	1.5773940
2.0000000	7.0000000	2.4377499	-0.8402748
2.0000000	8.0000000	-1.7404720	0.4972012
2.0000000	9.0000000	1.2977906	-0.3186495
2.0000000	10.0000000	-0.9967627	0.2166821
3.0000000	3.0000000	89.7686853	73.5279083
3.0000000	4.0000000	11.5130903	-32.9795890
3.0000000	5.0000000	-9.6928712	9.2222940
3.0000000	6.0000000	5.7555121	-3.4252595
3.0000000	7.0000000	-3.6190215	1.5750789
3.0000000	8.0000000	2.4404396	-0.8390769
3.0000000	9.0000000	-1.7404720	0.4972012
3.0000000	10.0000000	1.2909498	-0.3182189
4.0000000	4.0000000	89.7586546	73.5228643
4.0000000	5.0000000	11.5183567	-32.9761457
4.0000000	6.0000000	-9.6958163	9.2201569
4.0000000	7.0000000	5.7569752	-3.4241930
4.0000000	8.0000000	-3.6190210	1.5750818
4.0000000	9.0000000	2.4377502	-0.8402652
4.0000000	10.0000000	-1.7294829	0.4973518
5.0000000	5.0000000	89.7561321	73.5207987
5.0000000	6.0000000	11.5194577	-32.9751816
5.0000000	7.0000000	-9.6958179	9.2201517
5.0000000	8.0000000	5.7555121	-3.4252595
5.0000000	9.0000000	-3.6142229	1.5773987
5.0000000	10.0000000	2.4220355	-0.8405751
6.0000000	6.0000000	89.7561226	73.5208397
6.0000000	7.0000000	11.5183645	-32.9761467
6.0000000	8.0000000	-9.6928740	9.2222815
6.0000000	9.0000000	5.7479272	-3.4287401
6.0000000	10.0000000	-3.5914093	1.5770644
7.0000000	7.0000000	89.7586365	73.5228596
7.0000000	8.0000000	11.5130889	-32.9795814
7.0000000	9.0000000	-9.6804947	9.2271050
7.0000000	10.0000000	5.7129217	-3.4257562
8.0000000	8.0000000	89.7686701	73.5279598
8.0000000	9.0000000	11.4909285	-32.9853473
8.0000000	10.0000000	-9.6220694	9.2147729
9.0000000	9.0000000	89.8145514	73.5295401
9.0000000	10.0000000	11.3828216	-32.9356413
10.0000000	10.0000000	90.0059128	73.2887220

(0.5 λ SPACING, a/λ = 0.007)

TABLE 4

Mutual impedances for half-wavelength dipoles placed quarter-wavelength over a ground plane

I	J	R(I, J)	X(I, J)
1.0000000	1.0000000	108.5694008	47.5149937
1.0000000	2.0000000	104.8336029	1.9040360
1.0000000	3.0000000	82.2882748	-39.3902106
1.0000000	4.0000000	47.5651307	-63.7575197
1.0000000	5.0000000	9.5742015	-67.3936434
1.0000000	6.0000000	-22.6763697	-52.2415347
1.0000000	7.0000000	-42.4302673	-24.8814468
1.0000000	8.0000000	-46.8388138	5.5613376
1.0000000	9.0000000	-37.4422045	30.0353756
1.0000000	10.0000000	-19.3915830	41.9230771
2.0000000	2.0000000	114.9727516	32.5586176
2.0000000	3.0000000	105.0098057	-10.2410731
2.0000000	4.0000000	77.8872147	-46.1379061
2.0000000	5.0000000	40.4836049	-64.1881132
2.0000000	6.0000000	1.7812396	-62.3697081
2.0000000	7.0000000	-29.5050471	-44.0920849
2.0000000	8.0000000	-47.2008996	-16.7071426
2.0000000	9.0000000	-49.1454520	10.7511064
2.0000000	10.0000000	-37.4422178	30.0353892
3.0000000	3.0000000	110.8170729	25.9226706
3.0000000	4.0000000	98.3512259	-10.8208605
3.0000000	5.0000000	70.4526167	-41.6133494
3.0000000	6.0000000	33.7844133	-56.7907524
3.0000000	7.0000000	-3.0905012	-54.9883113
3.0000000	8.0000000	-31.9828107	-39.4697952
3.0000000	9.0000000	-47.2009153	-16.7071011
3.0000000	10.0000000	-46.8388305	5.5613940
4.0000000	4.0000000	103.4871559	30.2575455
4.0000000	5.0000000	91.7004814	-3.8080320
4.0000000	6.0000000	65.5209513	-34.6820970
4.0000000	7.0000000	31.2075570	-52.4955344
4.0000000	8.0000000	-3.0905417	-54.9882894
4.0000000	9.0000000	-29.5050998	-44.0920324
4.0000000	10.0000000	-42.4303088	-24.8813868
5.0000000	5.0000000	98.5409002	37.0384464
5.0000000	6.0000000	89.0846233	0.3257525
5.0000000	7.0000000	65.5209227	-34.6820865
5.0000000	8.0000000	33.7843471	-56.7907252
5.0000000	9.0000000	1.7811590	-62.3696680
5.0000000	10.0000000	-22.6764336	-52.2414856
6.0000000	6.0000000	98.5408735	37.0384526
6.0000000	7.0000000	91.7004328	-3.8080202
6.0000000	8.0000000	70.4525423	-41.6133451
6.0000000	9.0000000	40.4835086	-64.1881132
6.0000000	10.0000000	9.5741208	-67.3936310
7.0000000	7.0000000	103.4870796	30.2575352
7.0000000	8.0000000	98.3511400	-10.8208807
7.0000000	9.0000000	77.8871136	-46.1379504
7.0000000	10.0000000	47.5650411	-63.7575436
8.0000000	8.0000000	110.8169870	25.9225991
8.0000000	9.0000000	105.0097265	-10.2411596
8.0000000	10.0000000	82.2881994	-39.3902802
9.0000000	9.0000000	114.9726906	32.5584688
9.0000000	10.0000000	104.8335505	1.9039469
10.0000000	10.0000000	108.5693150	47.5148735

(0.5 λ SPACING, a/λ = 0.007)

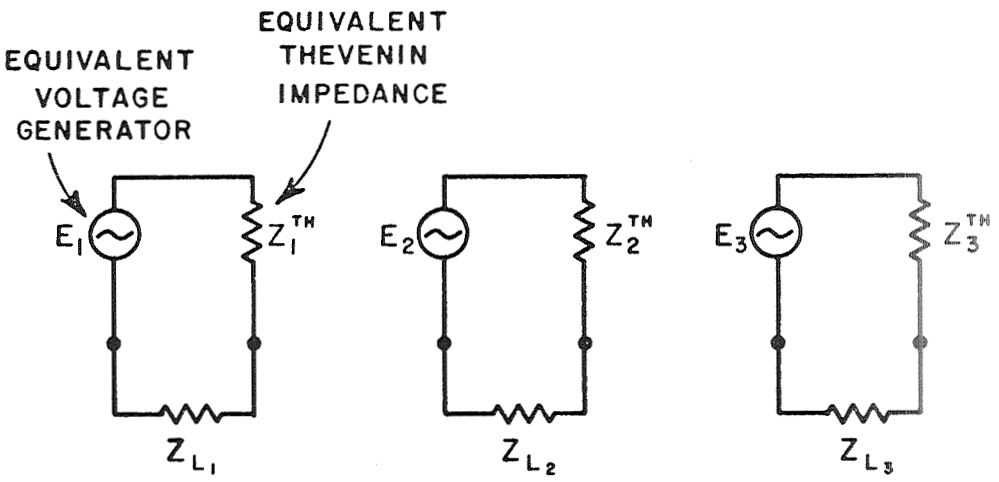

Fig. A4--Thevenin equivalent circuit representation of receiving array.

Z_1^{TH} the impedance seen looking into the terminals of element 1 can be found by evaluating the ratio V_1/I_1 with all internal sources set to zero. (An alternate method is to compute the ratio of open circuit voltage to short circuit current.) For this condition

(94) $$V_1 = Z_{11}I_1 + Z_{12}I_2$$

$$V_2 = Z_{21}I_1 + Z_{22}I_2 = -I_2Z_{L2}$$

where V_1, V_2 = terminal voltage at element 1 and 2 due to a single generator placed at the terminals of element 1.

$Z_{ij} = Z_{ji}$ = the mutual impedance between the ith and jth element.

Z_{L2} = load impedance placed across the terminals of element 2.

Solving this system of equations yields

$$Z_1^{TH} = \frac{Z_{11}Z_{22} + Z_{11}Z_{22} - Z_{12}Z_{21}}{Z_{22} + Z_{L2}} \tag{95}$$

Similarly the expression for Z_2 is given by

$$Z_2^{TH} = \frac{Z_{11}Z_{22} + Z_{22}Z_{L1} - Z_{12}Z_{21}}{Z_{11} + Z_{L1}} \tag{96}$$

To find E_1, the open circuit voltage, we set $I_1 = 0$ hence from Eq. (20)

$$\begin{aligned} E_1 &= V_1^{oc} + Z_{12}I_2 \\ V_2 &= V_2^{oc} + Z_{22}I_2 = -I_2Z_{L2} \end{aligned} \tag{97}$$

or

$$E_1 = V_1^{oc} - \frac{Z_{12}}{Z_{22} + Z_{L2}} \tag{98}$$

Similarly

$$E_2 = V_2^{oc} - \frac{Z_{21}}{Z_{11} + Z_{L1}} \tag{99}$$

It can be seen that the Thevenin impedance is again a constant; i.e., it is independent of amplitude or angle of arrival of an incident plane wave but does depend on the load termination of the other elements. The voltage generator varys in magnitude both with angle of arrival and load impedance.

APPENDIX III
CIRCUIT DIAGRAM FOR PROCESSING UNIT

This section presents the circuit diagram for a signal processor and briefly describes the components used. The schematic is given in Fig. A5. Except for the $\lambda/4$ delay line both the upper and lower halves are symmetrical.

A double-balanced mixer using four matched hot carrier diodes was used to perform the multiplication operation. The excellent balance of the mixer eliminated the need for null balance adjustment and minimized the interaction between the incoming and error signals.

A high gain discrete component operational amplifier with RC feedback was used for the integrator. A unity gain integrated circuit amplifier provided the required sign inversion.

Dual gate field effect transistors were used both to provide gain and to vary the weighting coefficient for each of the four channels of the signal processor. A single gate FET could have been used to provide power gain but the dual gate version is reported to have superior cross-modulation performance and greater dynamic range.

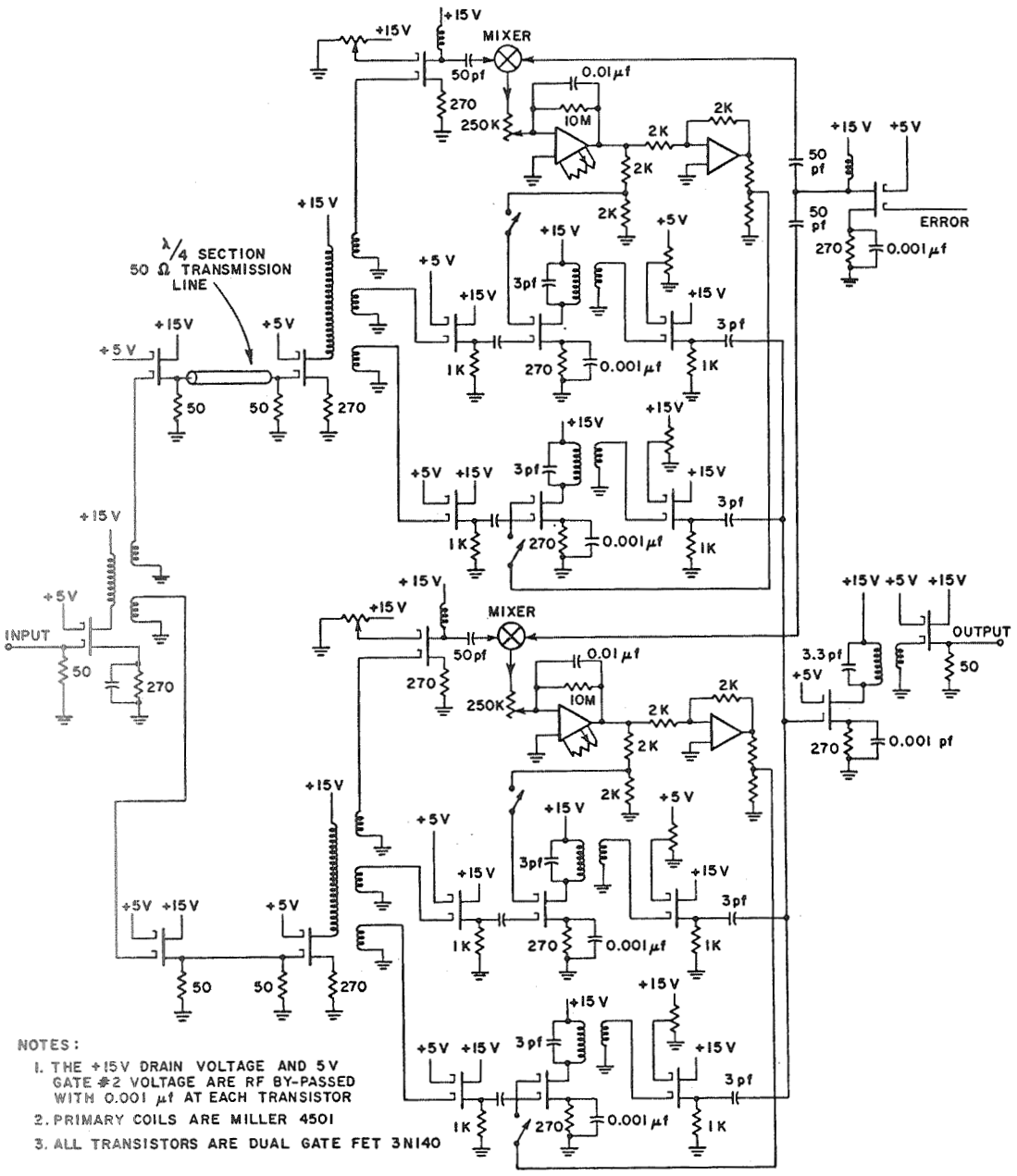

Fig. A5--Circuit diagram for signal processor.

The nearly infinite dc gate impedance of this device provides an excellent means for "freezing" the weighting coefficients. By simply disconnecting the control voltage from the gate, with a switch, the amplifier gain remains constant and one can then run an antenna pattern. The amplifier gain remains constant for several hours with no measurable change from the previous closed loop value.

APPENDIX IV
COMPUTER PROGRAM

For completeness this appendix contains the Fortran IV computer program used to compute the SNR curves of Chapter II. It consists primarily of a modification to a mutual impedance program previously written by Dr. J.H. Richmond. This program calculates the set of open circuit voltages (VOC), mutual impedances (ZMN), load currents (CUR), optimum SNR (SNO), and SNR resulting from uniform combining (SNU) for a linear array of parallel dipoles over a ground plane.

Input data include the number of dipoles (NDIP), interelement spacing in wavelengths (XC), height over ground plane in wavelengths (YC), diameter of dipoles in wavelengths (AL), halflength of dipole in wavelength (HL), and load impedance (ZL).

A detailed description of the electromagnetic principles involved in the numerical analysis can be found in Reference 12.

```
1    FORMAT(1X,8E15.7)
2    FORMAT(1X,8E15.7)
5    FORMAT(1H0)
7    FORMAT(7E10.5)
8    FORMAT(7I10)
11   FORMAT(1H1)
     COMPLEX ZMNP(15,15)
     COMPLEX ZL
     COMPLEX VOC(15)
     COMPLEX P(50),Q(50)
     COMPLEX ET1,ET2,EP1,EP2
     COMPLEX ETT(50),EPP(50)
     COMPLEX ETH,EPH
     COMPLEX Y11,Z11,ZIJ
     COMPLEX C(50,50),CJ(50)
     COMPLEX ZIP
     COMPLEX ZMN(15,15)
     COMPLEX YIJ(15,15),CK(15)
     COMPLEX CSC(20,20)
     COMPLEX CUR(15)
     DIMENSION JS(100)
     DIMENSION IPD(100)
     DIMENSION XC(10),YC(10)
     DIMENSION XD(10),YD(10)
     DIMENSION X(200),Y(200),Z(200)
     DIMENSION VOL(15),SNRO(15),SNRU(15)
     IDM=50
     IDK=15
     ISYM=2
     WRITE(6,11)
     TP=6.2831853
     ETA=376.72727
     TIME=CLOCK(.016667)
     WRITE(6,2)TIME
     NS=4
     HL=.25
     AL=.007022
     DO 270 II=1,2
     IF(II.EQ.1) NDIP=4
     IF(II.EQ.2) NDIP=10
     WRITE(6,8) NDIP
     XC(1)=0.
     XC(2)=.1
     XC(3)=.2
     XC(4)=.3
     XC(5)=.4
     XC(6)=.5
     XC(7)=.6
     XC(8)=.7
     XC(9)=.8
     XC(10)=.9
     YC(1)=.25
     YC(2)=.25
     YC(3)=.25
     YC(4)=.25
```

```
      YC(5)=.25
      YC(6)=.25
      YC(7)=.25
      YC(8)=.25
      YC(9)=.25
      YC(10)=.25
      IND=1
      IF(NS.LT.4)NS=4
      IG=NS/2
      NS=2*IG
      ND=NS-1
      JG(1)=IG
      DO 18 I=2,NDIP
      JG(I)=JG(I-1)+ND
   18 CONTINUE
      WRITE(6,8)NS
      N=NDIP*ND
      FIG=IG
      NP=NS+1
      EMC=10.
      WAVE=30000./EMC
      WRITE(6,2)EMC,AL,HL
      WRITE(6,5)
      AK=TP*AL
      HK=TP*HL
      TPL=TP
      DK=HK/FIG
      CDK=COS(DK)
      SDK=SIN(DK)
      DO 20 I=1,NDIP
      XD(I)=TPL*XC(I)
      YD(I)=TPL*YC(I)
   20 CONTINUE
      L=1
      DO 50 J=1,NDIP
      ZZ=-HK
      DO 40 I=1,NP
      X(L)=XD(J)
      Y(L)=YD(J)
      Z(L)=ZZ
      ZZ=ZZ+DK
      L=L+1
   40 CONTINUE
   50 CONTINUE
      J=2
      I=1
      DO 70 K=1,NDIP
      DO 60 L=1,ND
      IPD(I)=J
      J=J+1
      I=I+1
   60 CONTINUE
      J=J+2
   70 CONTINUE
      DO 100 K=1,NDIP
      XK=XD(K)
```

```
      YK=YD(K)
      DO 100 L=K,NDIP
      IF(L.NE.K)GO TO 74
      IF(K.EQ.1)GO TO 74
      DO 76 M=1,ND
      P(M)=Q(M)
76    CONTINUE
      GO TO 82
74    XL=XD(L)
      YL=YD(L)
      DDK=SQRT((XK-XL)**2+(YK-YL)**2)
      IF(L.EQ.K)DDK=AK
      DDP=SQRT((XK-XL)**2+(YK+YL)**2)
      SSK=.0
      DO 80 M=1,ND
      CALL SPARS(DK,CDK,SDK,DDK,SSK,ZIJ)
      CALL SPARS(DK,CDK,SDK,DDP,SSK,ZIP)
      P(M)=ZIJ-ZIP
      IF(L.EQ.K)Q(M)=P(M)
      SSK=SSK+DK
80    CONTINUE
82    CONTINUE
      JB=L*ND
      JA=1+ND*(L-1)
      IB=K*ND
      IA=1+ND*(K-1)
      DO 90 I=IA,IB
      IH=I-IA
      DO 84 J=JA,JB
      JH=J-JA
      M=1+IABS(JH-IH)
      C(I,J)=P(M)
84    CONTINUE
90    CONTINUE
100   CONTINUE
      DO 210 J=1,NDIP
      DO 180 I=1,N
180   CJ(I)=(.0,.0)
      K=JG(J)
      CJ(K)=(1.,0.)
      IF(J.EQ.1)CALL CRCUT1(C,CJ,N,IDM,ISYM,0)
      IF(J.GT.1)CALL CRCUT2(C,CJ,N,IDM,ISYM,0)
      DO 200 I=1,NDIP
      K=JG(I)
      YIJ(I,J)=CJ(K)
200   CONTINUE
      IF(IND.EQ.0)GO TO 210
      K=JG(J)
      PIN=REAL(CJ(K))
      PINT=30.*PIN
      TH=90.
      THR=.0174532*TH
      CTH=COS(THR)
      STH=SIN(THR)
      FIJ=120.*(CDK-COS(DK*CTH))/SDK/STH
      PH=.0
```

```
      DO 208 NTH=1,10
      PHR=.0174532*PH
      CPH=COS(PHR)
      SPH=SIN(PHR)
      DO 202 I=1,N
      J2=IPD(I)
      ANG=X(J2)*STH*CPH+Z(J2)*CTH
      ETT(I)=FIJ*CMPLX(COS(ANG),SIN(ANG))*SIN(Y(J2)*STH*SPH)
  202 CONTINUE
      ETH=(.0,.0)
      DO 204 I=1,N
      ETH=ETH+CJ(I)*ETT(I)
  204 CONTINUE
      GDT=(CABS(ETH)**2)/PINT
      CSC(J,NTH)=(.0,2.)*ETH/ETA
      PH=PH+10.
  208 CONTINUE
  210 CONTINUE
      DO 220 I=1,NDIP
      FI=I
      DO 220 J=I,NDIP
      FJ=J
      C(I,J)=YIJ(I,J)
  220 CONTINUE
      WRITE(6,5)
      DO 250 J=1,NDIP
      DO 230 I=1,NDIP
  230 CK(I)=(.0,.0)
      CK(J)=(1.,0.)
      IF(J.EQ.1)CALL CRCUT1(YIJ,CK,NDIP,IDK,2,0)
      IF(J.GT.1)CALL CRCUT2(YIJ,CK,NDIP,IDK,2,0)
      DO 240 I=1,NDIP
      ZMN(I,J)=CK(I)
  240 CONTINUE
  250 CONTINUE
      DO 260 I=1,NDIP
      FI=I
      DO 260 J=I,NDIP
      FJ=J
      WRITE(6,2)FI,FJ,ZMN(I,J)
  260 CONTINUE
      DO 270 K=1,5
      IF(K.EQ.1) ZL=(50.,0.)
      IF(K.EQ.2) ZL=(100.,0.)
      IF(K.EQ.3) ZL=(50.,-72.)
      IF(K.EQ.4) ZL=(112.,-72.)
      IF(K.EQ.5) ZL=(10000.,10000.)
      WRITE(6,11)
      WRITE(6,2)ZL
      DO 261 I=1,NDIP
      DO 261 J=1,NDIP
  261 ZMNP(I,J)=ZMN(I,J)
      DO 262 I=1,NDIP
  262 ZMNP(I,I)=ZMNP(I,I)+ZL
      DO 360 NTH=1,10
      NPHI=10*(NTH-1)
```

```
      WRITE(6,5)
      WRITE(6,8)NPHI
      DO 330 I=1,NDIP
  330 CK(I)=-CSC(I,NTH)
      CALL CROUT2(YIJ,CK,NDIP,IDK,2,0)
      DO 340 I=1,NDIP
      VOC(I)=-CK(I)
  340 CONTINUE
      IF(NTH.EQ.1)CALL CROUT1(ZMNP,VOC,NDIP,IDK,2,0)
      IF(NTH.GT.1)CALL CROUT2(ZMNP,VOC,NDIP,IDK,2,0)
      DO 346 I=1,NDIP
      CUR(I)=VOC(I)
      WRITE(6,1)CUR(I)
  346 VOL(I)=CABS(ZL*CUR(I))
      SNO=0.
      SUMV=0.
      DO 347 I=1,NDIP
      SNO=SNO+(VOL(I))**2
      SUMV=SUMV+VOL(I)
      FNDIP=NDIP
  347 SNU=(SUMV**2)/FNDIP
      SNRO(NTH)=SNO
      SNRU(NTH)=SNU
  360 CONTINUE
      WRITE(6,11)
      DO 361 NTH=2,10
      RSNO=SNRO(NTH)/SNRO(10)
      RSNU=SNRU(NTH)/SNRO(10)
      NPHI=10*(NTH-1)
      WRITE(6,5)
      WRITE(6,8)NPHI
      XX=10.*ALOG10(RSNO)
      YY=10.*ALOG10(RSNU)
  361 WRITE(6,2)XX,YY
  270 CONTINUE
      TIME=CLOCK(.016667)
      WRITE(6,2)TIME
      STOP
      END
```

GCROUT - FEN SOURCE STATEMENT - IFN(S) -

```
C       SET ISYM=2 IF MATRIX IS SYMMETRIC
C       SET IWR = 0 TO AVOID WRITEOUT
        SUBROUTINE CROUT1(C,S,N,IDM,ISYM,IWR)
    2   FORMAT(1X,8F15.7)
    5   FORMAT(1H0)
        COMPLEX C(IDM,IDM),S(IDM)
        IF(ISYM.NE.2)GO TO 8
        DO 6 I=1,N
        DO 6 J=I,N
        C(J,I)=C(I,J)
    6   CONTINUE
    8   CONTINUE
        DO 10 L=2,N
   10 C(1,L)=C(1,L)/C(1,1)
        DO 20 L=2,N
        LLL=L-1
        DO 20 I=L,N
        DO 11 K=1,LLL
   11 C(I,L)=C(I,L)-C(I,K)*C(K,L)
        IF(L.EQ.I)GO TO 20
        IF(ISYM.EQ.2)GO TO 15
        DO 12 K=1,LLL
   12 C(L,I)=C(I,I)-C(L,K)*C(K,I)
        C(L,I)=C(L,I)/C(L,L)
        GO TO 20
   15 C(L,I)=C(I,L)/C(L,L)
   20 CONTINUE
        ENTRY CROUT2(C,S,N,IDM,ISYM,IWR)
        DO 30 L=1,N
        IF(L.EQ.1)GO TO 30
        LLL=L-1
        DO 25 K=1,LLL
   25 S(L)=S(L)-C(L,K)*S(K)
   30 S(L)=S(L)/C(L,L)
        DO 35 L=2,N
        I=N-L+1
        II=I+1
        DO 35 K=II,N
   35 S(I)=S(I)-C(I,K)*S(K)
        IF(IWR.EQ.0)GO TO 50
        DO 40 I=1,N
   40   WRITE(6,2)S(I)
        WRITE(6,5)
   50   CONTINUE
        RETURN
        END
```

REFERENCES

1. Dolph, C.L., "A Current Distribution for Broadside Arrays which Optimizes the Relationship between Beam Width and Side Lobe Level," Proc. IRE, June 1946, p. 335
2. Uzkov, A.I., "An Approach to the Problem of Optimum Directive Antenna Design," Comptes Rendus (Doklady) de l'Academie de Sciences des l'USSR, 1946, p. 35.
3. Tai, C.T., "On the Optimum Gain of Uniformly Spaced Arrays of Isotropic Sources or Dipoles," Report 1522-1, March 1963, ElectroScience Laboratory (formerly Antenna Laboratory), Department of Electrical Engineering, The Ohio State University; prepared under Contract CRES 1090-1, for University of Kansas.
4. Jennetti, A.G., "Increased-Directivity Antennas," Ph.D. Dissertation, The Ohio State University, 1970.
5. Eberle, Jon W., "An Adaptively Phased, Four-Element Array of Thirty Foot Parabolic Reflectors for Passive (Echo) Communi-Cation Systems," Ph.D. Dissertation, The Ohio State University, 1964.

6. Svoboda, D.E,. "A Phase-Locked Receiving Array for High-Frequency Communications Use," IEEE Transactions on Antennas and Propagation, March 1964, p. 207.

7. Shor, S.W.W., "Adaptive Technique to Discriminate Against Coherent Noise in a Narrow-Band System," J. Acoust. Soc. Amer., January 1966, p. 74

8. Widrow, B., Mantey, P.E., Griffiths, L.J., Goode, B.B., "Adaptive Antenna Systems," Proc. of IEEE, December 1967, p. 2143.

9. Brennan, D.G., "Linear Diversity Combining Techniques," Proc. IEEE, pp. 1075-1102, June 1959.

10. Van Vleck, J.H., Propagation of Short Radio Waves, MIT Radiation Lab. Series.

11. Wulfsberg, Karl N., "Apparent Sky Temperatures at Millimeter-Wave Frequencies," Physical Sciences Research Papers, No. 38, July 1964, Air Force Cambridge Research Lab.

12. Richmond, J.H., "Computer Analysis of Three-Dimensional Wire Antennas," Report 2708-4, December 1969, ElectroScience Laboratory, Department of Electrical Engineering, The Ohio State University; prepared under Contract DOODO5-69-C-0031, Department of the Army, Aberdeen Proving Ground, Maryland.

NASA-Langley, 1971 — 10 CR-1778

NATIONAL AERONAUTICS AND SPACE ADMINISTRATION
WASHINGTON, D.C. 20546

OFFICIAL BUSINESS
PENALTY FOR PRIVATE USE $300

FIRST CLASS MAIL

POSTAGE AND FEES PAID
NATIONAL AERONAUTICS AND
SPACE ADMINISTRATION

POSTMASTER: If Undeliverable (Section 158
Postal Manual) Do Not Return

"The aeronautical and space activities of the United States shall be conducted so as to contribute . . . to the expansion of human knowledge of phenomena in the atmosphere and space. The Administration shall provide for the widest practicable and appropriate dissemination of information concerning its activities and the results thereof."

—NATIONAL AERONAUTICS AND SPACE ACT OF 1958

NASA SCIENTIFIC AND TECHNICAL PUBLICATIONS

TECHNICAL REPORTS: Scientific and technical information considered important, complete, and a lasting contribution to existing knowledge.

TECHNICAL NOTES: Information less broad in scope but nevertheless of importance as a contribution to existing knowledge.

TECHNICAL MEMORANDUMS: Information receiving limited distribution because of preliminary data, security classification, or other reasons.

CONTRACTOR REPORTS: Scientific and technical information generated under a NASA contract or grant and considered an important contribution to existing knowledge.

TECHNICAL TRANSLATIONS: Information published in a foreign language considered to merit NASA distribution in English.

SPECIAL PUBLICATIONS: Information derived from or of value to NASA activities. Publications include conference proceedings, monographs, data compilations, handbooks, sourcebooks, and special bibliographies.

TECHNOLOGY UTILIZATION PUBLICATIONS: Information on technology used by NASA that may be of particular interest in commercial and other non-aerospace applications. Publications include Tech Briefs, Technology Utilization Reports and Technology Surveys.

Details on the availability of these publications may be obtained from:

SCIENTIFIC AND TECHNICAL INFORMATION OFFICE

NATIONAL AERONAUTICS AND SPACE ADMINISTRATION

Washington, D.C. 20546